Erythrocyte apoptosis (erythroptosis) and anaemia in chronic HIV-1 infection: relationship with immune activation and viraemia

By

Stanley Loots

Dissertation presented for the degree of
Master of Science in Medical Sciences (Medical Virology) in the Faculty of Medicine and Health Sciences at
Stellenbosch University

Supervisor: Dr. Richard H. Glashoff
Co-supervisor: Dr. Hayley Ipp

December 2013

Declaration

By submitting this thesis/dissertation electronically, I declare that the entirety of the work contained therein is my own, original work, that I am the sole author thereof (save to the extent explicitly otherwise stated), that reproduction and publication thereof by Stellenbosch University will not infringe any third party rights and that I have not previously in its entirety or in part submitted it for obtaining any qualification.

Date: 27 November 2013

Verklaring

Deur hierdie tesis/proefskrif elektronies, verklaar ek dat die geheel van die werk hierin vervat, my eie, oorspronklike werk is, dat ek die enigste outeur daarvan (behalwe tot die mate uitdruklik anders aangedui), dat reproduksie en publikasie daarvan deur die Universiteit van Stellenbosch sal nie inbreuk maak op enige regte van derde partye, en dat ek vantevore in die geheel of gedeeltelik nie, ter verkryging van enige kwalifikasie.

Datum: 27 November 2013

Abstract

Introduction

Chronic HIV-1 infection is characterized by extensive inflammation/immune activation and also by anaemia. Macrophages and neutrophils produce reactive oxygen species (ROS) which can cause damage to surrounding cells, including erythrocytes. Damaged erythrocytes may die by apoptosis (erythroptosis) or be tagged for clearance by monocytes/ macrophages. In this study we investigated HIV-1-associated anaemia and erythroptosis in asymptomatic, untreated HIV-1 infected individuals and how it relates to oxidative stress and immune activation.

Materials and Methods

This cross-sectional study included 44 chronically HIV-1 infected individuals (CD4 count > 200) and 33 matched control uninfected individuals. CD4 count, viral load, and haemoglobin levels were measured. Red blood cells (RBCs) were stained with annexin V for determining *ex vivo* levels of erythroptosis. Erythrocytes were also subjected to oxidative stress (5mM H_2O_2 or 5mM ascorbic acid), in the presence or absence of N-acetyl cysteine (NAC). Finally, RBCs were also stained with CFSE, stimulated with H_2O_2 and then incubated with purified monocytes to monitor monocyte uptake of RBCs.

Results

Asymptomatic chronically HIV-1 infected individuals had reduced haemoglobin levels as compared to matched controls (12.9g/dL vs. 14.1g/dL, p=0.0172). The reduced haemoglobin was mirrored by significantly higher RBC-associated annexin V baseline expression in the HIV-1 infected group (13.4% vs. 10.4%, p=0.0189). Annexin V expression increased in both groups when stimulated with H_2O_2. Although NAC inhibited induced oxidative stress in both groups, the uninfected group displayed stronger inhibition. The *in vitro* oxidative stress induced percentage of apoptotic RBCs was significantly reduced in the control group (20±5.1% to 15±4.4%, p=0.0063), but not the HIV-1 positive group (18.3±5.0% to 16±5.2%, (p=0.0649)). There was a significant increase in the percentage inflammatory monocytes in the HIV-1 infected group, with the control group median inflammatory monocyte comprising 5.3±3.8% when compared to the HIV-1 positive group 8.3±3.5%, p=0.0054. In the HIV-1 infected individuals there was a higher number of inflammatory monocyte phagocytosing oxidatively stress-induced autologous RBCs compared to inflammatory monocyte phagocytosing un-stimulated RBCs (median monocyte/CFSE of 2.9% vs. 5.2% at 1 monocyte to 25 RBCs ratio, p=0.0803).

Conclusion

This study demonstrated a significant reduction in haemoglobin levels in untreated chronic HIV infection in a South African cohort. This anaemia was mirrored by significantly increase annexin V expression on RBCs. It was further shown that there was enhanced uptake of dying red blood cells by autologous monocytes. Treatments aimed at limiting oxidative stress or reducing immune activation may be beneficial in the management of anaemia in chronic HIV-1 infection.

Opsomming

Inleiding

Chroniese MIV-1 infeksie word gekenmerk deur uitgebreide inflammasie/immuun aktivering en ook deur anemie. Makrofage en neutrofiele produseer reaktiewe suurstof spesies (ROS), wat kan skade aan omliggende selle, insluitend rooibloedselle veroorsaak. Beskadigde rooibloedselle kan sterf deur apoptose (erythroptosis) of gemerk vir klaring deur monosiete/makrofage. In hierdie studie het ons ondersoek MIV-1-verwante bloedarmoede en erythroptosis in asimptomatiese, onbehandelde MIV-1 besmette individue en hoe dit verband hou met oksidatiewe stres en immuun aktivering.

Materiaal en metodes

Hierdie deursnee-studie ingesluit 44 chroniese MIV-1 besmette individue (CD4-telling> 200) en 33 ooreenstem beheer onbesmette individue. CD4-telling, virale lading, en hemoglobien vlakke gemeet is. Rooibloedselle (RBS) is gevlek met annexin V vir die bepaling van ex vivo vlakke van erythroptosis. Eritrosiete is ook onderwerp aan oksidatiewe stres (5 mm H_2O_2 of 5mM askorbiensuur), in die teenwoordigheid of afwesigheid van N-asetiel cysteïne (NAC). Ten slotte, is ook RBS gevlek met CFSE, gestimuleer word met H_2O_2 en dan geïnkubeer met gesuiwerde monosiete opname van RBS te monitor.

Resultate

Asimptomatiese chroniese MIV-1 besmette individue het verminder hemoglobien vlakke in vergelyking met ooreenstem kontroles (12.9g/dL teen 14.1g/dL, p=0,0172). Die verminderde hemoglobien is weerspieël deur aansienlik hoër RBC-verwante annexin V basislyn uitdrukking in die MIV-1 besmette groep (13,4% vs 10.4%, p=0,0189). Annexin V uitdrukking verhoog in beide groepe wanneer dit gestimuleer word met H_2O_2. Hoewel NAC geïnhibeer veroorsaak oksidatiewe stres in beide groepe, die onbesmette groep vertoon sterker inhibisie. Die *in vitro* oksidatiewe spanning persentasie van apoptotisch RBS was aansienlik verminder in die kontrole groep (20±5,1% tot 15±4,4%, p=0,0063), maar nie die MIV-positief is 1 groep (18,3±5,0% tot 16±5.2 %. (p=0,0649)). Daar was 'n beduidende toename in die persentasie opruiende monosiete in die MIV-1 besmette groep, met die kontrole groep mediaan opruiende monosiet bestaande 5,3±3,8% in vergelyking met die MIV-positief is 1 groep 8,3±3,5%, p=0,0054. In die MIV-1 besmette individue was daar 'n groter aantal inflammatoriese monosiet phagocytosing oxidatively stres-geïnduseerde lichaamseigen RBS in vergelyking met opruiende monosiet phagocytosing un-gestimuleer suspensie RBC

(mediaan monosiet/CFSE van 2,9% teen 5,2% op 1 monosiet tot 25 suspensie RBC verhouding , p=0,0803).

Gevolgtrekking

Hierdie studie dui op 'n beduidende afname in hemoglobien vlakke in onbehandelde chroniese MIV-infeksie in 'n Suid-Afrikaanse groep. Dit anemie is weerspieël deur aansienlik annexin V uitdrukking verhoog op RBS. Dit is verder getoon dat daar 'n verhoogde opname van die dood rooibloedselle deur lichaamseigen monosiete. Behandelings wat daarop gemik op die beperking van oksidatiewe stres of vermindering van immuun aktivering voordelig kan wees in die behandeling van anemie in chroniese MIV-1 infeksie.

Acknowledgement

I wish to thank the following individuals:

Dr. Richard Glashoff, my supervisor, for all his guidance and support

Dr. Hayley Ipp, my co-supervisor, for all her input and encouragement

The nursing staff from the Emavundleni Clinic for the collection of patient samples

Jan de Wit for assisting with CD4+ T cell counts

Dalene de Swardt for supervision, laboratory assistance and valuable advice

Keith Ryan Reddy for preparation of CD38 on CD8+ T cells samples

Mathilda Claassen for assisting with viral loads counts of HIV-1 positive samples

The HAIG group for all their support and advice

The Division of Medical Virology for accepting me and giving me the chance to sharpen my scientific skills

My parents for all their unlimited support and love over the last couple of years

My fellow students for advice, support and always being there to lend a helping hand

The Poliomyelitis Research Foundation (PRF) for funding

The NHLS at the Division of Haematology for providing full blood count data

Shahieda, Karmistha, Randall and Nafiisah for helping proof-read my thesis

My Lord Jesus for all the opportunities he has blessed me with, his unconditional love, the support and strength he has blessed me with and for always being there day and night

Table of Contents

Page

List of Figures

Page

List of Tables

Page

List of Abbreviations

AAOB	Ascorbic acid oxidative buffer
ABB	Annexin V binding buffer
ACD	Anaemia of chronic disease
AIDS	Acquired immune deficiency syndrome
APC	Allophycocyanin
ART	Antiretroviral therapy
ARV	Antiretroviral
BM	Bone marrow
bnAbs	Broadly neutralizing antibodies
CD14+CD16-	Classical monocyte subset
CD14+CD16+^{high}	Inflammatory monocyte subset
CD14+CD16+^{low}	Intermediate monocyte subset
cDNA	Complementary DNA
CFSE	Carboxyfluoresceinsuccinimidyl ester
cpz	Chimpanzee
CT	Cape Town
CTL	Cytotoxic T lymphocytes
DC	Dendritic cells
DPBS	Dulbecco's Phosphate Buffered Saline
dsDNA	Double-stranded linear DNA
dsRNA	Double-stranded RNA
EDTA	Ethylenediaminetetraacetic acid
EPO	Erythropoietin

ESCRT	Endosomal sorting complexes required for transport
FACS	Fluorescent Activated Cell Sorter
FBC	Full blood count
FH	Familial hypercholesterolemia
FITC	Fluorescein isothiocyanate
FMO	Fluorescence Minus One
GALT	Gut-associated lymphoid tissue
Gp	Glycoprotein
GPx	Glutathione peroxidase
GST	Glutathione-S-transferase
GT	Glutathione
H_2O_2	Hydrogen peroxide
HAART	Highly active antiretroviral therapy
Hb	Haemoglobin
Hct	Haematocrit
HCTP	HIV counselling, testing and prevention
hiFBS	High inactivated Fetal Bovine Serum
HIV	Human immunodeficiency virus
HM	Hemotrophic mycoplasmas
HREC	Human Research Ethics Committee
IL-1	Interleukin 1
IL-6	Interleukin 6
LDL	Low-density lipoproteins
LN	Lymph nodes
LPS	Lipopolysaccharide

M	Major
MHC	Major Histocompatibility complex
mRNA	Messenger RNA
N	Non-M/non-O
NAbs	Neutralizing antibodies
NAC	N-acetyl cysteine
NK	Natural killer cell
NNRTI	Non-nucleoside reverse transcriptase inhibitor
NRTI	Nucleoside analog reverse transcriptase inhibitor
O	Outlier
O_2	Oxygen
$ONOO^-$	Peroxynitrite
PAMPs	Pathogen-associated molecular patterns
PBMC	Peripheral Blood Mononuclear Cell
PCP	*Pneumocytis carinii* pneumonia
PCV	Packed cell volume
PE	Phycoerythrin
PerCP	Peridinin chlorophyll protein
PMN	Polymorphonuclear
PRRs	Pattern recognition receptors
PS	Phosphatidylserine
P-TEFb	Positive transcription elongation factor b
RBC	Red blood cell
RCC	Red cell count
RNA	Ribonucleic acid

RNAPII	RNA polymerase II
ROS	Reactive oxygen species
RT	Reverse transcriptase
SANAS	South African National Accreditation System
SD	Standard deviation
SIV	Simian immunodeficiency virus
sm	Sooty mangabeys
SOD	Superoxide dismutase
ssRNA	Single-stranded RNA
TB	Tuberculosis
TLR	Toll-like receptor
TNF α	Tumour necrosis factor α
UNAIDS	United AIDs
VQA	Virology Quality Assurance
WBCs	White blood cells
WHO	World Health Organization

Chapter 1: Introduction

Acquired immune deficiency syndrome (AIDS) was first described more than three decades ago in Los Angeles (CA, USA) (Beyrer *et al.*, 2012). Human immunodeficiency virus (HIV) is responsible for the development of AIDS and is the causative agent of the major AIDS pandemic. HIV-1 infection is characterized by a systemic pro-inflammatory milieu and persistent host immune system activation. The pro-inflammatory environment and chronic immune activation which is characteristic of chronic HIV-1 infection is also associated with anaemia (Weiss, 2009). Anaemia in HIV-1 may be due to either more rapid removal of erythrocytes from the blood circulation due to increased damage or death, or alternatively the bone marrow may be suppressed due to the inflammatory environment resulting in decreased erythrocyte production. Inflammation also promotes oxidative stress which is linked to cellular dysfunction and increased cell death. In the present study we have investigated the status of the erythrocyte compartment in untreated chronic HIV-1 infection, with a particular focus on the erythrocyte death (erythroptosis) and the sensitivity of erythrocytes to oxidative stress as a role player in anaemia in HIV-1 infection.

It has been well described that HIV-1 infection facilitates the production of reactive oxygen species (ROS) (Agrawal *et al.*, 2007). ROS in low to moderate levels are harmless but once they exceed optimal levels, they can become toxic to a cell. Glutathione (GT) is a type of anti-oxidant found in red blood cells that neutralises the low to moderate levels of ROS, however, higher levels of ROS depletes available glutathione and results in oxidative stress. Oxidative stress culminates in damage to the cell membrane, either directly or via the activation of caspases (Valko *et al.*, 2007). N-acetyl-cysteine (NAC) antioxidant is the precursor molecule for glutathione. NAC is a free radical scavenger that has been shown to neutralise the damaging effects of ROS (Kamboj *et al.*, 2010). In the current study, we investigated whether NAC could inhibit the damage sustained by RBCs in chronic HIV-1 infection.

Monocytes have an important function of clearance of dead, damaged or dying cells from the circulation host system. Damaged RBCs express phosphatidylserine at early stages of apoptosis and are thus primed for up-take by monocytes (Mikołajczyk *et al.*, 2009)(Weiss, 2009). Several studies have investigated phagocytic function in monocytes in HIV-1 infection, but none have investigated monocyte phagocytosed RBCs. In this study we investigated the different subtypes of monocytes and their phagocytic uptake capabilities of oxidatively stressed RBCs.

The current study has thus examined the erythrocyte compartment in chronic HIV-1 infection at several levels. Initially the total red cell count and haemoglobin levels between healthy and HIV-1-infected individuals were compared. A notable incidence of anaemia in HIV-1-infection

then led to the investigation of erythrocyte death (erythroptosis). The *ex vivo* level of erythroptosis was increased in HIV-1 patients. Experiments involving *in vitro* oxidative stressing of erythrocytes indicated that the cells from the infected and uninfected individuals showed similar levels of sensitivity and equivalent increases in erythroptosis. Also, the antioxidant NAC, although effective in minimizing induced oxidative stress, could not reverse the damage that had occurred *in vivo*. Having established that erythrocytes in HIV-1 infection have higher baseline levels of annexin V expression, we then investigated how this impacted on the monocyte compartment, as splenic monocytes are the primary cell type involved in erythrocyte removal from the circulation. The monocytes in the HIV-1-infected group were skewed toward the inflammatory phenotype and this subset of monocytes also displayed an enhanced phagocytic ability. In the study we showed that the level of erythroptosis impacts on the resultant phagocytosis, thus implicating enhanced removal of red blood cells in the development of anaemia in chronic HIV-1 infection.

Chapter 2: Literature Review

2.1. HIV-1/AIDS Epidemic Overview

AIDS was first described on June 5, 1981 in Los Angeles (CA, USA), but the causative viral agent was only discovered two years later (Beyrer *et al.*, 2012). In the original description of HIV-1 infection, patients showed symptoms of *Pneumocytis carinii* pneumonia (PCP), a rare opportunistic infection that was known to occur in people with significantly compromised immune systems (Helweg-Larsen *et al.*, 2009). The causative virus was isolated independently by Robert Gallo and Luc Montagnier in 1983 (Fauci, 2008). Human immunodeficiency virus (HIV-1), as it came to be known, originated from simian immunodeficiency viruses (SIV) in chimpanzees (cpz) (Wertheim *et al.*, 2009). The disease was first reported mainly in homosexual males in 1983 but within a decade the heterosexual epidemic came to predominate worldwide (Beyrer *et al.*, 2012). HIV consists of two subtypes: HIV-1 and HIV-2. HIV-1 originated from SIVcpz of central African chimpanzees, whereas HIV-2 originated from SIVsm of sooty mangabeys (sm) (Wertheim *et al.*, 2009).

The HIV-1 and HIV-2 viruses each have several subtypes. HIV-1 is divided into the following sub-groups M (major); O (outlier) and N (non-M/non-O). HIV-2 is divided into eight groups from A-H. The group M of HIV-1 is mainly responsible for the epidemic (and includes nine subtypes: A-D, F-H, J and K) (Wertheim *et al.*, 2009; Tebit *et al.*, 2011). HIV-1 infection in humans originated from cross-species infection by SIV, possibly due to contact with infected animals (bites, scratches) or contaminated meat (Worobey *et al.*, 2008).

HIV-1 infection represents one of the most severe infectious disease of the 20th century and is responsible for multiple human deaths (Volberding *et al.*, 2010). In 2011 HIV-1 was responsible for approximately 1.7 million HIV-1 related deaths (UNAIDS, 2012). HIV-1 transmission can be either horizontal or vertical. Vertical transmission occurs from HIV-1-infected mothers to their unborn infants during pregnancy or during the birth process. Horizontal transmission is mainly due to sexual contact. Other horizontal transmitting factors contributing to HIV-1 infection included contaminated needles used during intravenous drug administration, and contaminated blood used for blood transfusions (Khan *et al.*, 2007). AIDS is the end stage of untreated HIV-1 infection.

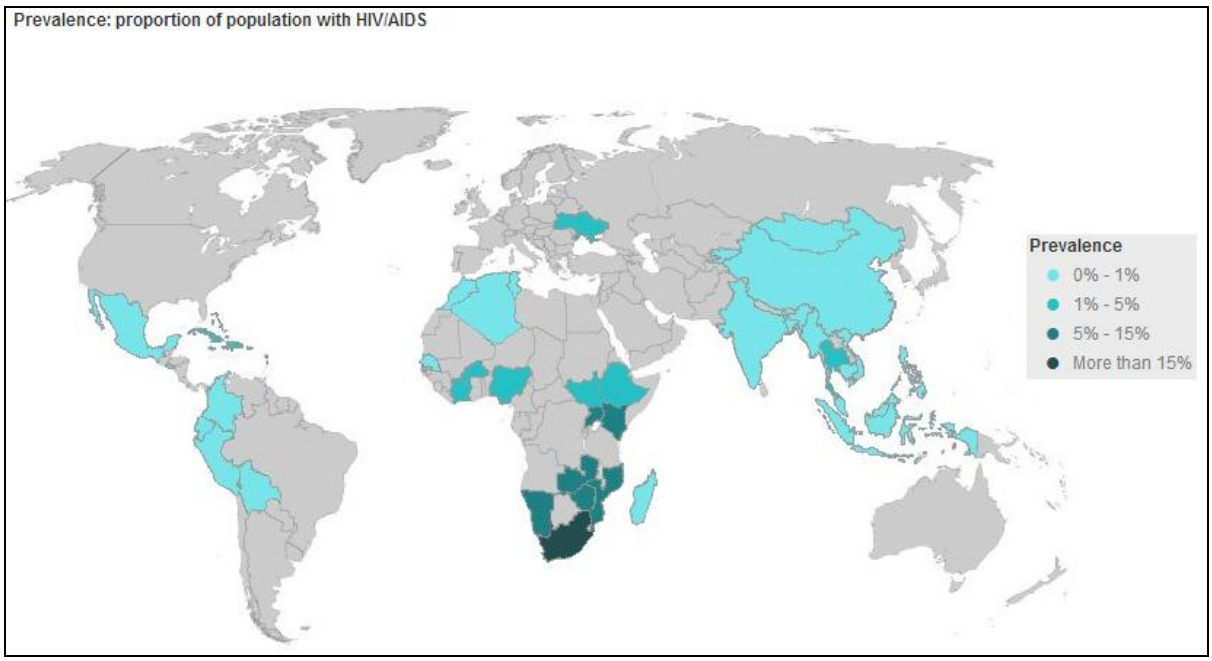

Figure 2.1. Prevalence of HIV-1 infection worldwide (2010).The world map represents the estimated prevalence of the 34 million individuals infected by HIV-1 at the end of 2011 (UNAIDS 2012). The darker the colour the greater the prevalence rate (http://maps.aidsalliance.org/map/global/2010/prevalence/)

Even though HIV-1 infection occurs worldwide, Sub-Saharan Africa, which includes only 3% of the world population, represents 69% of the global HIV-1 positive population (Lurie *et al.*, 2010). Sub-Saharan Africa also has the highest prevalence rate in the world with adult prevalence of more than 15% (Lurie *et al.*, 2010) as indicated in Figure 2.1 above.

People infected with HIV-1 can live approximately 11 years without anti-retroviral treatment (ART) and approximately 23 years on highly active (combination drug) antiretroviral therapy (HAART) treatment before developing AIDS or before dying (Harrison *et al.*, 2010). It has been estimated that there were 34 million people globally living with HIV-1 at the end of 2010. Only 6.6 million people were on ART from the 14.2 million people that were eligible to receive treatment in low to middle income countries at the end of 2010 according to the 2011 report released by the UNAIDS (http://www.unaids.org/en/resources/presscentre/pressreleaseandstatementarcHIV1e/2011/november/20111121wad2011report/).

HAART treatment can suppress viral replication of HIV-1 to such an extent that it is undetected by standard laboratory assays. The lower viral load results in lower levels of immune activation and decreased inflammation. If the use of HAART treatment is disrupted, the viral load may increase drastically (rebound effect) leading to recurrence of higher levels of immune activation and inflammation.

2.2 HIV-1 virus

2.2.1. Structure

HIV-1 is a retrovirus (family Retroviridae), belonging to the genus Lentivirus. It is a small enveloped ribonucleic acid (RNA) virus. HIV-1 consists of an inner cone-shaped core and a spherical matrix. The HIV-1 envelope lipid bilayer supports the gp41 glycoprotein (Gp) which is embedded within the membrane. The gp120 envelope glycoprotein is situated above and attached to the gp41 envelope glycoprotein. The combined structural unit comprising gp41 and gp120 is also referred to as the gp160 (Chakrabarti *et al.*, 2011).The p17 matrix protein is located beneath the lipid membrane, the structural component of the matrix capsid which encloses the core of the virus. The viral core structure is composed of p24 protein. The capsid proteins surround and protect the two single RNA strands and reverse transcriptase (RT) enzyme of the virus (Lever, 2009) as indicated in Figure 2.2.

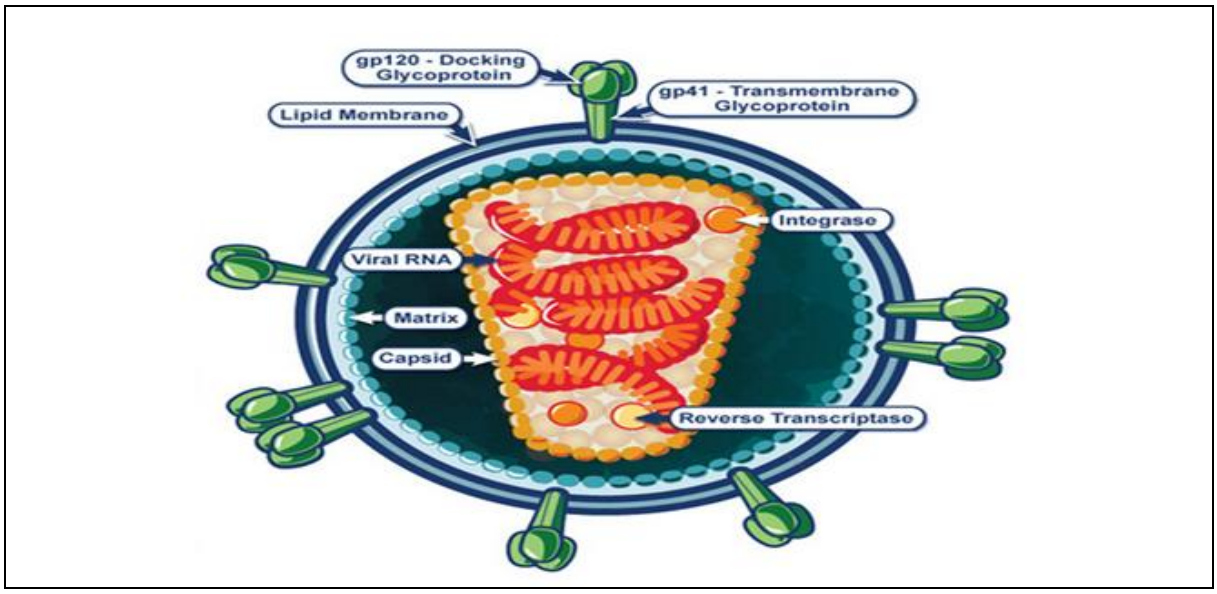

Figure 2.2. Structure of the HIV-1 virion. The HIV-1 virus RNA is surrounded by lipid bilayer containing glycoproteins gp41 and gp120, protecting it from immune attack before entering the cell. The p17 matrix protein and p24 capsid proteins (http://www.niaid.nih.gov/topics/HIV1aids/understanding/biology/Pages/structure.aspx).

The HIV-1 genome consists of only nine genes and is approximately 9kb in length. The nine genes viz. *gag, pol, vif, vpr, vpu, tat, rev, env* and *nef*, each play a critical role either in the structure of the virus or in the infection, replication and/or exocytosis processes (Watts *et al.*, 2009). The nine genes are categorized into three different groups i.e. structural (*gag, pol* and *env*), regulatory (*tat, rev* and *nef*) and accessory (*vif, vpr* and *vpu*) genes. The arrangement of HIV-1 genes is illustrated in Figure 2.3.

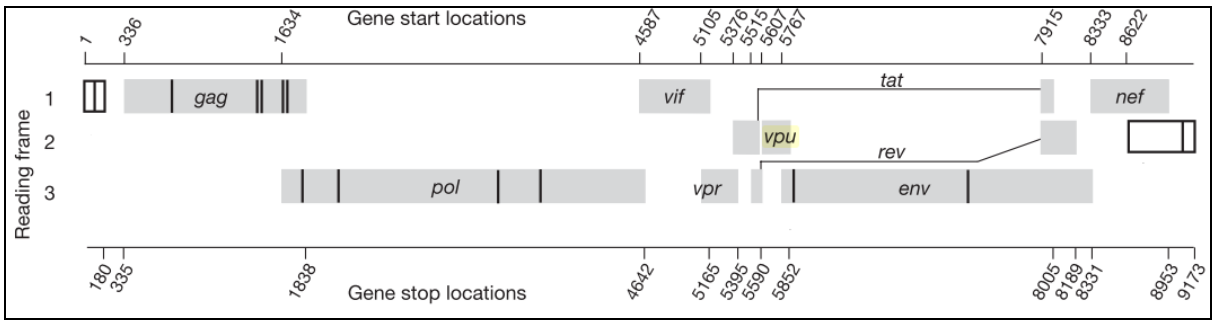

Figure 2.3. Diagram of the HIV-1genome.The HIV-1 genome consists of 9749 nucleotides. The genome is comprised of 9 genes (gag, pol, vif, vpr, vpu, tat, rev, env and nef) all having specific functions during HIV-1 infection, replication and spread (Watts et al., 2009).

HIV-1 virus infects cells in a slow, continuously progressive manner. Like all retroviruses, HIV-1 has a unique way of replicating involving reverse transcription which is shown in figure 2.4 and discussed in more detail below.

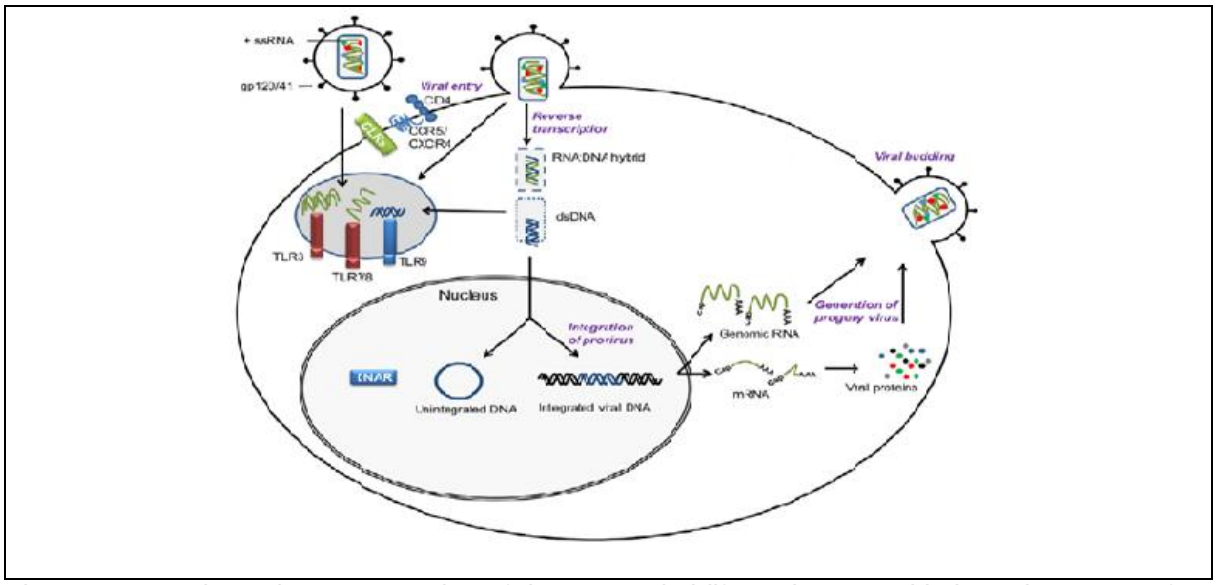

Figure 2.4. A schematic representation of the HIV-1 viral life cycle. HIV-1 binds to the CD4 surface marker and chemokine co-receptors (CCR5/CXCXR4) of the T lymphocytes. Toll-like receptors (TLR) of the T cell detects various forms of the viral infection and initiates an immune response. TLR3 recognises double stranded RNA (dsRNA), TLR7/8 recognises single stranded RNA (ssRNA) and TLR9 recognises double-stranded linear DNA (dsDNA) of the virus (Liu et al., 2008; Qu et al., 2009; Iwasaki et al., 2010). The virus goes on integrating the provirus DNA into the host DNA, replicating and finally exiting the cell through exocytosis. The virus repeats these steps in other uninfected cells (Mogensen et al., 2010). All these steps of the life cycle are explained below.

2.2.2. HIV-1 replication

2.2.2.1. Entry

The HIV-1 virion targets cells expressing the CD4 surface molecules (viral receptor) and one or more chemokine co-receptors (CCR5/CXCR4) (Chun *et al.*, 2012). These receptors define HIV-1 cell tropism. The main cell targeted during established HIV-1 infection is the

$CCR5^{+}CD4^{+}$ T lymphocyte a subset of T cells which is consequentially drastically reduced by HIV-1 infection (Funderburg *et al.*, 2012). It is noteworthy that mucosal $CD4^{+}$ T cells consist predominantly of memory $CD4^{+}$ T cells which express the HIV-1 co-receptor CCR5 and represent an activated status (Brenchley *et al.*, 2004). The envelope glycoprotein gp120 on HIV-1 interacts with CD4 surface marker on the T lymphocyte binding with a high affinity of 28 nM (Dey *et al.*, 2009). The envelope glycoprotein gp120 also attaches to the chemokine co-receptors CCR5/CXCR4 on the T lymphocyte (Briz *et al.*, 2006). The binding activates the gp41 glycoprotein allowing it to insert a terminal fusion peptide into the cell membrane of the T lymphocyte. The gp41 glycoprotein and terminal fusion peptide form a six-helix bundle formation allowing membrane fusion to occur. When fusion of the membranes is complete, the nucleocapsid is released into the cytoplasm of the T lymphocyte illustrated in Figure 2.5 (Wilen *et al.*, 2012).

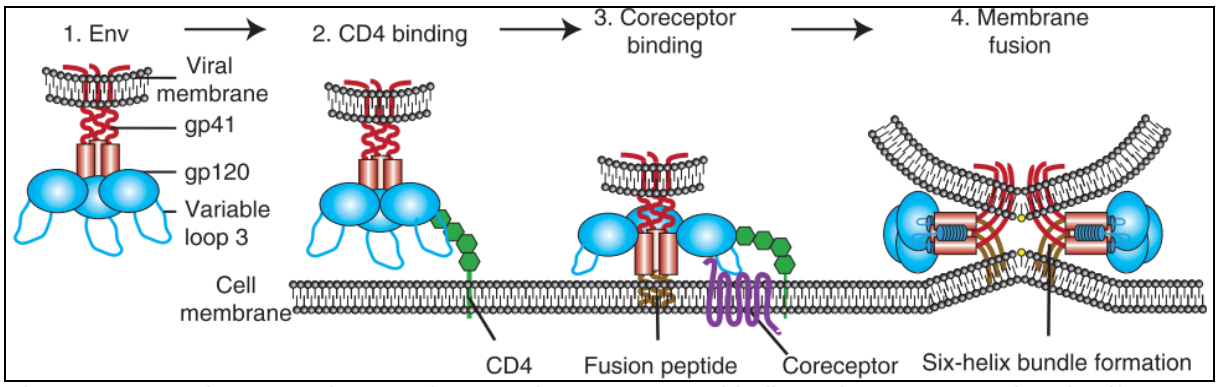

Figure 2.5. Attachment and entry of HIV-1 via GP120-CD4 binding. The HIV-1 attaches itself to CD4 positive cells via its gp120 protein. The gp120 protein can also bind to the CXCR4 or CCR5 chemokine co-receptors to gain access to the cell (Wilen et al., 2012).

2.2.2.2. Reverse Transcription and integration

Once inside the cell the HIV-1 enzyme known as reverse transcriptase, copies a single stranded RNA into a complementary DNA (cDNA) molecule. This double stranded viral DNA is then transported to host cell nucleus where it is integrated into the host DNA by a viral enzyme integrase (Zheng *et al.*, 2005). The integrated viral DNA can be transcribed and translated when the host cell is activated and host cell gene transcription is activate (illustrated in Figure 2.6.).

2.2.2.3. Transcription

Tat intensifies the HIV-1 transcription in infected CD4+ T lymphocytes. The HIV-1 Tat protein is responsible for placing the cellular positive transcription elongation factor b (P-TEFb) onto the integrated proviral DNA. The P-TEFb stimulates transcription by phosphorylating the C-terminal domain of the RNA polymerase II (RNAPII) (Trono *et al.*, 2010). The transcription of the provirus DNA produces viral messenger RNA (mRNA). The viral mRNA is translated into viral structural proteins and the viral enzyme RT within in the host cell cytoplasm (Jeang, 2012) illustrated in Figure 2.6.

2.2.2.4. HIV-1 assembly and budding

The assembly of the viral structural proteins and core particles occurs at the plasma membrane of the host cell. Gag plays a major role in the packing of viral RNA, forming of spherical particles by linking proteins and assembly of the virion. All of these occur at the same time. Once the virus is assembled it is released from the plasma membrane by the endosomal sorting complexes required for transport (ESCRT) machinery. Viral particles exit the cell by budding, a process in which the virus acquires its outer envelope. New virions are thus set free to infect other nearby cells (Sundquist *et al.*, 2012) illustrated in Figure 2.6.

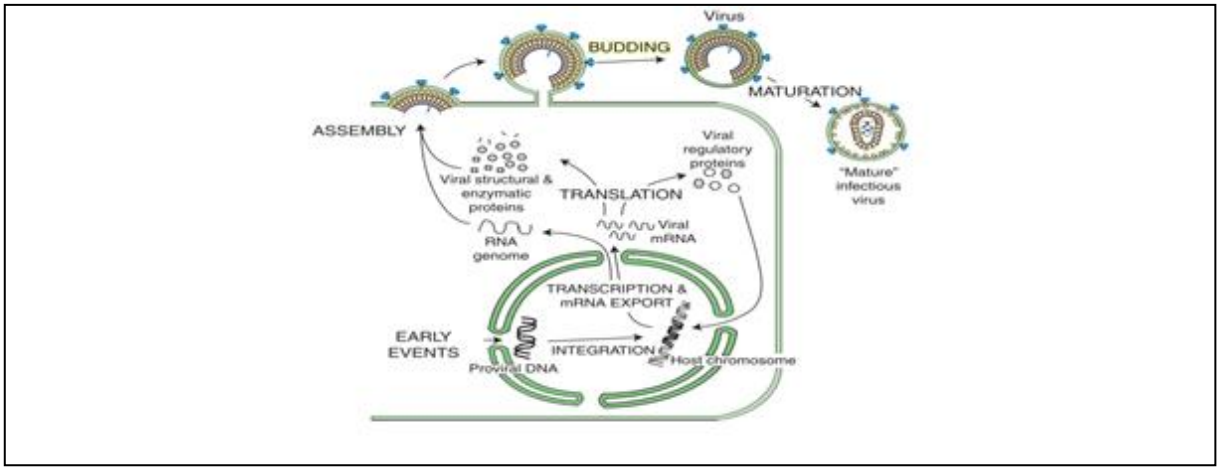

Figure 2.6. Representation of the production of a new HIV-1virion (reverse transcription, integration, transcription, assembly and budding) (Sundquist et al., 2012).

2.3. HIV-1 Pathogenesis

There are three phases in the pathogenesis of the HIV-1 infection, namely acute phase (also termed viremic), chronic phase (or latent) and late phase (full-blown AIDS). The first step in the pathogenesis process is the targeting and infection of $CD4^+$ T cells, leading to their depletion which is a characteristic feature of the acute phase (McMichael *et al.*, 2010). A

second step which begins simultaneously to the first and which becomes amplified and defines the chronic phase of infection is immune system activation (Boasso *et al.*, 2008). A third major step is the dysfunction and exhaustion of the immune system ultimately leading to impairment, opportunistic infections, malignancies and eventually death (Cassol *et al.*, 2010). The three phases are discussed in more detail below.

2.3.1. Acute HIV-1 pathogenesis phase (viremic)

The acute HIV-1 phase extends from viral entry or the detection of the viral RNA until the production of HIV-1 specific antibodies approximately 3-4 weeks from day of infection. These HIV-1 specific antibodies are indicative of the development of a functional humoral immunity. Initial invasion of the host triggers localized inflammation and activation of the innate immune system. Resident cells initially detect the presence of the virus and initiate the recruitment of additional lymphocytes, monocytes (macrophages) and other cells to the site of infection and localized inflammation. These recruited cells are in turn targeted by the virus for infection (Mogensen *et al.*, 2010). Initial infection usually occurs via the genital tract from where it spreads to secondary lymphoid organs after about a week. These secondary lymphoid organs include draining lymph nodes (LN) and gut-associated lymphoid tissue (GALT). It is unknown whether infection of the GALT is due to cells migrating from the LN and thus carrying virus there or by direct viral spread after release from infected cells in the LNs (Yan *et al.*, 2011). The GALT is a major storage site for lymphocytes. The majority of these T lymphocytes are activated effector memory CD4+ T cells expressing the chemokine receptors CCR5 (Chun *et al.*, 2012). HIV-1 replicates rapidly in the GALT and then plasma viraemia peaks between days 21-28 of infection. This rapid replication in the GALT leads to the destruction of the reservoir of helper T cells located there. The destruction of the reservoir helper T cells is irreparable in the GALT but circulating CD4+ T cell numbers are restored to almost normal levels in certain cases (Mogensen *et al.*, 2010). During the acute stage HIV-1 integrates itself into the DNA of some resting memory T cells and then enters dormant (non-replicative) stage. This dormant stage is known as viral latency and is an important adaptive mechanism of HIV-1 to escape the immune system (Cohen *et al.*, 2011). These resting cells also serve as viral reservoirs. The viral load decreases after 12-20 weeks as HIV-1 antigen specific CD8+ cytotoxic T lymphocytes (CTL) become active and eliminate infected cells and aid in establishing control of the infection (Mogensen *et al.*, 2010) illustrated in Figure 2.7.

2.3.2 Chronic HIV-1 phase (latent)

This stage of the HIV-1 infection begins after the viral load starts decreasing (and when CD4 count begins to recover), and also when HIV-1 specific antibodies are first detected. Patients not on any form of treatment can live approximately 11 years in the chronic phase, whereas those on ART treatment can live approximately 23 years (Harrison *et al.*, 2010). The defining concepts for chronic HIV-1 infection are: a low stable viral load (that is slowly increasing) resulting in continued enhanced immune activation; low mucosal CD4+ count and a relatively high (but decreasing) circulating CD4+ T cell count; stable CTL numbers, but also slowly decreasing as viral load increases over time (Ford *et al.*, 2009; Mogensen *et al.*, 2010). Increased immune activation and increased viral load leads to the depletion of CD4+ effector memory cells and also an accelerated cell turnover. The accelerated cell turnover produces naïve and central memory T cells to compensate for the depletion of the effector memory T cells in the gut. These cells are not very efficient in playing the role of the depleted CD4+ effector memory T cells (Brenchley *et al.*, 2004).

The naïve and memory CD4+ T cells that are produced express CCR5, thus resulting in more cells being available for HIV-1 infection (Picker *et al.*, 2005). The depletion of the CD4+ effector memory cells in the GALT also results in damage to the mucosal barrier. The mucosal barrier can no longer effectively constrain the natural flora in the gut. Gut bacteria (microbiota) and microbial products such as lipopolysaccharide (LPS) translocate into the peripheral blood (Haas *et al.*, 2011). The LPS contributes to the on-going chronic immune activation during HIV-1 infection by stimulating monocytes and other innate immune cells via the TLR4 (Seki *et al.*, 2012). HIV-1 constantly evolves to escape immune defences by undergoing multiple mutations. Once the CD4+ CCR5+ T cells become low the viral mutations may also change the cellular tropism of the virus from CCR5-tropic to CXCR4-tropic or dual tropic (CCR5 and CXCR4). Naïve/ memory T cells and monocytes/ macrophages expressing CXCR4 then also become targets for infection (Joshi *et al.*, 2011). During chronic infection the lymphoid tissue is also damaged by the virus. The damage also leads to the dysfunction of the thymus which results in insufficient/ dysfunctional T cell production (Ofotokun *et al.*, 2012) illustrated in Figure 2.7.

2.3.3 Late phase (AIDS)

The development of AIDS is due to the continued depletion of the CD4+ lymphocytes until a minimum threshold is reached (Joshi *et al.*, 2011). An effective immune response and immune defences in general are largely dependent on these lymphocytes. The dysfunction of immune defences gives way to opportunistic infections and malignancies, eventually leading to the death of the infected host (Rockstroh *et al.*, 2010).

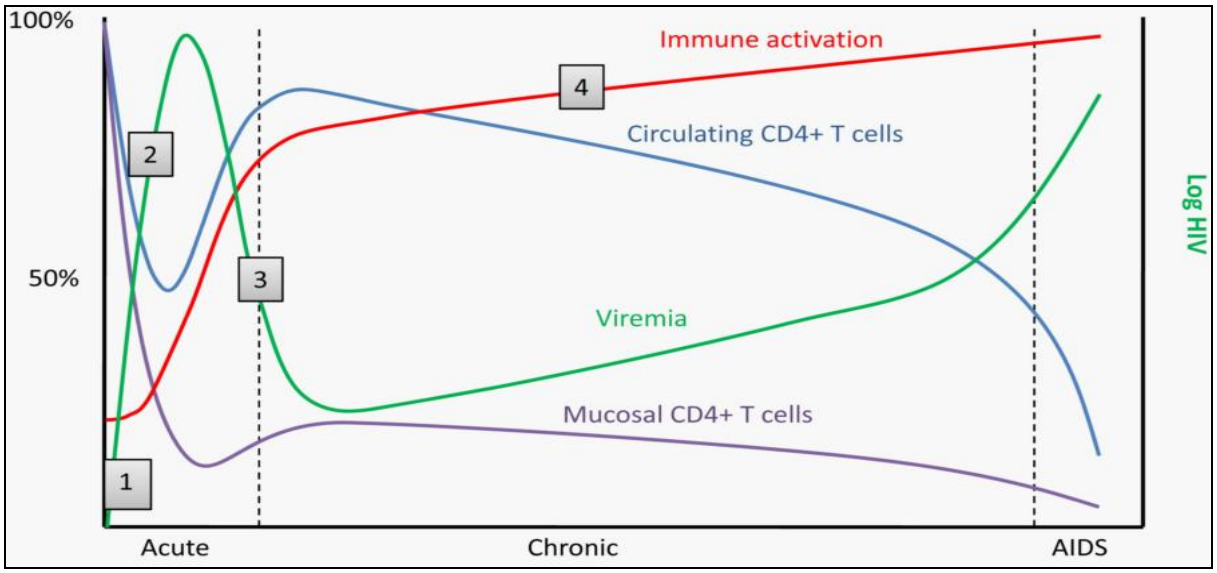

Figure 2.7. Representation of the immune system at the acute and chronic stages of HIV-1 infection leading to the development of AIDS. (1-2) Initiation of innate immune system is trying to prevent HIV-1 infection, (2-3) during inflammation numerous cells including activated T lymphocytes are recruited which are targeted to the virus, (3-4) viral load decreases to low levels at the start of chronic HIV-1 infection, (4) the persistent immune activation upheld by the HIV-1 infection and opportunistic infections leads to the development of AIDS (Mogensen et al., 2010).

2.4. Immune response in HIV-1 infection (innate, humoral and cell-mediated).

2.4.1. Innate immunity

Innate immunity includes barrier cells (such as epithelial cells), phagocytes (dendritic cells (DCs), monocytes and macrophages) and natural killer (NK) cells. These are the first line of defence against pathogens. These cells have both surface and intracellular pattern recognition receptors (PRRs), which bind to pathogen-associated molecular patterns (PAMPs) (Yan *et al.*, 2011; Vivier *et al.*, 2011). PRR engagement leads to cellular activation and enhancement of function. Macrophages will engulf pathogens while NK cells will kill infected cells. Infected cells that are activated, damaged or killed as a result of infection or early immune activity, release cytokines which in turn amplify inflammation. The on-going inflammation results in recruitment of monocytes and neutrophils to sites of infection but also begins the initiation of acquired immunity when dendritic cells migrate to LNs to initiate antigen-specific immunity (Gonzalez *et al.*, 2010).

2.4.2. Humoral Immune Response

The humoral immune response is not very effective in controlling HIV-1 infection (Alter *et al.*, 2010). HIV-1 causes B cells to produce large amounts of antibodies as evident by hypergammaglobulinemia, but these antibodies are not particularly effective. During the acute phase non-neutralizing antibodies that bind directly to the gp41 glycoprotein of HIV-1 are produced. Soon afterwards, additional non-neutralizing antibodies are produced that bind

directly to the gp120 glycoprotein. These non-neutralizing antibodies are not very effective in reducing HIV-1 infectivity (Nicely *et al.*, 2010). Autologous neutralizing antibodies (NAbs) are only produced weeks to months after initial infection which is too late to effectively neutralize infection, resulting in largely uncontrolled infections. The virus can also escape the NAbs by rapid mutation of the gp120 glycoprotein resulting in changing of antigenic determinants (Alter *et al.*, 2010).

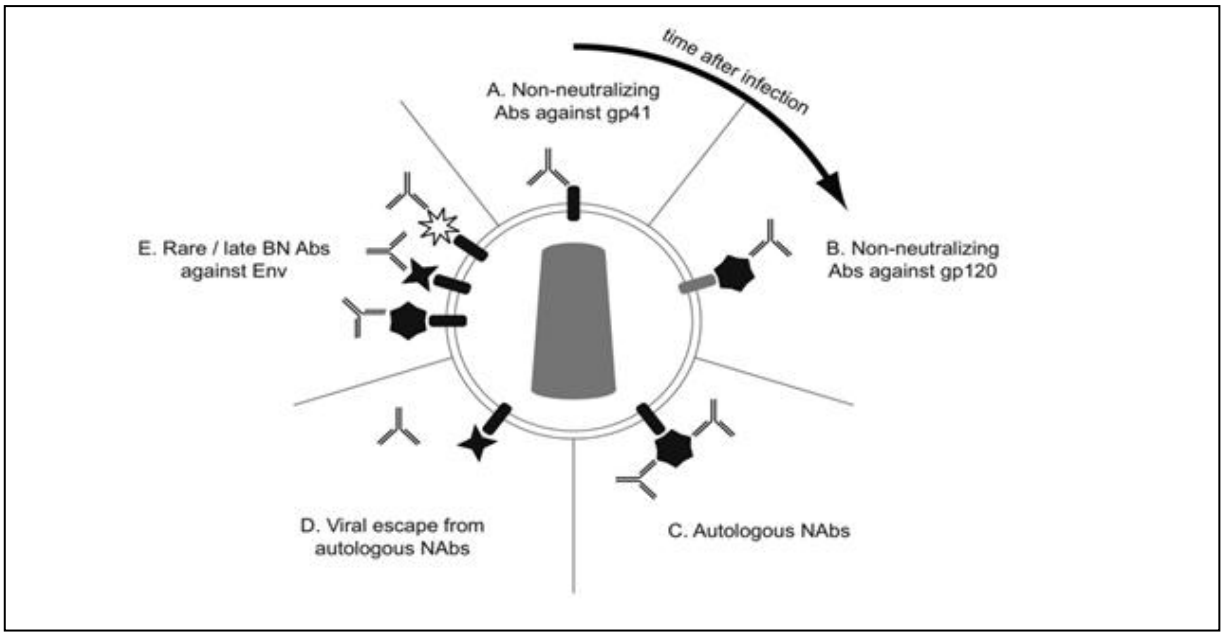

Figure 2.8. Representation of antibody response to HIV-1 at different stages. (A) Non-neutralizing antibodies responds to the gp41 of HIV-1: (B) Non-neutralizing antibodies respond to the gp120 of HIV-1 soon afterwards: (C) autologous neutralizing antibodies (NAbs) specific for HIV-1 are produced weeks to months after initial infection: (D) the virus mutates the gp120 in order to escape the Nabs: (E) some individuals produce Nabs for numerous gp120 mutations and is known as broadly neutralizing antibodies (bnAbs) (Alter et al., 2010).

2.4.3. Cell-mediated immune response

Unlike the humoral immune response that mediates its function by producing antibodies (see section 2.4.2), the cell-mediated immune response activates antigen specific T cells (CD4 and CD8) (Karanam *et al.*, 2009). Cell-mediated immunity is very important in the control of HIV-1 infection, as evidenced in animal experiments where adoptive transfer of CD8+ CTL to monkeys conferred protection. Cells that are infected with HIV-1 will present antigens on their cell surface via major histocompatibility complex (MHC) class I, thereby enabling cytotoxic CD8 T cells to recognize and kill them (via apoptosis induction) (Vivier *et al.*, 2011).

2.5. HIV-1-associated immune activation and apoptosis

Individuals infected with HIV-1 display elevated expression of markers of activation (both soluble (serum) and cell-associated (e.g. CD4+, CD8+, B cells, etc.)). These cells often also express elevated markers of apoptosis (Brenchley *et al.*, 2004). Pro-inflammatory cytokines (TNF-α, IL-1 and IL-6) are increased during immune activation (Seidler *et al.*, 2010). Increased CD8+ CTL activation also occurs which leads to higher expression of the activation marker CD38 on these cells. This marker has been correlated with HIV-1 disease progression (Barbour *et al.*, 2009). Untreated HIV-1 infected individuals display a high immune activation status and depletion of CD4+ T cells (Zeng *et al.*, 2011). The activation of the immune system produces a pro-inflammatory environment facilitating the replication of HIV-1. Increased replication leads to increased infection of host immune cells (primarily CD4+ T cells) contributing to the apoptosis of these cells. The apoptosis of these cells can occur directly or indirectly by mechanisms such as pro-inflammatory cytokines, viral peptides and other co-infections (Kirchhoff, 2009).

In addition to the well described changes in immune cells in chronic HIV-1 infection, changes in other compartments are known. Anaemia is a common complication in chronic HIV-1 infection. HIV-1-associated anaemia is the result of changes in the erythrocyte population of the infected host. As this study has focused on erythrocytes in chronic HIV-1 infection, some background is provided below.

2.6. Red Blood Cells (RBCs)

In 1668 the first red blood cell (RBC) was observed and described by the Dutch biologist and microscopist Jan Swammerdam (Mohandas *et al.*, 2008). RBCs form the majority (±45%) of whole blood. RBCs live approximately ±120 days (Bratosin *et al.*, 2009). Healthy RBCs have a biconcave shape that is necessary in small, tight and high force spaces. This shape allows for minimal membrane bending energy requirements needed to squeeze through these areas (Kaoui *et al.*, 2009). Erythrocytes originate from hematopoietic stem cells in the bone marrow. Five differentiation stages occur before the erythrocyte stage is reached. Hematopoietic stem cells generate pro-erythroblasts, which in turn give rise to erythroblasts, normoblasts, reticulocytes and eventually erythrocytes (illustrated in Figure 2.9). The progressive decrease in size and disappearance of the nucleus leaves an enucleated mature erythrocyte with a diameter of approximately 7-8µm (illustrated in Figure 2.10). Erythrocytes have one distinct surface marker on the cell membrane CD235a (Glycophorin A) (Lu *et al.*, 2008). Glycophorin A is a sialoglycoprotein (Berahovich *et al.*, 2010). The unique shape of erythrocytes is believed to be caused by glycophorin A (Karsten *et al.*, 2010). Erythrocytes have two major functions viz. transporting oxygen to muscles and organs and transporting

carbon dioxide from muscles and organs back to the lungs (Pittman, 2010)(Maitra *et al.*, 2011). In addition to their role in gaseous transport and exchange, they also play a role in coagulation and haemostasis (Zwaal et al., 1997).

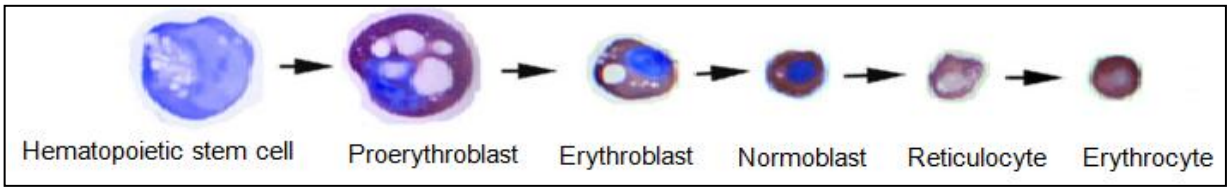

Figure 2.9. Schematic representation of erythrocyte differentiation from haematopoietic stem cell. The five stages prior to emergence of the mature erythrocyte are illustrated (Lu et al., 2008).

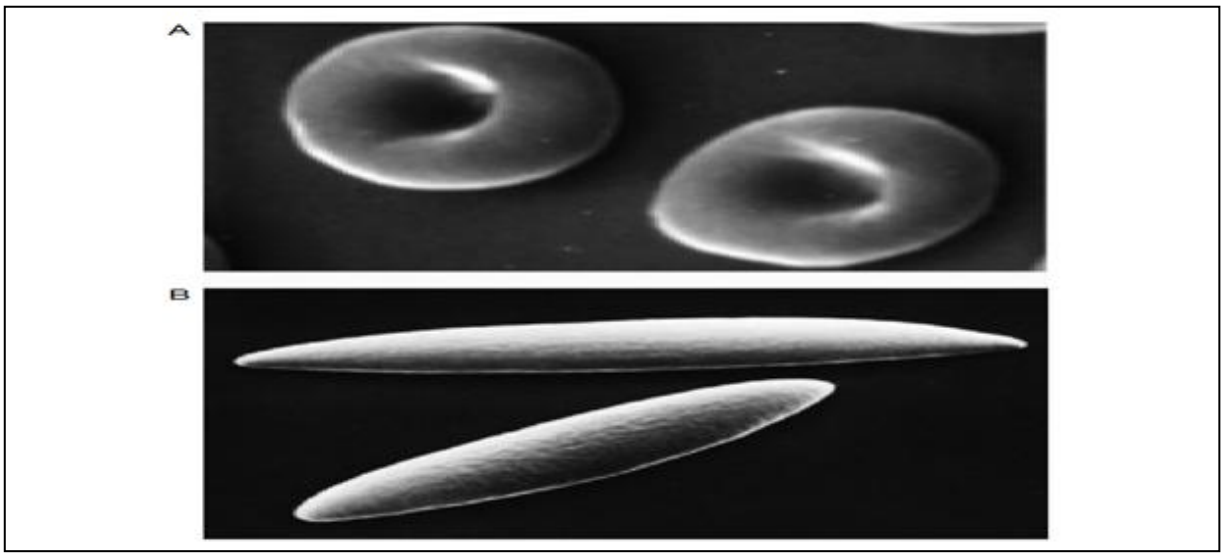

Figure 2.10. Scanning electron micrographic representations of erythrocytes.Erythrocytes are some of the smallest cells in the human body. Mature cells reach a width of 2µm and lengths of between 7-8µm. Cells have biconcave shape illustrated in Figure (A) from a top view and a cigar shape when viewing the cells from the side as in Figure (B) (Mohandas & Gallagher, 2008).

2.7. HIV-1 associated anaemia

RBCs contain the oxygen carrier molecule haemoglobin (Hb) which is also a marker of RBC compartment integrity. The integrity of the red cell compartment is also measured by the haematocrit (Hct), or packed cell volume (PCV). Anaemia is defined as either Hb or Hct below the normal level (Hb<13 g/dl and Hct<0.4 L/L) for age and gender (Quintó *et al.*, 2006; Meidani *et al.*, 2012). Anaemia has many different underlying causes such as iron deficiency or vitamin B12 folate deficiencies. In addition, anaemia is commonly found in individuals with diseases associated with chronic immune activation or inflammation, which is termed anaemia of chronic disease (ACD). HIV-1 infected individuals also develop chronic immune activation/inflammation and therefore the development of an associated anaemia is not unexpected and has been well described (Weiss, 2009). Continued immune activation leads to chronic production of several monocyte or neutrophil associated molecules, including

ROS. Unresolved inflammation thus alters the localized milieu (especially within lymphoid tissues) (Geissmann *et al.*, 2010). Anaemia in chronic HIV-1 may be related to unresolved inflammation and excessive ROS leading to RBC death. Based on Hb data in two independent studies it was found that individuals not on HAART treatment (i.e. treatment naïve) had a prevalence of anaemia of approximately 40%, whereas individuals on HAART treatment had a prevalence of 71% (Mildvan *et al.*, 2007; Meidani *et al.*, 2012).

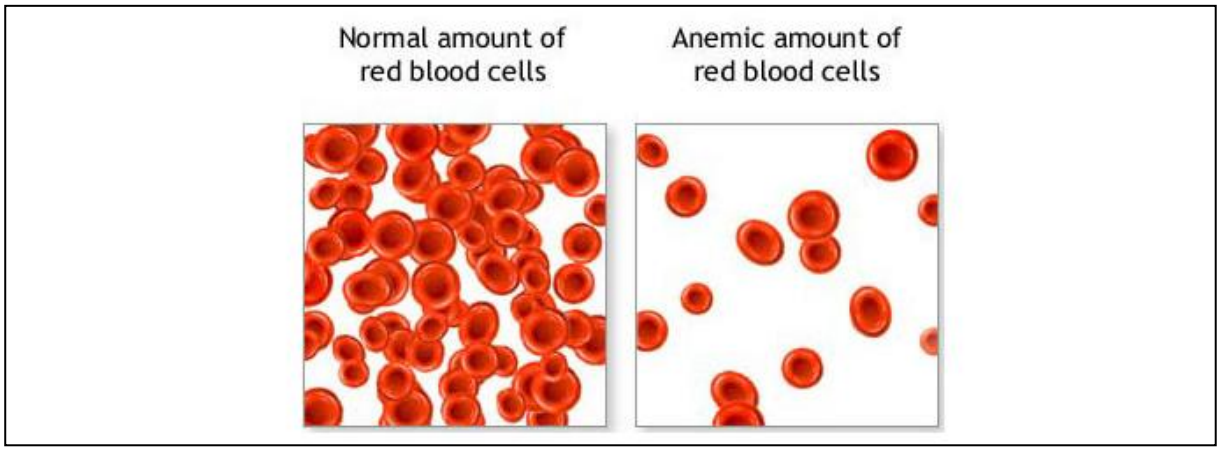

Figure2.11. The blood picture on the left illustrates the amount of RBCs in a healthy individual. The picture on the right illustrates a reduced amount of RBCs of an anaemic individual. http://www.pharmaceutical-networking.com/merck-mk-2578-for-treatment-of-anaemia-in-patients-with-kidney-disease/

Anaemia is a common problem in HIV-1-infection and has many underlying causes (Omoregie *et al.*, 2008). Chronic immune activation/inflammation is a key driving force in the progression to AIDS and is responsible for several complications associated with the infection. Anaemia which is the decrease of Hb (or loss of erythrocytes) can be due to: (1) increased RBC destruction; (2) increased up-take of prematurely aged or damaged RBCs by activated monocytes; and (3) decreased RBC production by the bone marrow (BM) (Ganz, 2006). Chronic inflammation results in both the production of hydrogen peroxide (H_2O_2) by various cells (e.g. neutrophils and macrophages) and the depletion of antioxidants such as glutathione (Fu *et al.*, 2010). Increased levels of ROS are thus the by-product of on-going inflammation and this has an impact on many cellular components, in particular the phospholipid bilayer of cell membranes. RBCs are also affected by ROS resulting in erythroptosis (Agrawal *et al.*, 2007).

Other chronic diseases, such as rheumatoid arthritis, produce a similar chronic inflammatory environment to that found in HIV-1 infection with the production of pro-inflammatory cytokines. IL-6 produced during a condition such as rheumatoid arthritis, inhibits the production of the hematopoietic growth factor erythropoietin (EPO) thus suppressing the

bone marrow production of erythrocytes and contributing to the development of anaemia (Raj, 2009; Steele *et al.*, 2012). During HIV-1 infection IL-6 is also produced thus also resulting in bone marrow suppression of erythrocyte production (Raj, 2009). Other factors may also be involved in contributing to the development of anaemia in these individuals. The iron located in erythrocytes could facilitate the replication of the HIV-1 and depletion of iron and resultant anaemia may be a side-effect of the promotion of cellular infection (Johnson *et al.*, 2012). Enhanced removal of RBCs in HIV-1 infection could also be due to elevated apoptosis or enhanced phagocytosis, or both (Cambos *et al.*, 2011). Ineffective production of RBCs by the bone marrow due to HIV-1-related dysplasia may also be a cause (Meidani *et al.*, 2012). Another mechanism of anaemia induction is the production of antibodies against RBC antigens which then cause autoimmune haemolytic anaemia. These antibody-coated RBCs are more rapidly removed from the system by splenic macrophages (Bain, 1997).

ARV therapy can directly impact on anaemia in both a positive and negative way. In a 2005 study in Nigeria HAART was observed to increase haematocrit and haemoglobin levels in HIV-1 infected individuals suffering from anaemia. HAART consisted of a combination of nevirapine + stavudine + lamivudine (Odunukwe *et al.*, 2005). In a 2008 study, also in Nigeria, it was found that HAART did not rectify anaemia owing to the fact that HAART in this study consisted of nevirapine + stavudine + zidovudine. The use of zidovudine instead of lamivudine has been linked to the development of anaemia. It has been suggested that zidovudine has a toxic effect on the bone marrow cells and could hinder the efficient production of haemoglobin as well as the transcription of the globin gene (Omoregie *et al.*, 2008). Nevirapine is a non-nucleoside reverse transcriptase inhibitor (NNRTI) and the other HAART drugs in this combination are nucleoside analog reverse transcriptase inhibitors (NRTI). It has been reported that HIV-1 patients suffering from anaemia are at a significantly higher risk for reduced survival (Odunukwe *et al.*, 2005). HAART drugs are chosen because they are effective against HIV-1; however, the development of anaemia may be a significant side effect of these drugs.

2.8. Monocytes

RBCs live for a short period of time (see section 2.6.) before they die or apoptose. The damaged/dying/dead cells need to be removed from the circulation. Monocytes have a distinct function of removing damaged/dying/dead cells from the circulation or from tissue. Monocytes are recruited to sites of infection during the innate immune response and are major producers of the pro-inflammatory cytokines tumour necrosis factor-α (TNF-α), interleukin-6 (IL-6) and interleukin-1 (IL-1) (Zimmermann *et al.*, 2010). These cytokines are produced when the monocytes are activated. Activated monocytes (and also macrophages) remove damaged/dying cells such as RBCs in the spleen (Fendel *et al.*, 2007; Swirski *et al.*, 2009). The innate immune functions of monocytes include immune defence in order to

protect the body from foreign invaders by phagocytosing infected cells and by the production of cytokines (Robbins *et al.*, 2010). The adaptive immune functions include differentiation into macrophages or DCs and acting as antigen presenting cells, maintaining homeostasis and also repairing of damaged tissue (Auffray *et al.*, 2009; Ziegler-Heitbrock *et al.*, 2010).

Monocytes make up a relatively small percentage of the human blood. The monocyte population comprises between 3-9% of the total leukocyte population (Ramoji *et al.*, 2012). Monocytes are formed from myeloid precursors derived from the bone marrow (Seidler *et al.*, 2010). Monocytes are found abundantly in the spleen but also circulating in the peripheral blood stream in lower concentrations. The spleen plays a role as a site for storage of monocytes that can be deployed quickly to sites of injury/infection (Swirski *et al.*, 2009). As mentioned above, the monocytes in the spleen also eliminate senescent and dead RBCs from circulation. Monocytes are located in the sub-capsular red pulp of the spleen (Swirski *et al.*, 2009). Monocytes do not live long with a half-life of about three days (Mosig *et al.*, 2009).

Several major subsets of monocytes have been described. The major differentiation is between classical CD14+CD16- monocytes and inflammatory CD14+CD16+^{high} monocytes. In certain schemes an intermediate monocyte population (CD14+CD16+^{low} is included (Mosig *et al.*, 2009; Zimmermann *et al.*, 2010). The differentiation of the two major monocyte subsets by flow cytometry is illustrated in Figure 2.12 and a schematic illustration of the three monocyte subsets in the blood is shown in Figure 2.13. The classical monocyte population makes up approximately 95% of the total monocyte population in healthy individuals with the remaining 5% being inflammatory monocytes (Mosig *et al.*, 2009). During chronic immune activation the inflammatory monocyte population increases significantly (Zhang *et al.*, 2011).

Monocytes have a cell diameter of 18-25µm, they are larger than lymphocytes and typically contain a kidney-shaped nucleus and intermediate granularity. Figure 2.14. shows a monocyte in a normal blood smear. Monocytes produce reactive oxygen species in low concentrations which act as signalling molecules that perform homeostatic functions. These functions include maintaining the cell cycle, metabolism and intercellular signalling transduction pathways (Federico *et al.*, 2007).

When persistent infection and inflammation occurs as in HIV-1 infection, the over production of ROS by monocyte may deplete the available glutathione levels and this impacts on surrounding cells, promoting their death (Federico *et al.*, 2007).

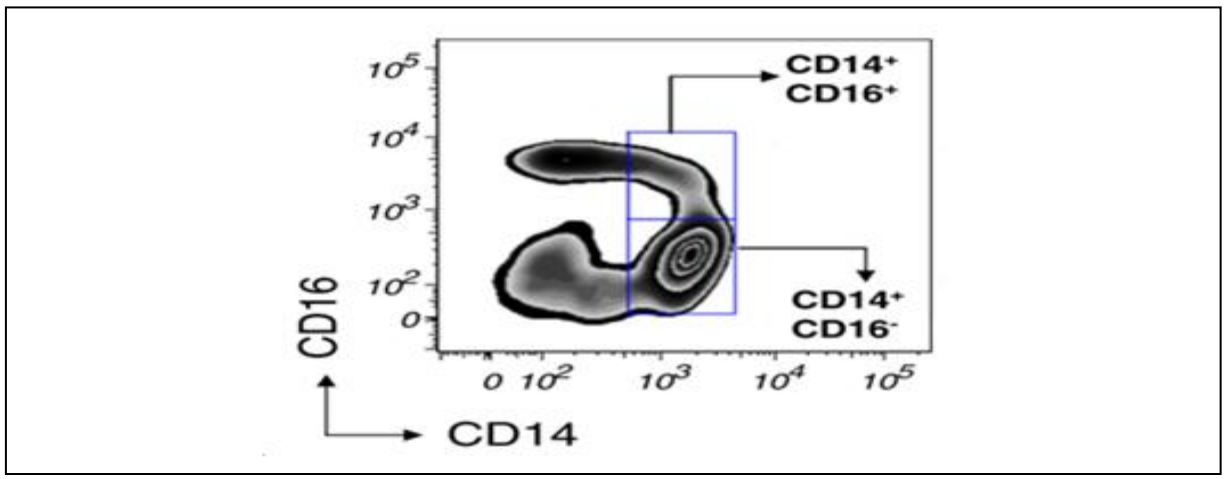

Figure 2.12. The analysis of monocytes by flow cytometry. The monocytes were gated on in a FSC versus SSC dot plot. The density plot on the illustrates the two major subsets of CD14+ monocytes examined in this study (Ansari et al., 2012)

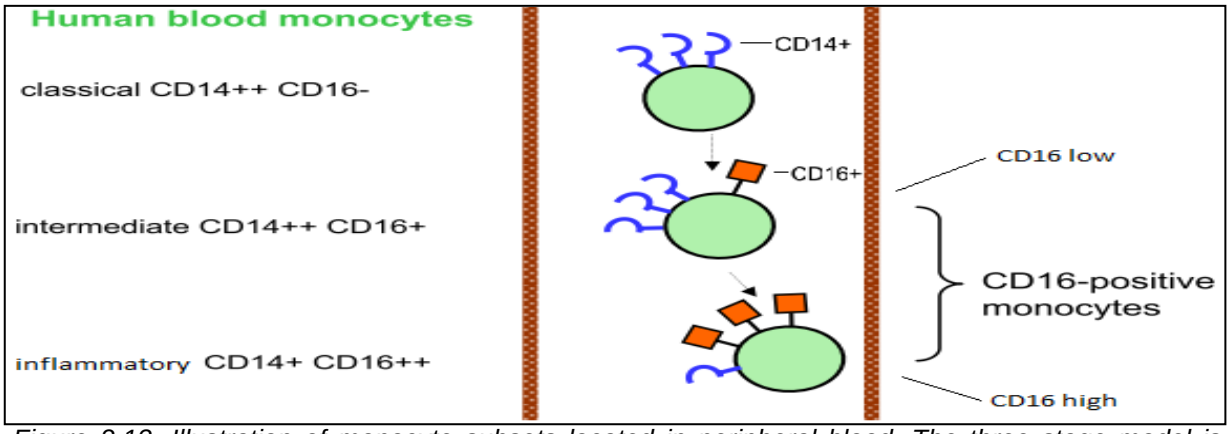

Figure 2.13. Illustration of monocyte subsets located in peripheral blood. The three stage model is schematically illustrated and the defining surface markers are indicated (Ziegler-Heitbrock et al., 2010).

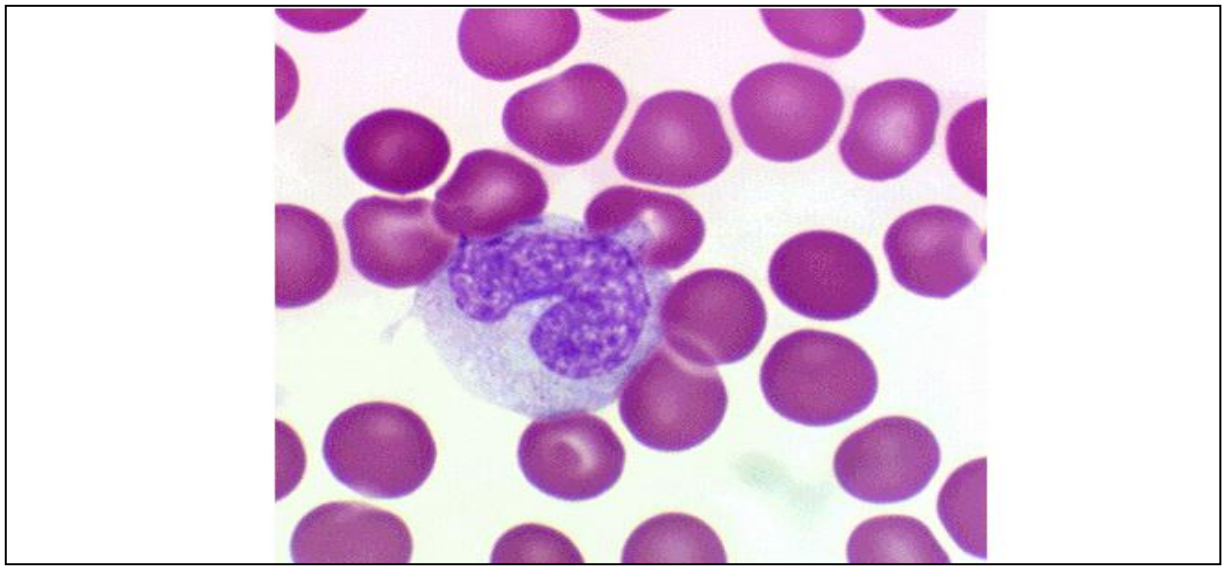

Figure 2.14. Blood smear showing monocyte and erythrocytes. *Monocytes are bigger and complex when compared to erythrocytes. Erythrocytes are between 7-8µm in size compared to the monocyte that is between 18-25µm in size. Monocytes contain a nucleus and granules unlike erythrocytes. http://www.vetmed.vt.edu/education/curriculum/vm8054/labs/lab6/lab6.htm*

2.9 Reactive Oxygen Species (ROS)

Inflammatory cells such as monocytes routinely produce ROS as part of their normal cellular metabolism. Oxygen (O_2) is one of the key elements that humans need to survive and also the essential element of ROS. Oxygen circulates through the body and has various functions. Low to moderate levels of ROS are beneficial to the host. These low/ moderate levels of ROS play physiological roles in various cellular responses and protect the host against infectious agents (Valko *et al.*, 2007). Homeostasis between the beneficial and/or harmful effects of intermediate species is crucial in living organisms (Federico *et al.*, 2007).

The balance between production and removal of ROS is mediated by antioxidants (e.g. superoxide dismutase (SOD), glutathione peroxidise, glutathione-S-transferase and glutathione (GT), etc.) that mop up these destructive molecules (Valko *et al.*, 2007). The imbalance in redox status and the enhanced production of intermediate reactive species progressively consumes the antioxidant defences, leading the cells to develop oxidative stress (as illustrated in Figure 2.15). Cells such as RBCs can respond to the oxidative stress either by enhancing their antioxidant potential (by increasing production of antioxidant molecules) or by activating cytoplasmic caspases that induce programmed cell death (apoptosis), which in the case of RBCs is known as erythroptosis (Herrera *et al.*, 2001)(Bratosin *et al.*, 2009).

Phosphatidylserine (PS) is a phospholipid found on the inner leaflet of all cell membranes (including RBCs). When RBCs are exposed to sufficient levels of oxidative stress the PS will transfer to the outer leaflet of the membrane. It is unknown whether the shift of the PS from

the inner to the outer leaflet is a form of programmed apoptosis or whether the membrane fatty acids are being stimulated by the oxidative stress itself. This transfer of the PS on RBCs is a sign of early apoptosis (erythroptosis) (Berg *et al.*, 2001). The oxidation or peroxidation of plasma membranes and other cellular structures, if unchecked, may culminate in the death of the cell and ultimately, could contribute to disease development. It is on this basis that oxidative stress is increasingly being implicated in the pathogenesis of multiple acute and chronic inflammatory human diseases (Lum *et al.*, 2001)(Lang *et al.*, 2004).

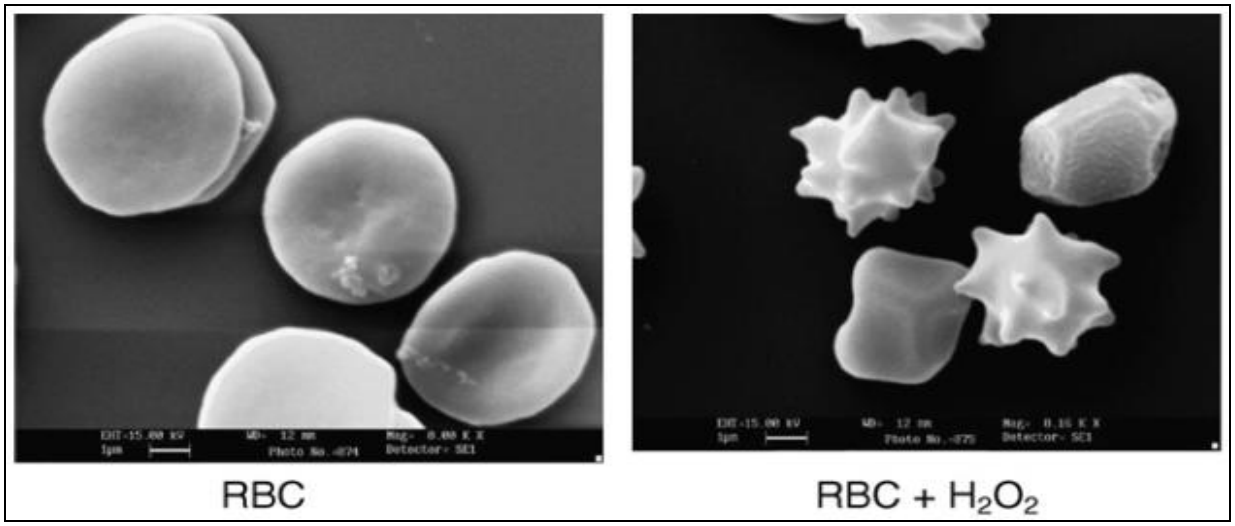

Figure 2.15. Healthy RBCs versus oxidative induced RBCs. The picture on the left illustrates a normal RBC structure. The picture on the right hand side illustrates the RBC deformation due to oxidative stress caused by H_2O_2 stimulation (Ajila et al., 2008).

2.10. Detection of erythroptosis

During chronic conditions such as HIV-1 infection, various cells are damaged. These cells need to be eliminated in order to maintain homeostasis. Apoptotic cells display PS on the external surface of the cell membrane allowing them to be phagocytosed following detection by scavenger receptors on monocytes/macrophages. Apoptosis can be measured by determining the level of binding of annexin V to the exposed PS on damaged cells (Demchenko, 2012).

Annexin V is a molecule that binds specifically to PS on cells membranes in a calcium dependent manner (Yan *et al.*, 2008). Annexin V can be conjugated to a fluorescent marker such as FITC. FITC is excited at a wavelength of 488nm. The annexin V bound to the PS on apoptotic cells can then be measured by flow cytometry as illustrated in Figure 2.16.

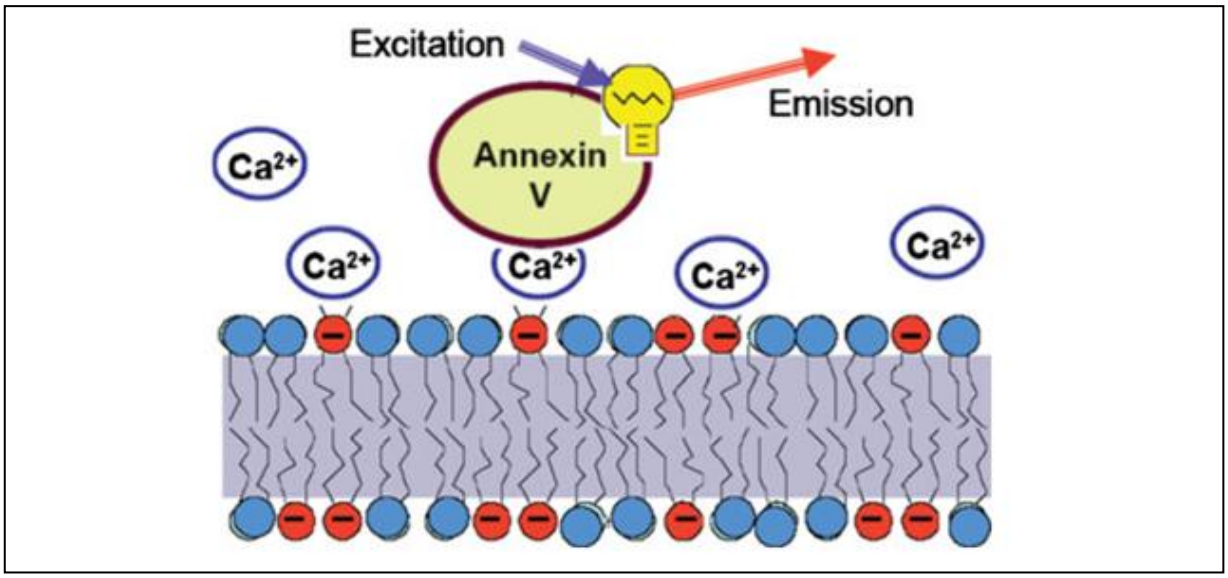

Figure 2. 16. Illustration of PS (circles with negative signs in them) transferring to the outer leaflet of a cell membrane and is a sign of early apoptosis. Annexin V is a calcium dependant antibody that is conjugated to a fluorescent marker binding to the exposed PS and allows for detection by flow cytometry when excited with laser light (Demchenko, 2012).

2.11. Hypothesis

- The study hypothesis was chronic stable HIV-1 infection is accompanied by anaemia (decrease Hb.), due to elevated erythroptosis. The elevated erythroptosis is linked to ROS damage and may be reversible through antioxidant treatment. Finally, increased erythroptosis is linked to changes in monocyte subset distribution, with HIV-1 infected individuals having a predominance of phagocytic pro-inflammatory monocytes.

2.12. Aims of study

To investigate

- The relationship of anaemia with red cell death (erythroptosis)
- Compare Hb, Hct, RCC between HIV infected and uninfected groups
- Measure levels of spontaneous (*ex vivo*) + induced erythroptosis in the two groups
- Whether antioxidant (NAC) can rescue RBCs from erythroptosis in both groups
- To determine relationship between RBC death, Hb and RBC parameters and immune activation status in the two groups
- To assess autologous monocyte uptake of RBCs in the two groups
- Total monocyte count vs. functional response
- To compare classical vs. inflammatory monocyte response to RBCs and measure level of erythroptosis

3. Methodology

3.1. Study Participants

All donors were recruited from Emavundleni, a HIV Counselling, Testing and Prevention (HCT) Clinic, in Crossroads, Cape Town. The prevention clinic employs the national HCT testing algorithm with accredited rapid tests. Inclusion criteria: age >21 years; clinically asymptomatic with CD4 counts >200 cells/µl at initial screen. Not on antiretroviral therapy. Exclusion criteria: Concurrent infections, tuberculosis (TB) or anti-TB therapy. Ethical Considerations: The study was approved by the University of Stellenbosch Ethics committee HREC N07/09/197 and the University of Cape Town REC 417/2006 and performed according to the declaration of Helsinki.

A total of 44 HIV-1 positive (HIV-1) and 33 matched HIV negative (negative control) whole blood samples were collected from the clinic. HIV-1 positive donors' statuses were confirmed with the use of an ELISA rapid HIV+ test. Once HIV status was confirmed, donors were bled and CD4 count determined. Original CD4 determinations were performed by the clinic associated laboratory one month prior to blood collection for the current study. Donors with original absolute CD4 counts of above 200 cells/µl were included on the study. Donors were not on any antiretroviral (ARV) treatment (i.e. treatment naive). HIV-1 positive donors were re-assessed for CD4 count on the day of blood donation. There were 6 HIV-1 positive individuals who had a CD4 count <200 cells/µl when CD4 counts were measured on day of blood collection (i.e. 1 month after initial CD4 count). These 6 HIV-1 individuals were included within the study. All patients were also asymptomatic for other diseases with no underlying infections or conditions at the time of blood extraction. Donors were properly informed that their blood would be used for research purposes in the study and they signed consent forms presented to them in their mother tongue. Demographics of study participants are presented in Table 4.1 in the results section in chapter 4.

3.2. Whole blood collection and Transport

Whole blood was collected by venipuncture by a qualified nursing sister at the walk-in clinic. Both ethylenediaminetetraacetic acid (EDTA) 5ml and Sodium Heparin 10ml vacutainer tubes (BD Biosciences, San Jose, CA, USA) were used. A total of 15ml whole blood was collected from each donor. Blood tubes were transported to the laboratory by the clinic courier service. Bloods reached the laboratory within 3-4 hours of collection. At arrival at the laboratory the specimens were immediately processed.

3.3. Viral Load

2.5ml EDTA blood was aliquoted and transferred to a sterile 5ml BD Falcon tube (BD Biosciences, San Jose, CA, USA) and centrifuged (Heraeus Megafuge 2.0 R, Germany) for 10 minutes at 375xg at 20ºC (room temperature). Plasma (500µl) was aliquoted into a pre-labelled sterile Eppendorf tube. Samples were then delivered by hand to the routine viral load testing laboratory in the Division of Medical Virology (NHLS, Tygerberg, Cape Town, South Africa) and samples were tested within 8 hours of blood collection. The Abbott RealTime HIV-1 viral load assay was performed on samples. This test has a detection range of 40 to 10,000,000 copies/mL. HIV RNA levels in the plasma were quantitated by nucleic acid amplification. The assay is validated against a viral standard from the Virology Quality Assurance (VQA) Laboratory of the AIDS Clinic Trail Group and accredited by the World Health Organization (WHO). The assay is also South African National Accreditation System (SANAS) approved. SOP number HAE1455.

3.4. CD4 Count

EDTA blood (300µl) was aliquoted from the 5ml EDTA tube for CD4 count measurement. The BD MultiTEST™ CD3 FITC/ CD8 PE/ CD45 PerCP/ CD4 APC Reagent (BD Biosciences, San Jose, CA, USA) and TruCOUNT tubes (BD Biosciences, San Jose, CA, USA) were used for CD4 count determination. TruCOUNT tubes were labelled with study participant numbers. MultiTEST reagent (antibody mix) (20µl) was added into the bottom of the TruCOUNT tube containing a steel retainer, above the bead pellet. Pre-aliquoted EDTA blood (50µl) was then added to the tube. The tubes were vortexed and left to incubate for 15 minutes at room temperature in a dark area. After incubation, 450µl of Fluorescent Activated Cell Sorter (FACS) lysing solution (BD Biosciences) was added, vortexed and again left to incubate for another 15 minutes at room temperature. Analysis of the sample was performed on a flow cytometer (Becton Dickinson FACSCalibur with MultiSET™ software). The CD4 counts were validated to control samples (LymphoSure) purchased from Synexa Life Sciences (Cape Town, SA).This method is the standard CD4 standard operating procedure (SOP number VIRO 00016.5) used in the Division of Medical Virology, which has been accredited by SANAS.

3.5. Full Blood Counts

Full blood count (FBC) measurements were performed in the Haematology Division of the National Health Laboratories Services (NHLS Tygerberg Hospital, Cape Town, SA). EDTA blood samples were run through the Siemens ADVIA 2120 system, which uses cytochemistry and flow technology. FBC results and white blood cell (WBC) differential

parameters were collected from the machine printout. These measurements are also SANAS accredited. The FBC parameters relevant to this study included RBC count, Hb levels, haematocrit (HCT) levels and monocyte count and percentages (of total leukocytes) (SOP number GPL0866).

3.6 CD38 expression on CD8 T lymphocytes labelling and gating

3.6.1. CD8 T cell labelling

CD38 expression on CD8 T cells was used as a marker for immune activation in this study (see Chapter 2 section 2.5.). Whole blood (50µl) from the 10ml heparin tube was aliquoted into a sterile 5ml BD Falcon tube (BD Biosciences, San Jose, CA, USA). An antibody cocktail was prepared containing the following antibodies (based on recommended volumes): 10µl CD3 (FITC), 10µl CD8 (PerCP) and 5µl CD38 (APC). All antibodies in this procedure were purchased from Becton Dickinson (BD Biosciences, San Jose, CA, USA). The antibody cocktail (25µl) was then added to each sample. Samples were incubated for 20 minutes in a dark area at room temperature. After incubation, 500µl lysing solution (BD Biosciences, San Jose, CA, USA) was added to each tube. Tubes were placed in a dark area and left to incubate for 15 minutes at room temperature. After incubation cells were washed by adding 300µl staining buffer to each tube. Samples were centrifuged for 10 minutes at 300xg at 20°C. Supernatant was removed and discarded. Pellet was re-suspended by adding 500µl staining buffer and was vortexed. Samples were analysed on the same day by flow cytometry (BD FACS-calibur, BD Biosciences, San Jose, CA, USA).

3.6.2. CD8 T cell gating and analysis

The total lymphocyte population in a FSC versus SSC dot plot was gated (G1=R1). Fifty thousand G1 gated events were gathered during the CD38/CD8 T lymphocyte acquisition. A second gate was created (G2=R2) on the CD3 positive population in a SSC versus CD3 plot generated from the G1 gated population. Expression of CD8 and CD38 (the activation/inflammation marker) were then measured in a two colour “quad stat” plot of CD8 versus CD38 (Figure 3.3.).

3.7. *In vitro* RBC preparation, stimulation with oxidative stressors, annexin V labelling and analysis

3.7.1. Stimulation with oxidative buffers

Sodium heparinised blood (10µl) was pipetted into 5ml BD Falcon tubes (BD Biosciences, San Jose, CA, USA) and was used to carry out each stimulation. Donor samples (13

negatives and 14 positives) were stimulated with 2 different oxidative stressors for varying time periods. The effects of the different oxidative stressors were evaluated. Un-stimulated cells (negative control) were incubated with Dulbecco's Phosphate Buffered Saline (DPBS, contains no Ca^{2+} or Mg^{2+}, Gibco, Invitrogen Corporation, UK), while test samples were exposed to either hydrogen peroxide (H_2O_2) (final concentration of 5mM) or an ascorbic acid oxidative buffer (DPBS + 5mM sodium-L-ascorbate (Sigma-Aldrich, UK) + 0.4 mM copper (II) sulphates (Sigma-Aldrich, UK)) (Cambos *et al.*, 2011). H_2O_2 or ascorbic acid oxidative buffer (AAOB) (10µl) was added to each tube containing 10µl blood as previously optimized in our laboratory (S. Loots, BSc Honours thesis, unpublished). Samples stimulated with 5mM H_2O_2, were incubated for 1 hour at 37ºC at 5% CO_2. Oxidative buffer stimulations were carried out for three different time periods (30 minutes, 1 hour to 2 hours) at 37ºC at 5% CO_2.

After incubation, RBCs were washed by adding 500µl 1x annexin V binding buffer (ABB) (Biolegend) to each tube and centrifuged at 300xg for 5 minutes at room temperature. Supernatant was carefully removed without disturbing the pellet and supernatant was discarded. Cells were then stained with 2.5µl annexin V (FITC) (eBioscience, San Diego, CA) as recommended by manufacturer (see section 3.10). AAOB stimulation was discontinued after comparison of 27 samples (13 controls and 14 positive samples) as the level of red cell apoptosis was not significantly different to that induced by H_2O_2. Including the 27 samples stimulated with either H_2O_2 or AAOB an additional 50 samples were stimulated with H_2O_2 alone after discontinuation of AAOB.

3.7.2. Impact of the anti-oxidant NAC

The impact of the antioxidant N-acetyl cysteine (NAC) on H_2O_2-induced stress was evaluated. Blood was incubated in the presence or absence (control) of various concentrations (2.5mM, 5mM and 10mM) of NAC (Sigma-Aldrich, UK) during stimulation with 5mM H_2O_2 as described above in section 3.7.1. NAC was added to cells in 48 samples (20 controls and 28 positive) with the three different concentrations of NAC indicated above. The NAC was added 30 seconds prior to H_2O_2 stimulation and then throughout the stimulation period. The same washing, staining procedures as previously described in section 3.7.1. and analysis procedures as described in section 3.13 were followed.

3.8. RBC purification, CFSE labelling, stimulation and measuring of up-take by purified monocytes

3.8.1. Purification of RBCs from whole blood using Peripheral Blood Mononuclear Cell (PBMC) extraction method

Whole blood (1ml) was aliquoted from a 10ml Sodium Heparin vacutainer tube (BD Biosciences, San Jose, CA, USA) and pipetted into a 15ml BD Falcon tube (BD Biosciences, San Jose, CA, USA) and diluted with 9ml DPBS. The 10ml Sodium Heparin tube containing the remaining 9ml whole blood was stored overnight at 4ºC in a refrigerator (K.I.C., South Africa) prior to monocyte purification as described in section 3.9. Initially 20ml Histopaque-Ficoll® (Sigma-Aldrich, UK) was added to a 50ml Leucosep tube (BD Biosciences, San Jose, CA, USA) and centrifuged for 1 minute at 375xg at room temperature to ensure the Histopaque-Ficoll® was gathered underneath the frit. The 10ml diluted blood prepared above was added to upper level of the 50ml Leucosep tube (BD Biosciences, San Jose, CA, USA) and centrifuged for 10 minutes at 300xg at room temperature. Plasma was extracted and discarded with the use of a bulb pipette (BD Biosciences, San Jose, CA, USA). RBCs were removed from the bottom of the tube and transferred to a 5ml BD Falcon tube (BD Biosciences, San Jose, CA, USA). 1ml RPMI + 5% heat inactivated Fetal Bovine Serum (hiFBS) (PAA: The cell culture company, Piscataway, NJ, USA) was added to the tube. Tubes were placed overnight in an incubator (NUAIRE™, US AUTOFLOW CO_2 Water-Jacketed Incubator) at 37ºC and 5% CO_2 concentration.

3.8.2. RBC preparation including CFSE staining of RBCs and stimulation for phagocytosis

Monocyte uptake of un-stimulated and H_2O_2-stressed RBCs was then investigated. RBCs were stained with 2.5mM Carboxyfluoresceinsuccinimidyl ester (CFSE, Invitrogen, CA, USA) prior to oxidative stress induction. Before stimulation with H_2O_2, purified RBCs were stained with the intracellular stain CFSE according to methods of Cambos *et al.*, 2011. 200µl RBCs were pipetted into a 5ml BD Falcon tube and 200µl CFSE with a 2.5mM final concentration was added to the tube. Tube received a quick vortex to ensure proper mixing of cells and intracellular stain. The tube was then placed in a dark room and left to incubate for 15 minutes at room temperature. After incubation stained RBCs were washed by adding 1ml Sep medium and centrifuged for 5 minutes at 300xg at room temperature. Supernatant was extracted and discarded and stained RBCs were removed and pipetted to sterile 5ml BD Falcon tube.

Stained cells were washed by adding 500µl DPBS to each tube and then centrifuged at 300xg for 5 minutes. Stained RBCs (7µl) were aliquoted and pipetted into adjusted volume of

DPBS in order to have a total of 250 000 cells and used as is for the un-stimulated RBC control experiments. The remaining RBCs were stimulated with H_2O_2 as previously described above see section 3.7.1. Stimulated cells were washed by adding 500µl DPBS to each tube and centrifuged at 300xg for 5 minutes at room temperature to ensure no further stimulation could take place. After washing, 7µl of stimulated RBCs were aliquoted and transferred to the same adjusted volume of DPBS as the un-stimulated to ensure the stimulated RBC dilution had the same concentration. These stained and pre-stimulated RBCs were added to purified monocytes obtained from the same donors (see section 3.9. below).

3.9. Monocyte purification using a 2 step (enrichment plus positive selection) procedure

3.9.1. Enrichment of monocytes by negative selection (RosetteSep).

An illustration of this procedure is provided in figure 3.1. A. The 10ml Sodium Heparin tube containing the 9ml donor blood from section 3.8.1.was mixed before it was centrifuged for 10 minutes at 375xg at room temperature. Plasma was discarded and 4ml of the blood was aliquoted to a 15ml BD Falcon tube (BD Biosciences, San Jose, CA, USA). RosetteSep® Human Monocyte Enrichment Cocktail (STEMCELL Technologies, North America) (200µl) was added and mixed with the 4ml whole blood and left to incubate for 20 minutes at room temperature. RosetteSep® Human Monocyte Enrichment Cocktail enriches the monocyte fraction by removing cells expressing CD2, CD3, CD8, CD19, CD56, CD66b, CD123 and glycophorin A (i.e. T and B lymphocytes, NK cells, neutrophils, RBCs, granulocytes and dendritic cells (DCs)), thus leaving an enriched monocyte population. 15ml Histopaque-Ficoll® (Sigma-Aldrich, UK) was pipetted into a sterile 50ml BD Falcon tube (BD Biosciences, San Jose, CA, USA). The tube containing the 4ml blood was diluted with an additional 6ml medium consisting of DPBS + 2% heat inactivated (hi) FBS + 1mM EDTA referred to as Sep medium from now on.

The 10ml diluted blood mentioned above containing the enriched antibody cocktail was extracted and carefully added to the tube containing the Histopaque-Ficoll® (Sigma-Aldrich, UK). Tubes were centrifuged at 375xg for 30 minutes at room temperature. The interface monolayer containing the monocyte enriched layer (7.5ml) was carefully removed and transferred to a sterile 50ml BD Falcon tube (BD Biosciences, San Jose, CA, USA). Sep medium (27.5ml) was added to the 50ml BD Falcon tube to give a final volume of 35ml. The tube containing the enriched monocytes underwent a wash step with centrifugation for 10 minutes at 375xg at room temperature. The supernatant was discarded and the pellet was gently re-suspended in 4ml DPBS. 50µl cell suspension was aliquoted and stained with 50 µl

Turks staining solution (0.02% crystal violet, 7% glacial acetic acid in water)(Sigma-Aldrich, UK) and cells were counted under a light microscope (Nikon, Eclipse E200, Japan). The 4ml cell suspension was centrifuged for 10 minutes at 375xg at room temperature. The monocyte purity (see section 3.11.2) obtained was <60% using this method alone, therefore an additional positive selection procedure was also used, as discussed below.

3.9.2. Purification of monocytes from the enriched monocyte fraction by positive selection

An illustration of this procedure is provided in Figure 3.1. B. The enriched monocytes isolated during the RosetteSep® monocyte procedure (see section 3.9.1.) did not generate a sufficiently pure cell population therefore an additional purification technique was applied. After monocyte enrichment (see section 3.9.1.) the tube was centrifuged to form a cell pellet at the bottom of the tube containing the enriched monocytes. The supernatant was discarded. Sep medium (100µl) was added to the tube and pipetted up and down slowly to re-suspend the pellet. EasySep® Human CD14+ positive selection cocktail (STEMCELL Technologies, USA) (10µl) was added to the tubes as specified by the manufacturer. Tubes were incubated at room temperature for 15 minutes. After incubation, 5µl of magnetic-nanoparticles (STEMCELL Technologies, USA) were then added and mixed as instructed by manufacturer. Tubes were inserted into specialized immunomagnets (STEMCELL Technologies, USA) made for use in this technique. Magnets were placed on a flat surface for 5 minutes. Magnets still containing tubes were inverted after 5 minutes to discard unattached cells (i.e. non- selected cells). Tubes were removed from the magnets and 2.5ml Sep medium was added in order to re-suspend cells adhering to the sides of the tube. Tubes were placed back into the magnets and the process repeated another 4 times ensuring no unwanted cells remained. After the fifth and final wash the tubes were removed from the magnets and cells were gently washed from the side of the tubes by adding 1ml Sep medium. The monocyte purity obtained after this method routinely exceeded 75%.

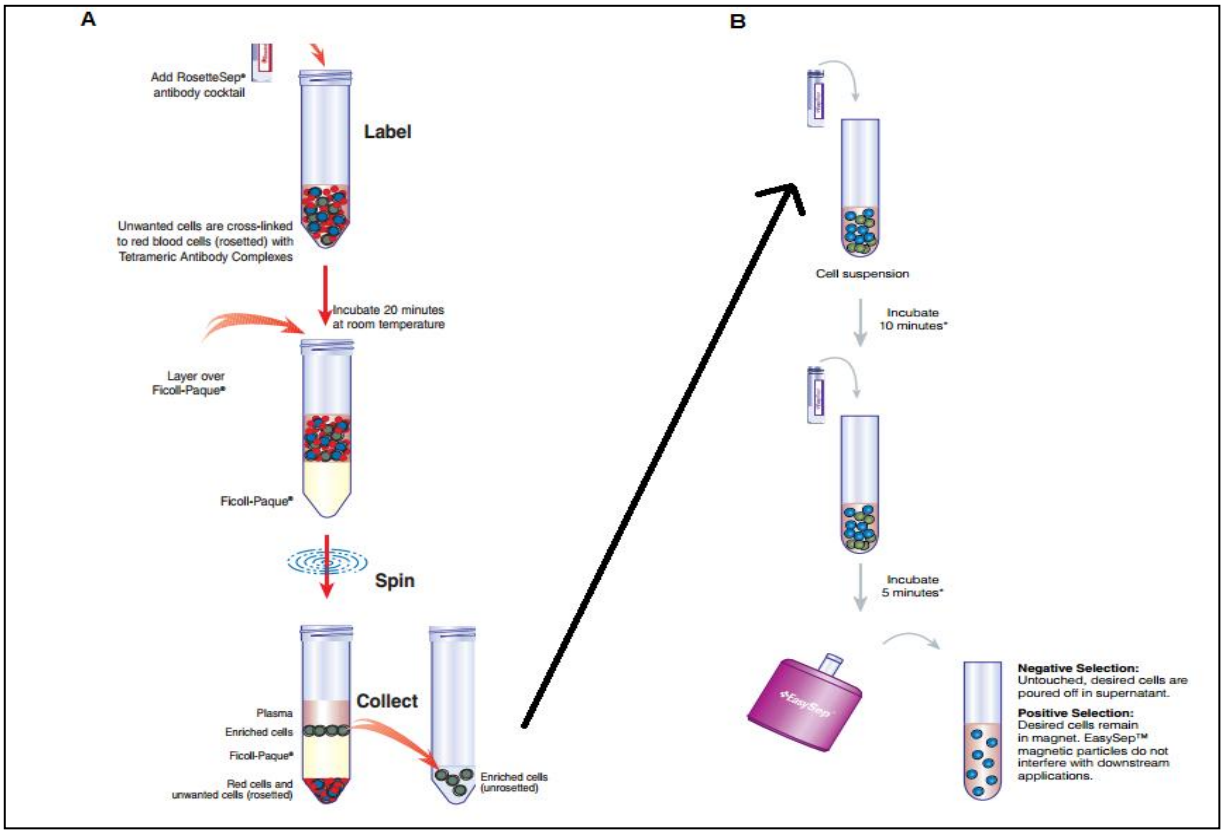

Figure 3.1. The two different methods used to obtain the highest possible monocyte purity from whole blood.The method on the left hand (A) is the enrichment of monocytes by negative selection (RosetteSep). The method on the right (B) is the purification of monocytes by positive selection following the enrichment step.

3.10. Flow cytometry antibody cocktail preparation

Antibody cocktails were prepared for (a) RBC apoptosis analysis (b) measuring monocyte purity (c) measuring phagocytosis of RBCs by monocytes and (d) measuring activation of cytotoxic T lymphocytes as a general marker of immune activation. Manufacturer, fluorochrome, clone and isotype details are shown in Table 3.1. All antibodies were kept in a 4°C fridge (K.I.C., model, South Africa) and were placed on ice when in use. Cocktail 1 for RBC apoptosis analysis consisted of four markers: CD45 PerCP (leukocyte marker), CD235a APC (Glycophorin A; RBC marker), CD41a PE (platelet marker) and annexin V FITC (phosphatydilserine marker). Cocktail 2 measuring monocyte purity consisted of four markers: CD45 FITC (leukocyte marker), CD3 PE (T lymphocyte marker), CD16 PerCP and CD14 APC (monocyte/ macrophage markers). Cocktail 3 measuring CFSE stained RBC phagocytosed by monocytes consisted of two markers CD14 APC (monocyte marker) and CD16 PerCP (inflammatory monocyte/macrophage marker). Cocktail 4 measuring the activation of cytotoxic T lymphocytes consisted of three markers CD8 PerCP (lymphocyte marker), CD3 FITC (lymphocyte marker), and CD38 APC (activation marker). Staining procedures are explained in section 3.11.

RBCs were stained with cocktail 1 after stimulation of cells (see section 3.10.). In phagocytosis experiments RBCs were stained with CFSE before stimulation (see section 3.8.2.). Monocytes were stained with cocktail 2 to measure the purity of monocytes isolated. CFSE stained RBCs were added to the monocyte stained with cocktail 3 to measure phagocytosis of dead/dying RBCs by monocytes.

Antibody titrations were performed to determine the optimal volume of each monoclonal antibody required for this study. The final titrated volumes of individual antibodies are indicated in Table 3.1. The intracellular stain (CFSE) was diluted with 2ml PBS to obtain a final concentration of 5mM.

Table 3.1. Antibodies used in this study.

Cocktails	Antibodie	Fluorochrome	Manufacturer	Clone	Type	Host	Final titration volume (µl)
Cocktail 1 RBCs	CD45	PerCP	BioLegend	HI30	IgG1	Mouse	2.5
	CD235a	APC	eBiosciences	HIR2/GA-R2	IgG2b	Mouse	2
	CD41a	PE	eBiosciences	HIP8	IgG1	Mouse	2.5
	Annexin V	FITC	eBiosciences	N/A	N/A	N/A	2.5
Cocktail 2 Monocyte purity	CD45	FITC	BioLegend	HI30	IgG1	Mouse	3
	CD14	APC	BioLegend	M5E2	IgG2a	Mouse	4
	CD16	PerCP	BioLegend	3G8	IgG1	Mouse	4
	CD3	PE	BioLegend	UCHT1	IgG1	Mouse	3.5
Cocktail 3 Monocyte phagocytosis	CD14	APC	BioLegend	M5E2	IgG2a	Mouse	4
	CD16	PerCP	BioLegend	3G8	IgG1	Mouse	4
Cocktail 4 Immune activation	CD3	FITC	BD Biosciences	UCHT1	IgG1	Mouse	10
	CD8	PerCP	BD Biosciences	SK1	IgG1	Mouse	10
	CD38	APC	BD Biosciences	HB7	IgG1	Mouse	5

PerCP = Peridinin chlorophyll protein; APC = Allophycocyanin; PE = Phycoerythrin; FITC = Fluorescein isothiocyanate

3.11. Staining Protocol

3.11.1. RBC staining with cocktail 1 (CD41a, CD45, CD235a and annexin V) to measure RBC apoptosis

Antibodies were placed in a dark area on ice prior to staining procedure. RBCs were stained in 5ml BD Falcon tubes. After H_2O_2 stimulation, 10µl whole blood was washed. ABB (500µl) was added to tubes and centrifuged at 300xg for 5 minutes at room temperature. This washing step removed any unwanted H_2O_2 left in the tube and also provided calcium to the cells for annexin V antibody binding. Supernatant was removed and discarded. Both stimulated/un-stimulated whole blood was stained using cocktail 1: (see Table 1. section 3.10.). Samples were incubated in the dark for 15 minutes at room temperature. After incubation, stained samples underwent another wash step, adding 500µl PBS and were centrifuged at 300xg for 5 minutes at room temperature to ensure that no unbound antibodies remained. Supernatant was removed and discarded. 500µl Staining buffer (0.4% Heat-inactivated Fetal Bovine Serum (Gibco, Invitrogen Corporation, UK) in PBS) was added to tubes followed by a quick vortex. Tubes were stored in the dark until acquisition on the flow cytometer.

3.11.2. Staining of monocytes with cocktail 2 (CD45, CD3, CD14 and CD16) to measure purity and subset distribution

Purified monocytes were stained with Turks solution (see section 3.9.1.) and counted under a light microscope in order to calculate how many cells were obtained within 4ml. Tubes containing purified monocytes were centrifuged for 15 minutes at 375xg at room temperature. Supernatant was discarded and pellet was re-suspended in 1ml PBS. The number of cells was then adjusted to $1X10^5$ cells/ml. The tube containing the $1X10^5$ cells/ml monocytes was stained using cocktail 2 (see Table 1. section 3.10.). Tubes were incubated for 15 minutes in a dark room at room temperature. 1ml Sep medium was added to tubes and tubes were centrifuged for 15 minutes at 375g at room temperature. Supernatant was removed and discarded and pellet re-suspended in 1ml Sep medium.

3.11.3. Staining of monocytes with cocktail 3 (CD14 and CD16) to measure phagocytosis of CFSE labelled RBCs

Purified monocytes were counted under a light microscope. Tubes containing purified monocytes were again centrifuged for 15 minutes at 375xg at room temperature. Supernatant was discarded and pellet was gently re-suspended in 1ml PBS. The number of cells/ml could then be adjusted to the volume $1X10^5$ cells/ml. The adjusted volume was then

aliquoted and transferred to a sterile 5 ml BD Falcon tube. The tube containing the $1X10^5$ monocytes was stained using cocktail 3 (see Table 1. section 3.10.). Tubes were incubated for 15 minutes in a dark room at room temperature. 1ml Sep medium was added to tubes and tubes were centrifuged for 15 minutes at 375xg at room temperature. Supernatant was removed and discarded and pellet re-suspended in 1ml Sep medium prior to adding RBCs.

3.11.4. Evaluating monocyte uptake of RBCs (erythrophagocytosis)

Pre-stained monocytes and CFSE stained RBCs were added together in various monocyte:RBC ratios (1:25, 1:50, 1:100). After monocytes were counted under a light microscope and RBC count was obtained from FBC data, cell numbers were adjusted in order to obtain the different ratios of monocyte to RBCs. One set of tubes comprising of monocytes with un-stimulated RBCs and the second set contained the stimulated (H_2O_2 treated) RBCs. Tubes were incubated for 1 hour at 37°C at 5% CO_2 concentration. After incubation period the non-phagocytosed RBCs were lysed by adding 1ml 1X FACS lysing solution (BD Biosciences, San Jose, CA, USA) and left at room temperature for 10 minutes. Tubes were centrifuged for 15 minutes at 375xg at room temperature and supernatant was discarded and the pellet was again re-suspended with 1ml FACS lysing solution and left at room temperature for 10 minutes. Tubes were centrifuged for a second time for 15 minutes at 375xg at room temperature and supernatant was discarded. Pellet was re-suspended with 300µl staining buffer and tubes were vortexed. Tubes were stored in a dark place to ensure no antibody denaturation occurred until acquisition on the flow cytometer.

3.12. Flow Cytometry

Data was acquired and analysed on a Becton Dickinson FACSCalibur flow cytometer (BD Biosciences, San Jose, CA, USA). The CellQuest™ software (BD Biosciences, San Jose, CA, USA) was used during acquisition/analysis stages of the study. Fluorescence Minus One (FMO) analysis was performed at the initiation phase of flow cytometric analysis in order to ensure correct placement of quadrant stats and precise delineation of the positive versus negative marker expression.

3.12.1 Analysis of RBC apoptosis in presence/absence of anti-oxidant (NAC)

Un-stimulated and H_2O_2 stimulated RBCs treated with or without NAC were assessed. For data acquisition on RBCs, using FSC height versus SSC height, 100 000 gated events were collected. RBCs express CD235a (glycophorin a) and the gating strategy was designed around the expression of this key marker. Using FSC height versus SSC height, the RBC population could be amplified and clearly observed and were gated (G1=R1) as illustrated

figure 3.2 A. Cells positively expressing the CD235a (RBC marker) in a SSC versus CD235a dot plot were then also gated (G2=R2). Other key markers CD41a (platelet specific) and CD45 (white blood cell specific) were assessed in order to ensure leukocytes plus platelets were excluded. The dot plots that followed illustrating the percentage annexin V expression was expressed as a combination of G1+G2 (i.e. G3=R1+R2). Measurement of erythroptosis (RBC specific death) is illustrated in Figure 3.2.D.

3.12.2. Monocyte purity and subset distribution

A dot plot (CD14 vs. CD16) was constructed to determine monocyte subset distribution. Ten thousand FSC height versus SSC height gated events were gathered during purified monocyte data acquisition. The monocyte subsets on a forward versus side scatter dot plot and were gated (G1=R1). The key markers, CD14 and CD45 were the main focus point for the gating strategy on monocytes. Cells were gated on the CD3 negative CD45 positive events (G2=R2) in a CD3 versus CD45 dot plot. Using G2=R2, the cells fluorescing dual positivity for CD14 versus CD45 were gated (G3=R3). Using G2=R2 the cells fluorescing dual positively for CD14 and CD16 in a CD16 versus CD14 dot plot was gated (G4=R4) illustrated in Figure 3.4. G3+G4 were then used in a histogram to measure CD14 expression and so were used to obtain our percentage purified monocyte population illustrated in figure 3.5.

3.12.3. Monocyte up-take of RBCs (erythrophagocytosis)

Ten thousand FSC height versus SSC height gated events were gathered during functional (i.e. phagocytosis) monocyte acquisition. The monocyte subsets in a FSC height versus SSC height dot plot was gated on (G1=R1). The key markers, CD14 and CD16 (monocyte markers) were the main focus point for the gating strategy on monocytes. CFSE stained RBCs (see section 3.11.3.) were evaluated within the CD14 positive CD16 negative or dual CD14 and CD16 positive monocyte population. Cells fluorescing positively for both CD14 and CD16 or positively for only CD14 and negatively for CD16 were gated (G2=R2) on. The dot plots that followed illustrating the percentage monocytes expression as a combination of G1+G2 (G3=R1+R2).

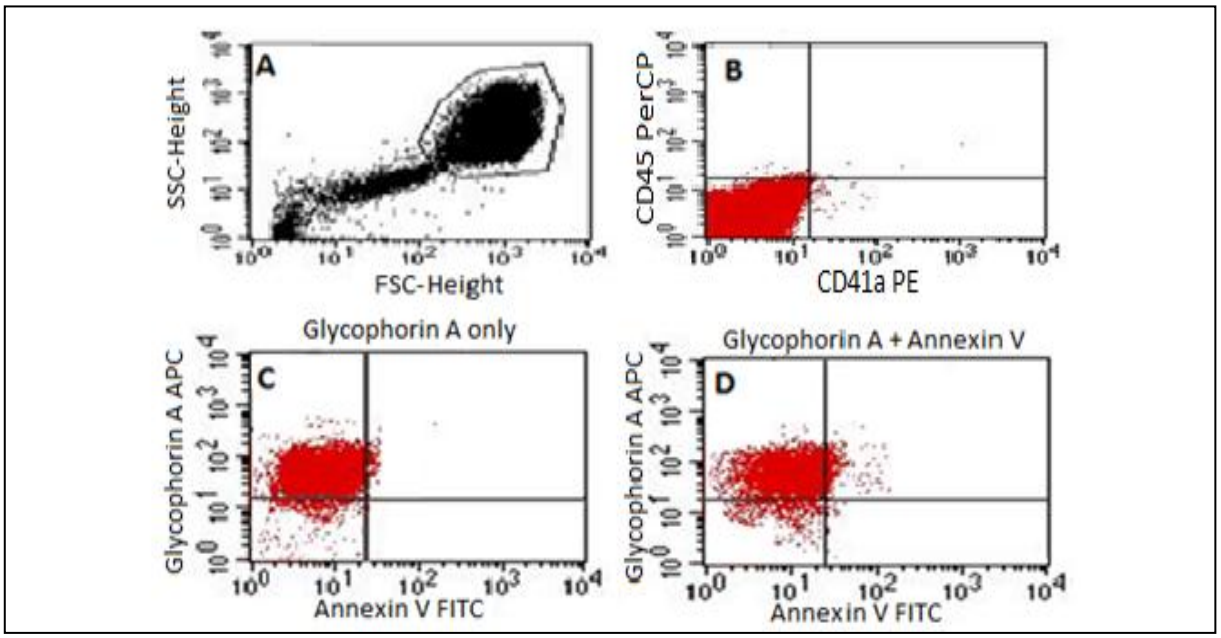

Figure 3.2. RBC gating and measurement of RBC damage. Illustrates the unstained gated RBCs in order to determine the double negative populations. These double negative populations indicated where quadrants were set. (A) Represents the gating of the non-purified erythrocytes in the FSC versus SSC; (B) illustrated that little to no platelets and white blood cells (WBCs) are present in the gated RBC population (C) Illustrates example of baseline annexin V expression and (D) example of annexin V expression on stimulated RBCs

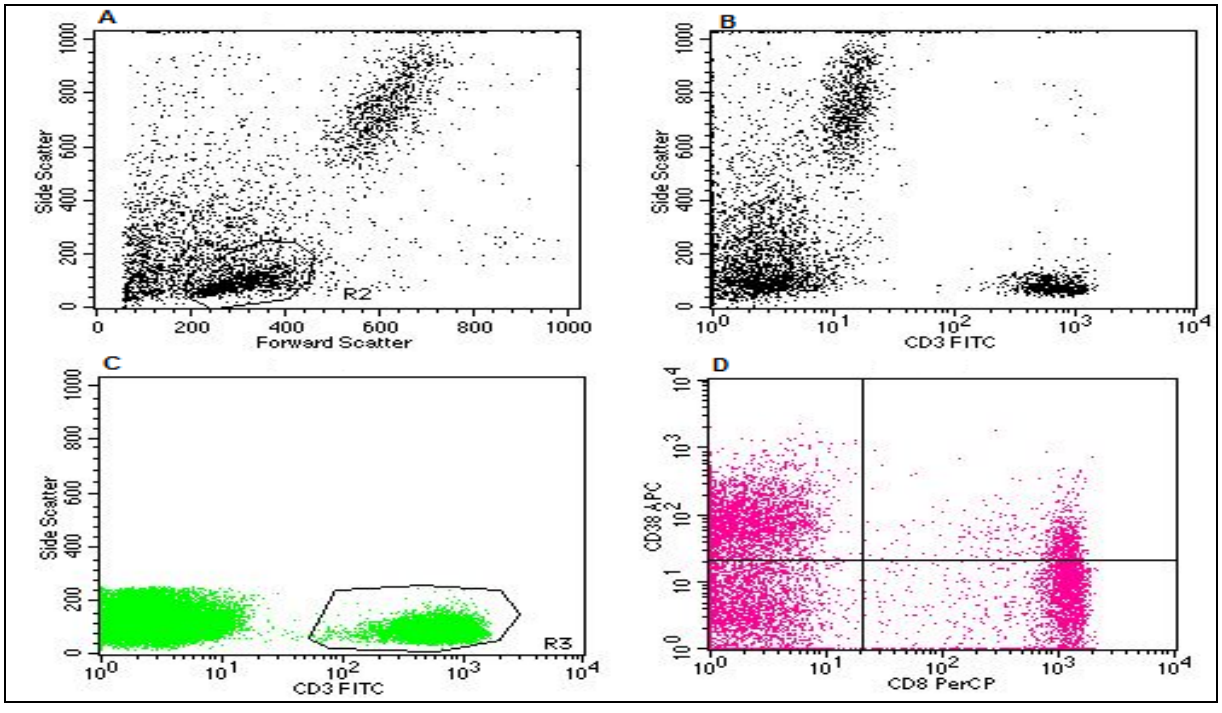

Figure 3.3. Gating strategy and measuring of CD38 expression on CD8+ CTL. Dot plot A illustrates the gating of the lymphocyte population based on forward vs. side scatter. Dot plots B and C illustrate the CD3+ sub-population, when no gate (B) or the lymphocyte gate (C) was defined. The dot plot (D) illustrates the number of CD8+ CTL expressing the CD38+ inflammatory marker (upper right hand quadrant) of the CD3 gated events.

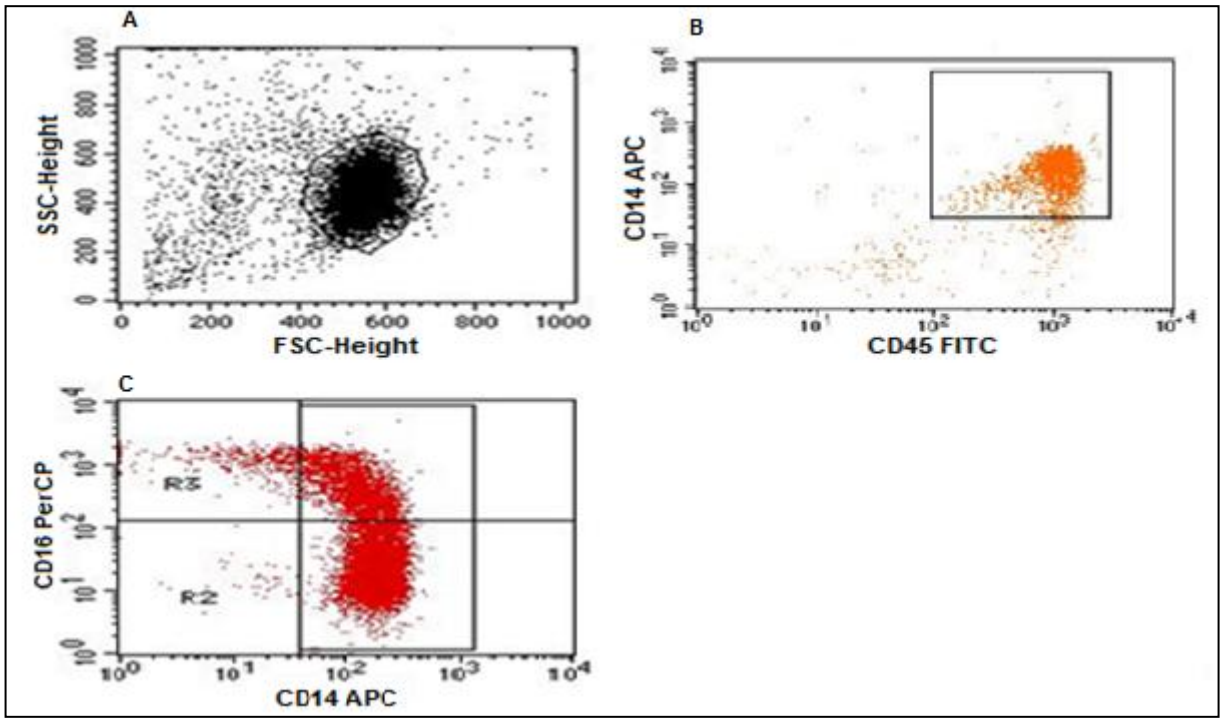

Figure 3.4. Purified monocyte gating and subtype identification. Dot plot A represents the purified monocyte population, showing gating region based on forward versus side scatter. Dot plots B Illustrates the gating on the CD45+CD14+ population to ensure only wanted cells are included Dot plot C illustrates the different monocyte populations we focused on namely the classical CD14+CD16- population located in the bottom right hand corner and the activated CD14+CD16+ population located at the top right hand corner.

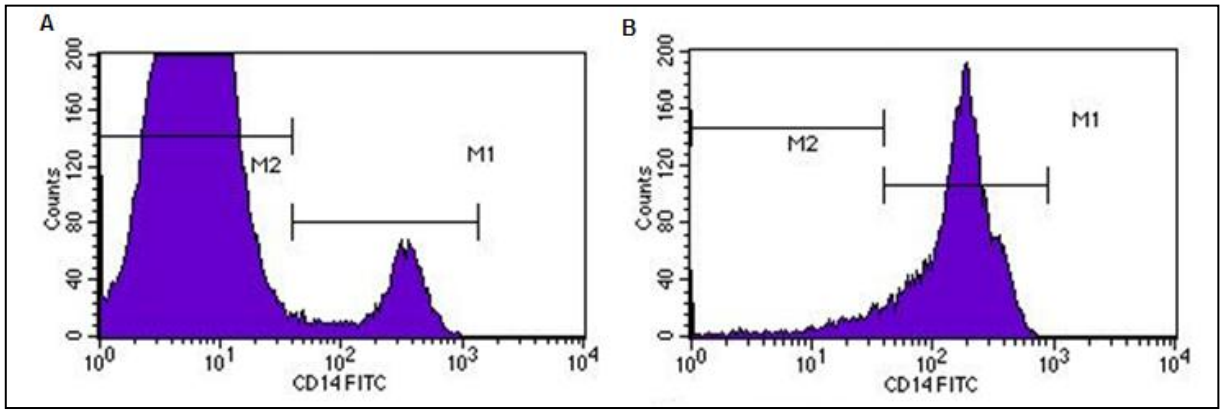

Figure 3.5. Monocyte % (M1) obtained before and after purification. Histogram (A) illustrates the CD14 monocyte population obtained from whole blood (B) the CD14 positive monocyte population after purification in order to determine the monocyte purity (see figure 4.19.).

4. Resuls

4.1. Patient Demographic

A total of 77 individuals were recruited from the HIV counselling, testing and prevention (HCTP) clinic (Emavundleni), situated in Crossroads, Cape Town (CT) which forms part of the Desmond Tutu HIV Foundation. These 77 individuals included 33 HIV negative (control group) and 44 HIV positive individuals. Most of the data generated in this study were non-parametric and are presented showing median values plus/minus standard deviation (SD). The median age in years in the control group was 26±9.3 (range 20-58) compared to a median age of 29.5±9.4 (range 23-56) in the positive group. Basic indicators of HIV-1 infection (CD4 count, viral load, immune activation) as well as other parameters important for the current study (RBC count, Hb, Hct, monocyte count and monocyte %) were determined using fresh blood samples and methodologies outlined in the Materials and Methods section above. Correlations between these basic parameters were performed and are presented. These data are presented in Table 4.1

The majority of the data are illustrated graphically using box-and-whisker plots generated following statistical analyses using the GraphPad Prism 5 software (GraphPad Software, CA, USA). The “box” in the graphs represents the interquartile range (25-75 percentile confidence limits). The line present in the box indicates the median and the “whiskers” located at the top and bottom of the box represents the 10-90 percentile confidence limits. Data falling outside the 10-90 percentile range (outliers) are indicated as dots. A p value of ≤0.05 was indicative of statistical significance and is illustrated on the graphs with a bar. Correlations of various parameters were also performed within groups with a p value ≤0.05 indicating statistical significance and r value =>0 indicating a positive relationship and an r value =<0 indicating a negative relationship.

Table 4.1. Patient demographic (data is shown as median values ±SD)

	Control	HIV	p-value
Number of samples	33	44	N/A
Age (years)	26±9.3	29.5±9.4	N/A
Age range	20-58	23-56	N/A
Number of Males	11	8	N/A
Number of Females	22	36	N/A
CD4 (cells/µl)	929±288.3	410±234.6	<0.0001

CD4 range	470-1691	19-980	N/A
RBC count ($x10^6$ cells/µl)	4.7±0.5	4.2±0.7	0.0009
RBC count ($x10^6$ cells/µl) range	3.7-5.9	2.8-6.9	N/A
Hb (g/dl)	14.1±1.9	12.9±1.8	0.0172
Hb range	7.7-18	8.4-17.5	N/A
Haematocrit (l/l)	0.43±0.1	0.39±0.1	0.0071
Haematocrit (l/l) range	0.27-0.55	0.26-0.55	N/A
Monocytes ($x10^3$ cells/µl)	0.32±0.2	0.27±0.1	0.0350
Monocytes ($x10^3$ cells/µl) range	0.18-0.57	0.15-0.44	N/A
Monocytes %	4.9±2.7	5.9±1.6	0.0246
Monocytes % range	3.2-8.6	3.2-9.9	N/A
Viral load (copies/ml) log	N/A	4.1±1.4	N/A
Viral load (copies/ml) log range	N/A	0.0-6.2	N/A
Activation marker CD38/8 T cell %	10.7±10.3	27.0±17.7	<0.0001
Activation marker CD38/8 T cell % range	2.3-25.4	5.5-48.8	N/A

Control = HIV-1 non-infected patients; HIV positive = HIV-1 infected patients

4.2. Basic indicators for HIV-1 infection measured *ex vivo*

4.2.1. CD4 counts

The control group had a median CD4 count more than double the HIV positive group. The control group had a median of 929±288.3 cells/µl when compared 410±234.8 cells/µl in the HIV positive group, p<0.0001 see Figure 4.1.

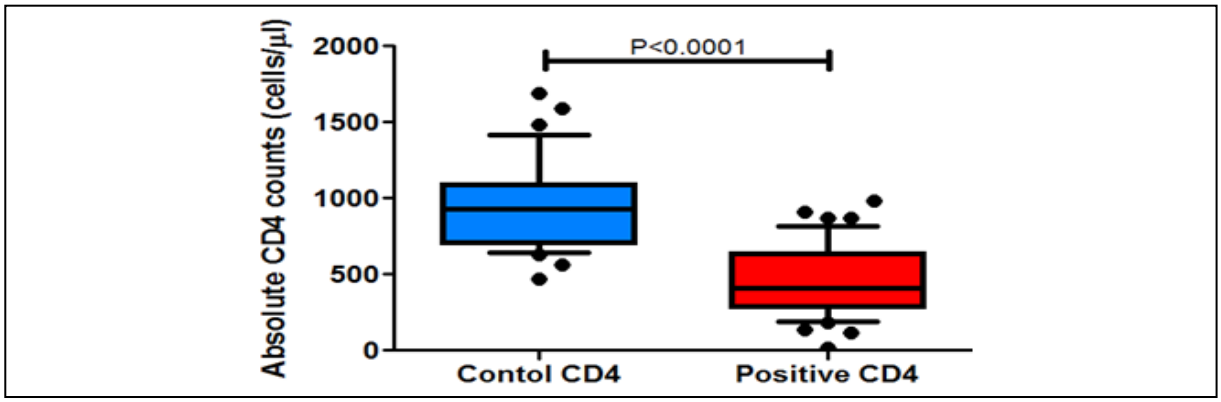

Figure 4.1. Box-and-whisker plot illustrating CD4 count data between the 2 groups. The box-and-whisker plot illustrates the CD4 counts in the two study groups. There was a statistically significant difference between the two groups: HIV-1 median 410±234.6 vs. HIV-1 uninfected median 929±288.3, p=<0.0001.

4.2.2. Red Blood Cell (RBC) Count

RBC Counts were obtained by full blood count (FBC). The control group had a higher median RCC of $4.7x10^6$±0.5 cells/µl when compared to the median RCC of the HIV positive group of $4.2x10^6$±0.7 cells/µl (p=0.0009) see figure 4.2. The decreased RBC count is indicative of anaemia in the HIV-1 infected group and is confirmed by the haemoglobin data presented below.

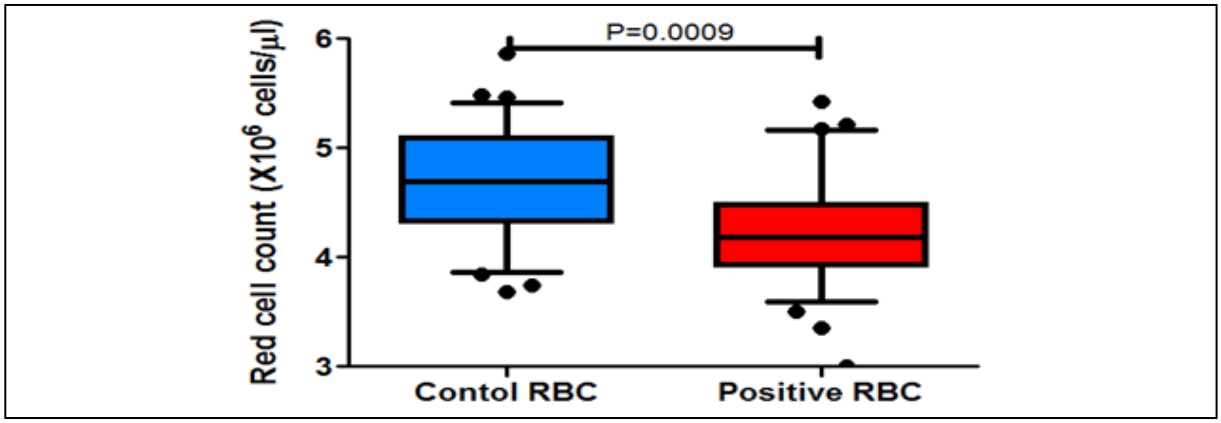

Figure 4.2. Box-and-whisker plot illustrating RBC count between the 2 groups. These data were obtained from routine full blood counts (FBCs). There is a statistically significant difference between the RCC of the two groups with the HIV + group showing a $0.5x10^6$ cells/µl statistical decrease when compared to the control group with a p=0.0009.

4.2.2.1. Correlations of RBC count with basic indicators of HIV

No statistically significant correlations were detected between the RCC and CD4 count or viral load tests as shown in Table 4.2. This would appear to indicate that neither the CD4 T cell subset changes nor the plasma viral load were directly implicated in the RBC decrease. This may be due to limited sample size and the selection of a study cohort in which HIV-1 infection was asymptomatic. Although there appears to be a positive relationship between CD4 count and RCC, and a negative relationship between VL and RCC the absence of statistical significance, implies that the two important clinical indicators of HIV-1 diseases progression were not causally linked to RBC count. Correlations with immune activation CD38/8 are discussed below.

Table 4.2. Correlation values of RCC with CD4 count and viral load.

RBC count	Control		HIV-1 infected	
	r-value	p-value	r-value	p-value
CD4 count	-0.0651	0.7188	0.1168	0.4848
Viral load (log)	N/A	N/A	-0.003	0.9851

4.2.3 Haemoglobin levels

Haemoglobin levels were obtained by routine FBC of fresh blood samples. The control group had a median Hb level of 14.1±1.9 g/dl compared to 12.9±1.8 g/dl in the HIV-1 positive group, p=0.0172 see figure 4.3. The significantly decreased Hb levels are consistent with anaemia and the decreased RBC count.

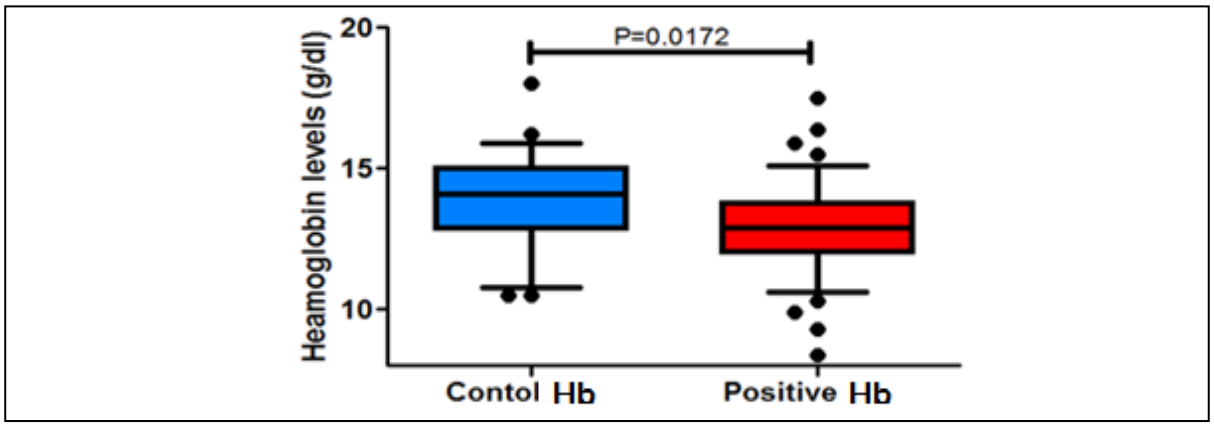

Figure 4.3. Haemoglobin levels between the 2 groups. The box-and-whisker plots illustrate the haemoglobin (Hb) levels as measured by FBCs between the two groups. There was a statistically significant difference between the Hb level of the two groups with the HIV + group (12.9±1.8 g/dl) showing a statistical decrease when compared to the control group (14.1±1.9 g/dl) with a p=0.0172.

4.2.3.1 Correlations of Hb with basic indicators of HIV

As with the RBC count data, no statistically significant correlations were detected between the Hb and CD4 count or viral load tests as shown in Table 4.3.

Table 4.3. Correlation of Hb with CD4 count and viral load

Hb	Control		HIV-1 infection	
	r-value	p-value HIV	r-value	p-value
CD4 count	0.1277	0.4788	0.1447	0.3862
Viral load (log)	N/A	N/A	-0.0599	0.7098

4.2.4. Haematocrit levels

Haematocrit (or packed cell volume) levels were obtained by routine FBC. The control group had a median of almost double that of the HIV positive group. The control group had a median of 0.43 (43%)±0.05 l/l compared to 0.27 (27%)±0.08 l/l in the HIV positive group, p=0.0071 , illustrated in Figure 4.4.

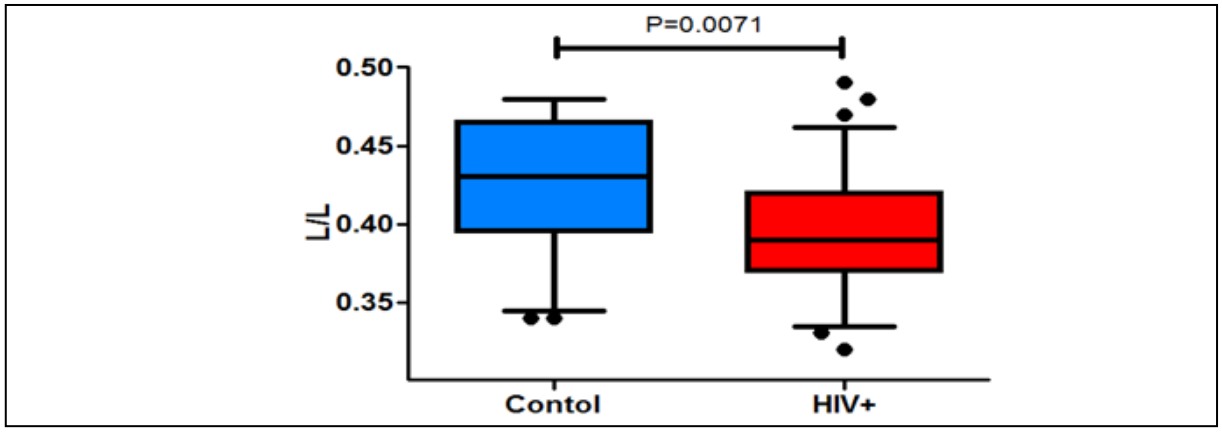

Figure 4.4. Haematocrit levels between the 2 groups. The box-and-whisker plot illustrates the haematocrit obtained from FBCs between the two groups. There was a statistically significant difference between the haematocrit level of the two groups with the HIV + group (0.27 (27%)±0.08 l/l) showing a statistical decrease when compared to the control group (0.43 (43%)±0.05 l/l), p=0.0071.

Hct data showed a similar trend to both RBC and Hb data, and again a significant difference between the two groups. All the red cell parameters show profound targeting and significant changes to the red cell compartment, even though our study cohort was “healthy” individuals with relatively high CD4 counts.

4.2.4.1. Correlations of Hct with basic indicators of HIV

No statistically significant correlations were detected between the Hct and CD4 count or viral load tests as shown in Table 4.4. The absence of statistical significance was most likely due to sample size, especially since the HIV-1 infected group was selected for their “healthy” status and relatively high CD4 count.

Table 4.4. Correlations of Hct with CD4 count and viral load

Hct	Control		HIV-1 infection	
	r-value	p-value	r-value	p-value
CD4 count	0.0683	0.7058	0.1044	0.5385
Viral load (log)	N/A	N/A	-0.0224	0.8893

4.2.5. Annexin V baseline

A novel component of this study was an assessment of RBC apoptosis (erythroptosis) by measuring surface expression of PS molecules as detected by annexin V binding. Annexin V was measured at baseline (*ex vivo*) before any stimulation in order to determine the levels of damage to the RBCs sustained *in vivo*. The control group had a lower median % annexin V positive RBC value at baseline 10.4±5% when compared to the HIV-1 positive group of 13.4±4.7%, p=0.0189 see figure 4.5.

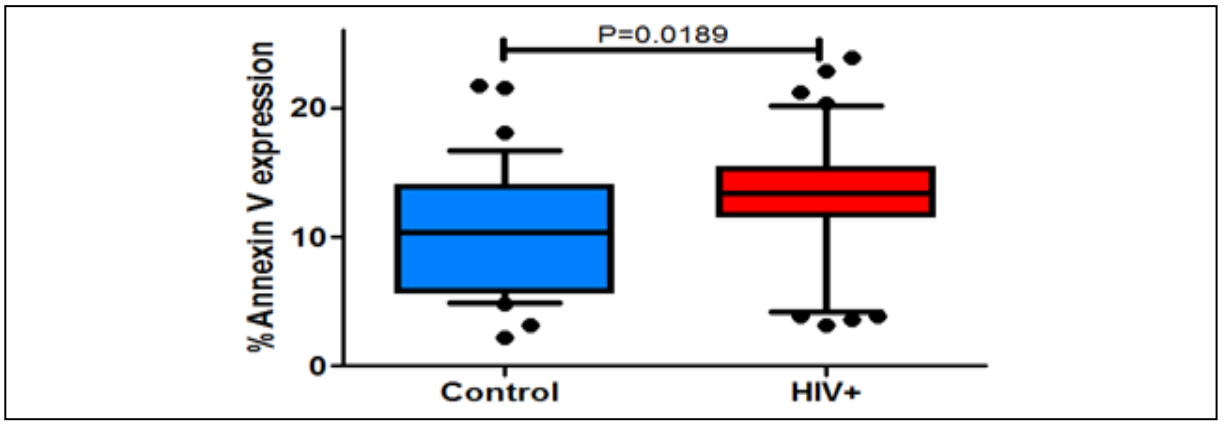

Figure 4.5. Annexin V baseline expression on damaged RBCs ex vivo. The box-and-whisker plot illustrates the annexin V baseline data measured ex vivo between the two groups. There was a statistically significant difference between the annexin V baseline of the two groups with the HIV-1 positive group showing a statistical increase when compared to the control group with a p=0.0189.

The significantly increased baseline annexin V (28.8% higher in the HIV-1 infected group) was indicative of higher levels of erythrocyte death by erythroptosis.

4.2.5.1. Correlations of annexin V with basic indicators of HIV

Correlations were performed between annexin V baseline and various other study parameters, illustrated in Table 4.5. A significant negative correlation between annexin V baseline and RBC count was observed in the control group. This confirmed that the decreased RBC count was biologically associated with RBC apoptosis as measured by annexin V binding. No statistical correlation was observed in the HIV positive group, however. This finding is in accordance with the lack of correlation of the RBC paramaters with standard clinical HIV-1 indicators.

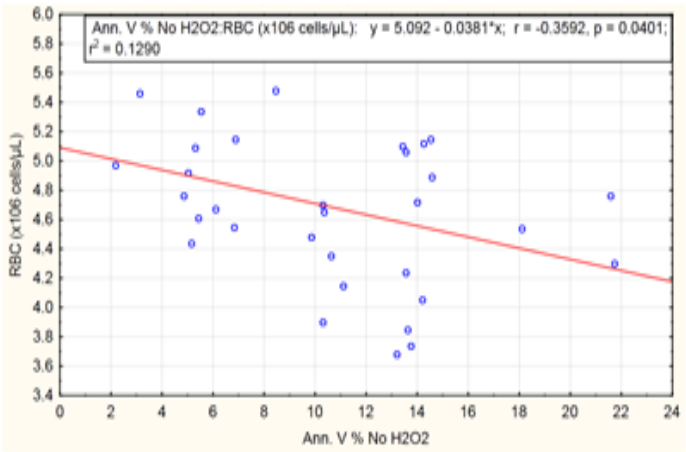

Figure 4.6. Annexin V baseline versus RBC count correlation. The scatterplot illustrates a negative correlation between annexin V baseline expression and RBC in the control group. There was a statistically significant difference with a p=0.0401 and r=-0.3592

Table 4.5. Correlations of annexin V baseline with basic HIV; red blood cell and immune activation parameters.

Annexin V baseline	Control		HIV-1 infection	
	r-value	p-value	r-value	p-value
CD4 count	-0.0702	0.4229	0.1443	0.6753
RCC count	N/A	N/A	0.1219	0.4305
Hb level	-0.2322	0.1934	0.1785	0.2462
Hct level	-0.1583	0.3790	0.2215	0.1535
Viral load	N/A	N/A	0.0189	0.9067
CD38/8	0.2330	0.1920	0.0447	0.7720

4.2.6. Absolute Monocyte Counts

Absolute monocyte counts were obtained from routine FBC and differential count. Absolute monocyte counts were lower in the HIV-1 infected group. The control group had a median monocyte count of $0.32x10^3$±0.1 cells/µl when compared to the HIV-1 positive group $0.27x10^3$±0.08 cells/µl. The decrease was statistically significant, p=0.035. See figure 4.7. Even though there was a statistically significant decrease, this was not clinical significant as it is still within the normal range of 0.1-0.8 cells/µl. The decrease in monocytes may be due to pooling in the tissues at sites of inflammation and infection at this stage of the disease. The decrease may also be indicative of increased monocyte apoptosis or decreased production from the bone marrow, or a combination of all of these (Gama *et al.*, 2012).

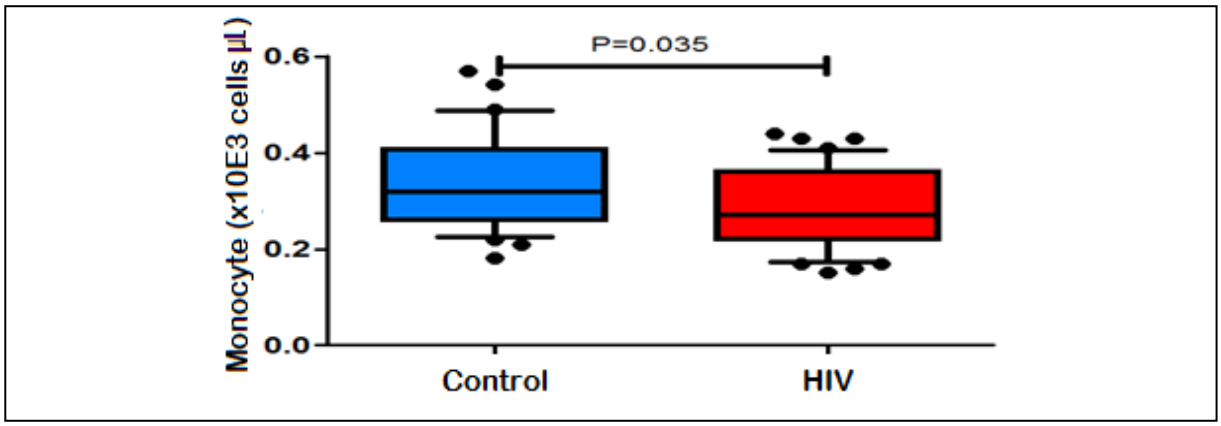

Figure 4.7. Monocyte counts obtained from FBC differentials. The box-and-whisker plot illustrates the monocyte counts between the two groups. There was a statistically significant difference between the two groups with the HIV + ($0.27x10^3$±0.08 cells/µl) group showing a statistically lower number of monocytes when compared to the control group ($0.32x10^3$±0.1 cells/µl), p=0.035.

The relationship of total monocyte count to HIV-1 clinical indicators and to red cell parameters was determined statistically. No significant correlations were obtained, indicating that changes to the monocyte compartment occurred relatively independently to changes in both standard clinical parameters and red cell parameters.

Table 4.6. Correlation of monocyte count with basic HIV indicators; RBC parameters and immune activation levels. No statistically significant correlations were detected with the monocyte count.

Monocyte count	Control		HIV-1 infection	
	r-value	p-value	r-value	p-value
CD4 count	0.0202	0.9111	0.1579	0.3576
RCC count	-0.3265	0.0637	0.1301	0.4177
Hb level	-0.0129	0.4406	-0.1390	0.9361
Hct level	-0.1689	0.3473	0.0804	0.6172
CD38	-0.0607	0.7372	-0.1438	0.3698
HIV-1 viral load	N/A	N/A	-0.1091	0.5084

4.2.7. Blood monocyte percentage

Blood monocyte percentages as a percentage of total leukocytes, were obtained by routine FBC and automated differential count on the Siemens Advia 2012. The control group had a median monocyte % of 4.9±2.7% when compared to the HIV-1 positive group 6±1.6%. See Figure 4.6. Even though there was a statistical significant decrease, there was not a clinically significant change, as the normal range is 2-10%. The higher monocyte percentage in the HIV-1 positive group may be due to a relative increase in proportion to the total leukocyte count as a result of the decreased CD4 counts, which also constitute a fraction of the total leukocytes. Please see results of absolute monocyte counts above.

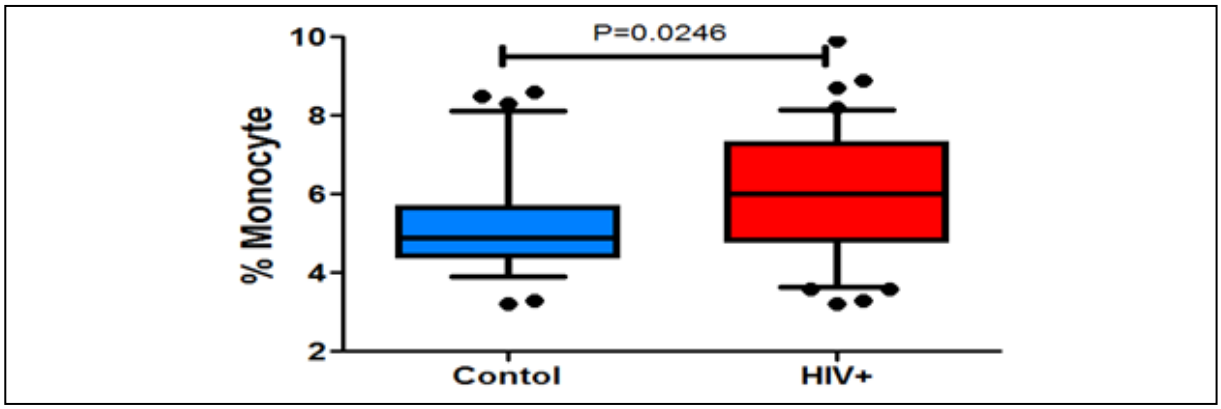

Figure 4.8. Monocytes as a percentage of total leukocytes obtained from FBC and differential counts. The box-and-whisker plot illustrates the monocyte % (of total leukocytes) data between the two groups. There was a statistically significant difference between the two groups with the HIV-1 + group showing a statistically higher monocyte % (6±1.6%) when compared to the control group (4.9±2.7%) with a p=0.0246.

4.2.7.1. Correlations of monocyte % with basic indicators of HIV and other red blood cell parameters

The monocytes were correlated with the basic clinical indicators of HIV-1 infection (CD4 and viral load) as well as RCC, Hb, Haematocrit, and annexin V baseline) in order to determine significant relationships.

4.2.7.2.. Relationship of Monocyte % with RCC

Correlations were performed between monocyte % and red cell counts. There was a significant negative correlation in the control group indicating that as the monocyte percentage increased the RCC decreased. There was no statistical correlation in the HIV positive group.

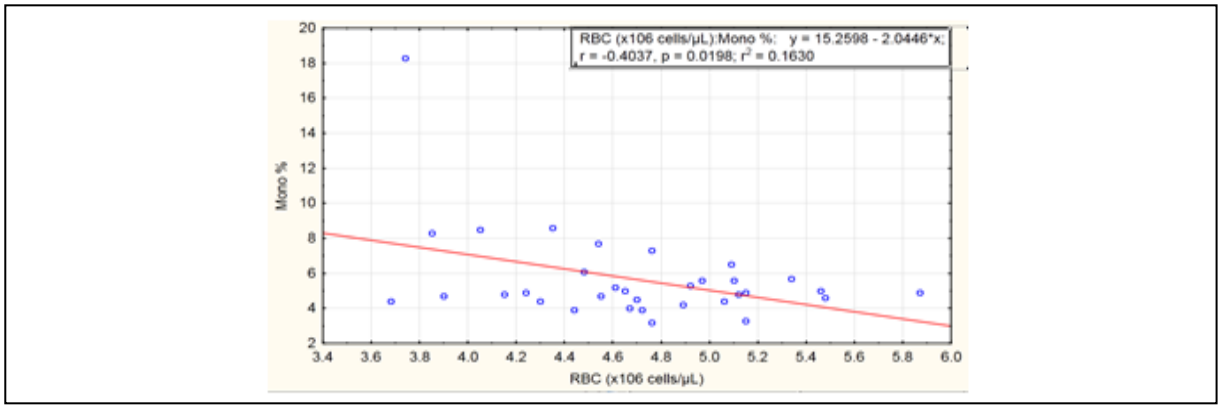

Figure 4.9. Monocyte % versus RBC count correlation. The scatterplot illustrates a negative correlation between the monocyte % and RBC in the control group. There was a statistically significant difference with a p=0.0198 and r=-0.4037

4.2.7.3. Relationship of monocyte % with Hb

Correlations were performed between monocyte % and Hb level. There was a significant negative correlation in the control group indicating that as the monocyte percentage increased the Hb level decreased. There was no statistical correlation in the HIV positive group. This finding confirms the relationship between monocyte % and RBC count discussed above.

The negative relationship between monocyte % and RBC parameters was not apparent in the HIV-1 infected group, confirming that altered percentages of monocytes (due to changes in CD4 counts) disrupted the relationship which was observed in the uninfected donors.

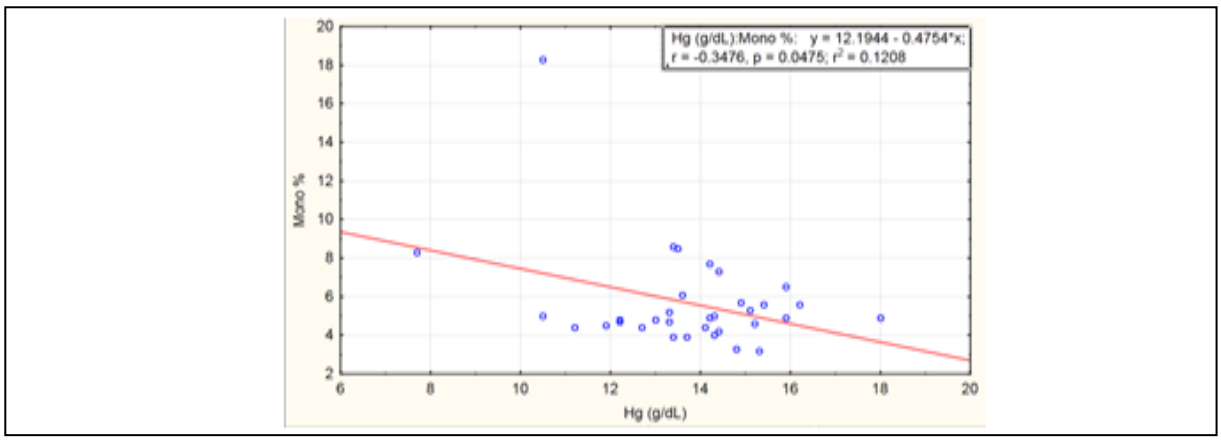

Figure 4.10. Monocyte % versus Hb level correlation. The scatterplot illustrates a negative correlation between the monocyte % and Hg level in the control group. There was a statistical significant difference with a p=0.0475 and r=-0.3476

The other parameters did not show statistically significant correlations with monocyte percentages, as indicated in Table 4.7. These findings should be considered in the light of the relationships of standard parameters to total monocytes, as discussed below.

Table 4.7. Correlations of monocyte % with basic HIV indicators

Monocyte %	Control		HIV-1 infection	
	r-value	p-value	r-value	p-value
CD4 count	-0.3227	0.0670	-0.0227	0.8953
RCC count	-	-	-0.1830	0.2521
Hb	-	-	-0.2877	0.0682
Hct	-0.3414	0.0519	-0.2487	0.1169
Annexin V baseline	0.2164	0.2264	-0.2482	0.1176
HIV-1 viral load	N/A	N/A	0.8010	0.6280-

4.2.8. Expression of the activation marker CD38 on CD8+ T cells

HIV-1 infection leads to the activation of various cells including CD8+ T cells. CD38 is a well-defined activation marker, particularly well-researched in the context of HIV-1 infection and serving as a marker for general immune activation status (Vollbrecht *et al.*, 2010). The HIV positive group had almost 3 times the % of CD8 T cells expressing CD38 as did the control group. The control group had a median % CD8 T cells expressing CD38 of 10.7±10.3 % vs. 28.8±17.3 % in the HIV-1 positive group, p<0.0001. See figure 4.11.

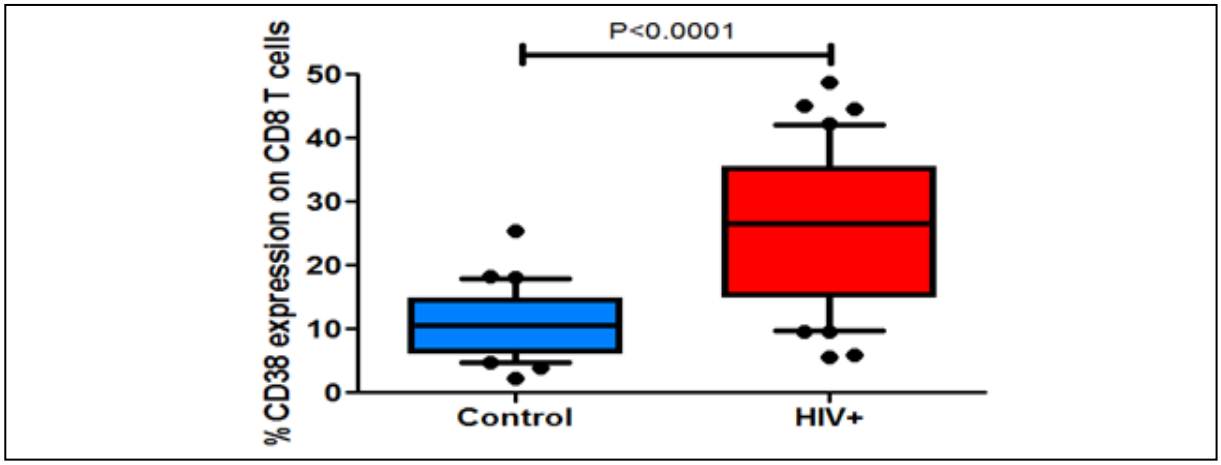

Figure 4.11. Immune activation measured by the expression of the activation marker CD38 on CD8+ T cells. The box-and-whisker plot illustrates the CD8 activation marker CD38 data between the two groups. There is a statistically significant difference between the two groups with the HIV + group showing a statistical increase when compared to the control group with a p<0.0001.

The dramatic increase in percentage activated CD8+ T cells is in accordance with published literature. The relationship of immune activation (as determined by CD38 expression) to other parameters was assessed by statistical correlation.

4.2.8.1. Relationship of % CD38+ CD8+ T cells with basic clinical indicators of HIV-1 disease; red cell parameters and monocyte count

The % CD38 expressing CD8+ T cells was correlated with the basic indicators of HIV (CD4, viral load), red cell parameters (RCC, Hb, Haematocrit, annexin V baseline), plus monocyte percentage and monocyte count in order to determine significant relationships.

4.2.8.2. % CD38 expressing CD8+ T cells and CD4 count

There was a negative correlation between CD4 cell count and CD38 on CD8 T cells in both study groups indicating that as the activation of CD8+ T cells increased the CD4 count decreased. However, this correlation was not statistically significant in the control group, but

reached statistical significance in the HIV positive group (p=0.0169). This indicates a relationship between activated CD8+ T cells and CD4 T cells, as previously published by others (Steel *et al.*, 2008).

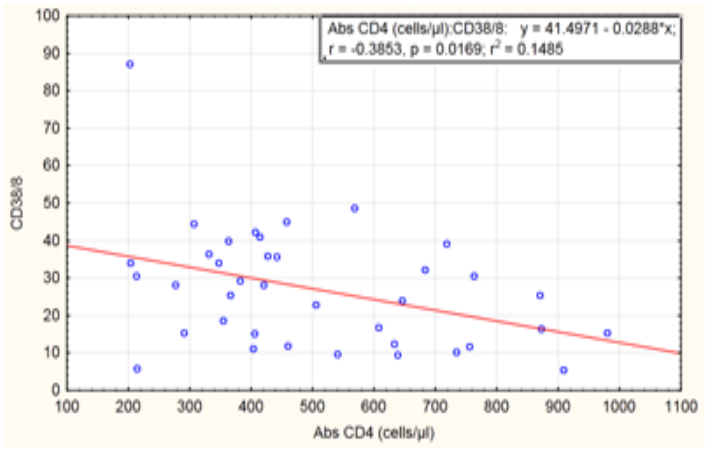

Figure 4.12. CD4 count versus CD38/8 correlation. The scatterplot illustrates a negative correlation between the absolute CD4 count and CD8 activation marker CD38 in the HIV+ group. p=0.0169 and r=-0.3853

4.2.8.2. CD38 on CD8 correlating with viral load

Correlations were performed between CD38/CD8 T cells and viral load in the HIV-1 infected group. There was a significant positive correlation indicating that as the viral load increased, activation of CD8+ T cells increased. See figure 4.13. The significant relationship between CD4 count, viral load and CD38 expression, shows the inter-relatedness of these parameters and the importance of these markers, even in a study cohort of “healthy” HIV-1 infected individuals.

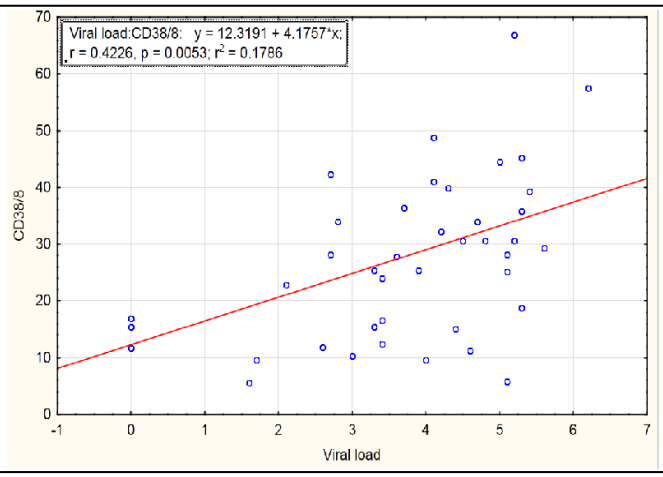

Figure 4.13. VL versus CD38/8 correlation. The scatterplot illustrates the correlation between the viral load (log) and the activation marker CD38 on CD8 T lymphocytes in the HIV+ group. This was statistically significant with a p=0.0053 and r=0.4226

CD38 did not correlate with other parameters (see Table 4.8). This appears to indicate the changes in red cell parameters and monocytes were not directly related to immune activation. This may be due to the sample size and the selection of a "healthy" HIV-1 infected cohort with fairly high CD4 count. Interestingly, despite the lack of a significant association, a negative relationship in the HIV-1 negative group between immune activation and Hb, Hct, monocyte count was noted, indicating that higher immune activation may impact on these parameters.

Table 4.8. Correlations of CD38 on CD8 T cells with other parameters

CD38 on CD8	Control		HIV-1 infection	
	r-value	p-value	r-value	p-value
CD4 count	-0.1606	0.3720	-	-
RCC	-0.0544	0.5094	0.1190	0.7259
Hb	-0.0216	0.9048	-0.1493	0.3333
Hct	0.0312	0.8634	-0.2487	0.1169
Monocyte count	0.0813	0.6529	-0.1639	0.3058
Monocyte %	0.1578	0.3806	0.1981	0.2145
Annexin V baseline	0.2390	0.1804	0.2482	0.1176

4.3. RBC oxidative stress and efficacy of the antioxidant NAC

4.3.1. RBC induced oxidative damage (erythroptosis) measured by annexin V expression

Our findings indicated that there was a significant decrease in RBCs, Hb and Hct in HIV-1 infected individuals (see sections 4.2.2.-4.2.4.), therefore, we wanted to investigate the role of oxidative stress on these changes. In order to evaluate this we stimulated cells *in vitro* with an oxidative stressor (H_2O_2) and then measured the % expression of annexin V. The relative amount of oxidative damage was determined by the increase in annexin V expression as illustrated in figure 4.14.

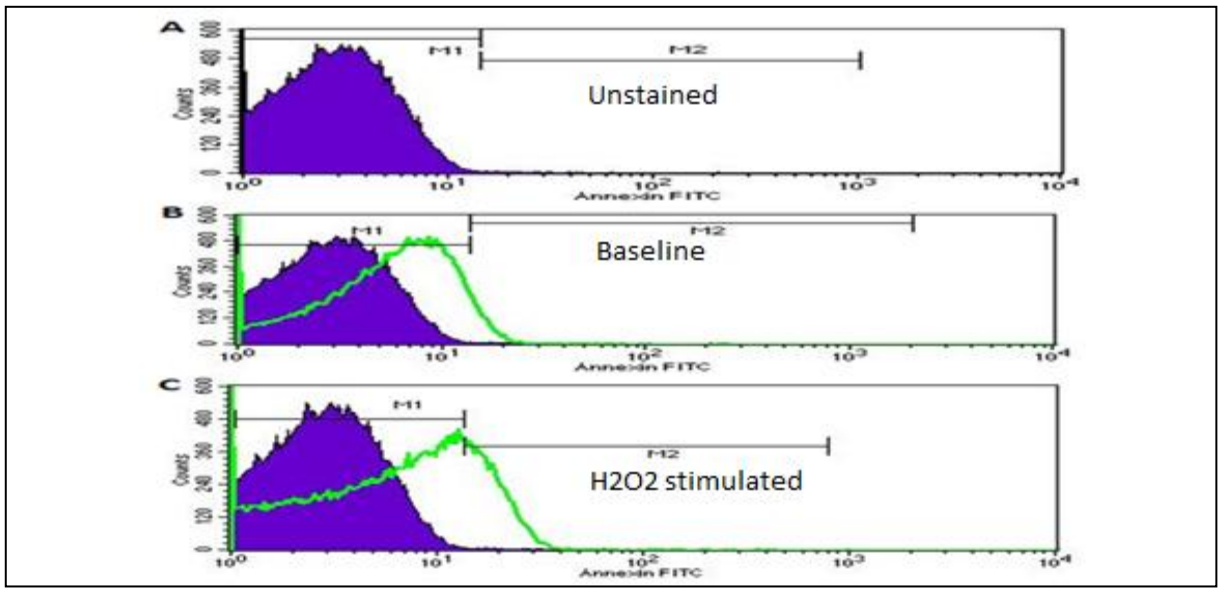

Figure 4.14. Expression and measurement of % annexin V. The histograms illustrate the percentage annexin V expression on gated RBCs as detected by flow cytometry. . (A) Presents unstained and un-stimulated RBCs, showing the placement of the markers M1 and M2 indicating the separation of populations negative and positive for annexin V, respectively. (B) Presents stained but un-stimulated RBCs i.e. baseline annexin V expression (14.4±6.9 %). (C) Presents stained and H_2O_2 stimulated RBCs and the increased annexin V expression (19±6.8 %).

The damage RBCs sustain after induction of oxidative stress *in vitro* with 5mM H_2O_2 for an hour was measured by annexin V expression. The technique used was previously optimized in 2010 in our laboratory. In section 4.2.5.the damage RBCs sustained *in vivo* was measured and illustrated as annexin V baseline. The control group had a median annexin V baseline of 10.4±5% when compared to the HIV-1 positive group of 13.4±4.7%, p=0.0189 indicating that RBC damage was already occurring *in vivo*. The oxidative stress was then induced on RBCs with 5mM H_2O_2 for 1 hour and the annexin V levels measured. The control group had an induced median annexin V % of 15.4±7.4% when compared to the HIV-1 positive group of 18.5±6.8%, p=0.0232, see Figure 4.15. Both groups had an approximate 5% increase in annexin V expression after induced oxidative stress see Figure 4.17. This similar level of induced damage *in vitro* led us to deduce that the RBCs from HIV-1 positive individuals are not more sensitive to oxidative stress when compared to the RBCs from the control group

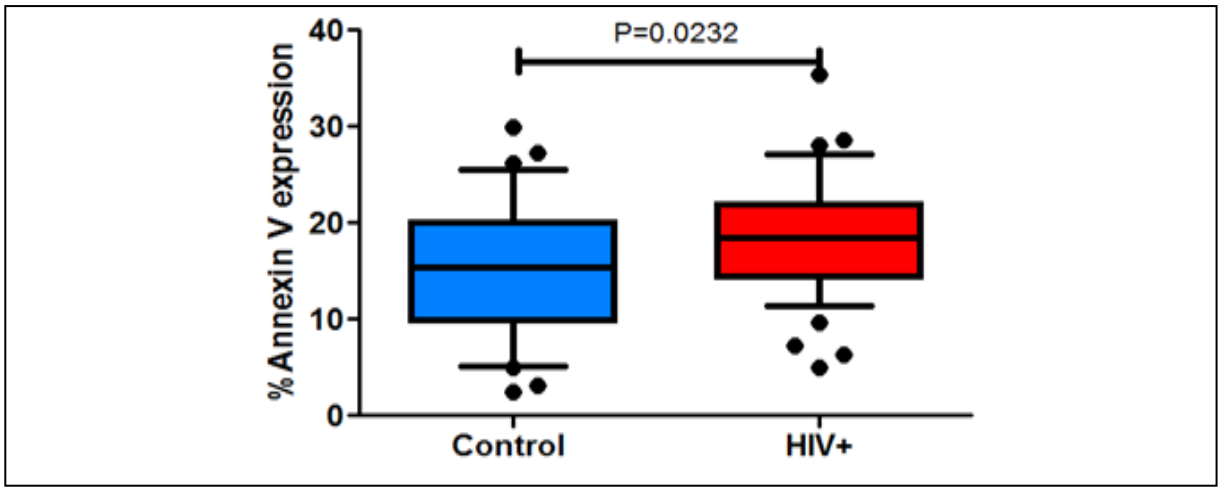

Figure 4.15.Induction of oxidative stress in vitro on RBCs and annexin V measurement. The box-and-whisker plot illustrates the annexin V expression following induced oxidative stress stimulation on homologous RBCs between the two groups. The data illustrated here indicates the damage RBCs sustained after in vitro induced oxidative damage while the baseline annexin V indicates the damage the RBCs sustain while in vivo illustrated in figure 4.5. There is a statistically significant difference between the annexin V expression of the two groups with the HIV + group showing a statistical increase when compared to the control group with a p=0.0232.

4.3.2. Comparison of induced oxidative stress using an oxidative buffer (DPBS + 5mM sodium-L-ascorbate (Sigma-Aldrich) + 0.4 mM copper (II) sulphates) vs. H_2O_2

The % annexin V expression between the control group (n=13) and HIV-1 (n=14) infected group were compared when RBCs were stressed with two oxidative stressors in order to determine which stressor would deliver optimal results. It has been reported in the literature that H_2O_2 is unstable and therefore other oxidative stressors in a buffered format may produce more consistent results. The control group had a median annexin V % of 15.7±9.2% after stimulation with H_2O_2 when compared to the HIV-1 positive group of 18.9±7.3%, p=0.0079. There was a significant difference in the control group when H_2O_2 stimulated samples compared to the un-stimulated samples. Oxidative buffer stimulated samples in the control group were 12.1±8.3% compared to the H_2O_2 stimulated samples 15.7±9.2%, p=0.0082. There was a significant difference in the HIV-1 infected group when H_2O_2 stimulated samples were compared to the un-stimulated samples as well as the oxidative buffer stimulated samples (see Figure 4.16 and Table 4.9.).

There was no significant difference within the groups between the un-stimulated and oxidative buffer stimulated samples. There were, however, significant differences between the control group and the HIV-1 infected group at each time point when samples were either un-stimulated or oxidative buffer stimulated (see Figure 4.16 and Table 4.9.).

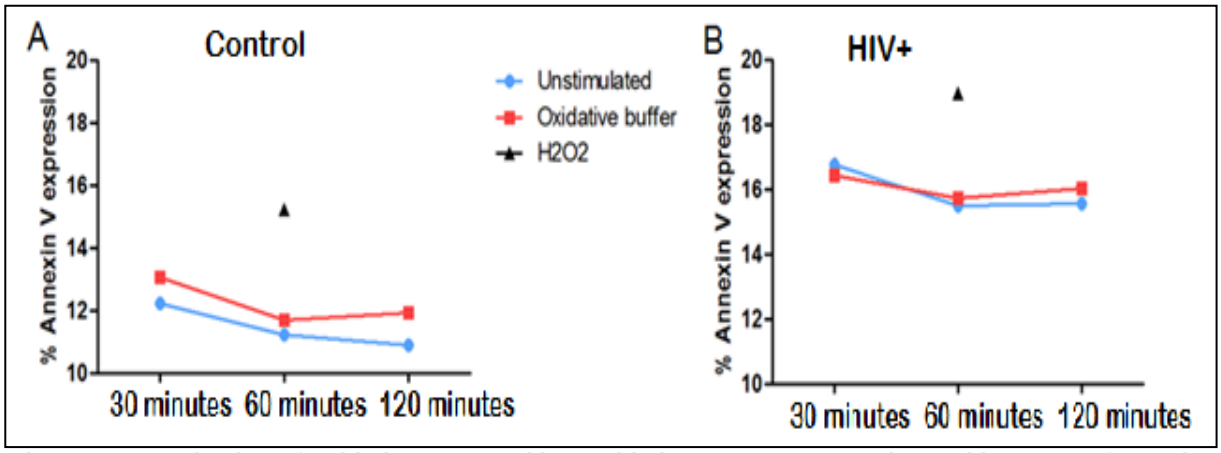

Figure 4.16. Induction of oxidative stress with 2 oxidative stressors over time. This was performed to compare whether the oxidative buffer would present better results compared to the unstable H_2O_2. The graph illustrates the median % annexin V expression on RBCs between the two groups with control group on the left in graph A and the HIV-1 infected group on the right in graph B. The groups were either un-stimulated and sampled at three time points (indicated as blue solid circles), stimulated with a 5mM H_2O_2 for 1 hour (represented as black solid triangle) or stimulated with an oxidative buffer (DPBS + 5mM sodium-L-ascorbate (Sigma-Aldrich) + 0.4 mM copper (II) sulphates)(indicated as solid squires) at three different time stages (represented as red solid squares). There was no statistically significant difference between the un-stimulated and oxidative buffer stimulated samples within the two groups. There was a statistical significant difference between the H_2O_2 and the un-stimulated and oxidative buffer stimulated samples at the 60 minutes time point in both groups. There was also significant differences between the un-stimulated as well as oxidative buffer stimulated samples at each time point between the control group and the HIV-1 infected group. Standard deviation and p values are indicated above and median values with SD are also presented in table 4.9. below. The SD was not indicated on the graph for clarity purposes. The highest level of annexin V expression data were obtained from the 5mM H_2O_2 concentration and the 30 minute time point with the oxidative buffer.

The SD and median values relating to figure 4.16. are illustrated in table 4.9 below. The 30 minute stimulation with the oxidative buffer presented the highest annexin V expression in both groups. It may be that annexin decreases over time as annexin positive cells enter late apoptosis and degrade, so not being included in the RBC gate. The samples were only stimulated for an hour with H_2O_2 as this presented optimal annexin V expression when technique was optimised in 2010 in our laboratory. The median and standard deviation annexin V baseline and stimulation of both groups are illustrated in Table 4.9.

Table 4.9. Representation of % annexin V expression at each stage of induced oxidative stress of figure 4.16

Form of stimulation and time	Control	HIV+
H_2O_2 60 minutes	15.7±9.2	18.9±7.3
Unstimulated 30 minutes	12.2±7.8	17±10.8
Oxidative buffer 30 minutes	13.2±9.2	16.6±10
Unstimulated 60 minutes	11.5±7.9	15.7±9.9
Oxidative buffer 60 minutes	12.1±8.3	16.1±10.1
Unstimulated 120 minutes	10.7±7.6	15.9±11.1
Oxidative buffer 120 minutes	12.4±8.8	16.2±10.8

4.3.3. Induction of oxidative stress using H_2O_2

Due to no apparent difference in use of H_2O_2 vs. the oxidative buffer, further experiments were performed using H_2O_2 alone. At baseline level indicated in section 4.2.5. there was a statistically higher annexin V expression in the HIV-1 infected individuals 13.4±4.7% when compared to the healthy non-infected group 10.4±5% with a p-value of 0.0189. After stimulation with H_2O_2 the annexin V expression increased in both groups indicated above (4.2.9.). The HIV-1 infected individuals expressed a statistically higher annexin V level 18.5±6.8 when compared to the healthy non-infected group 15.4±7.4% with a p value of 0.0232. There was also a statistical difference between the baseline level and induced oxidative stressed level within each group. The HIV-1 infected individuals had a p value of $p<0.0001$, and the healthy non-infected individuals also had a $p<0.0001$. The median and standard deviation annexin V baseline and stimulation levels of both groups are illustrated in Table 4.10.

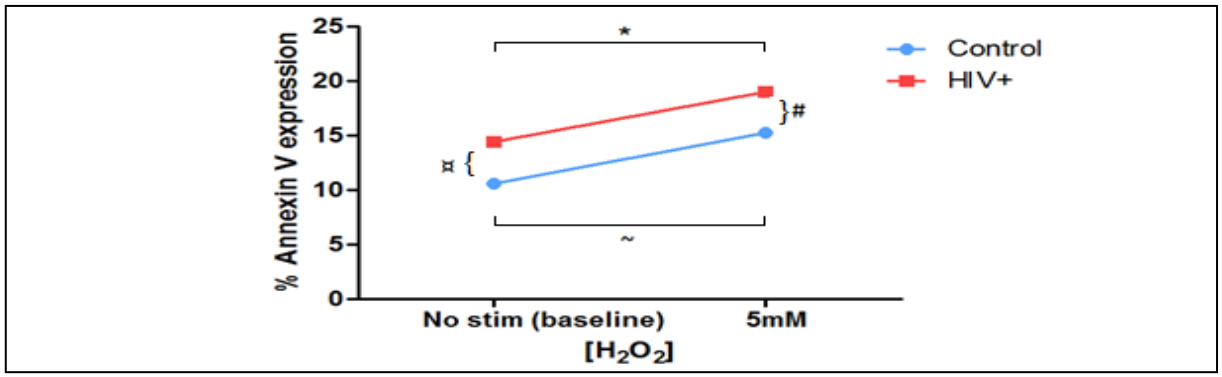

*Figure 4.17. Comparison of oxidative damage on RBCs between the two groups at baseline and after inducing oxidative stress with 5mM H_2O_2 for 1 hour. The graph illustrates the median % annexin V expression data either un-stimulated/ stimulated with H_2O_2 between the control group (n=33) and HIV group (n=44) There are statistically significant difference between the annexin V baseline and stimulated annexin V expression in the two groups with the HIV + group showing a statistically higher level to the control group at both points of measurement (un-stimulated and stimulated). There were statistical significant differences between baseline levels as well as between induced oxidative stress levels of annexin V expression between the two groups as well as within each group. The significant difference at baseline annexin V expression between the two groups p=0.0189, is illustrated as ¤. The significant difference after induced oxidative stress between the two groups, p=0.0232 is illustrated as #. The significant difference between baseline level and after induced oxidative stress within the control group, p<0.0001 is illustrated as ~. The significant difference between baseline level and after induced oxidative stress within the HIV-1 group, p<0.0001 is illustrated as *.*

Table 4.10. Representation of % annexin V expression when un-stimulated or stimulated

Form of stimulation	Control	HIV+
Un-stimulated Baseline median	10.4±5	13.4±4.7
Stimulated H2O2 median	15.4±7.4	18.5±6.8

In summary, the data presented in figure 4.17 indicates that although HIV-1 infected individuals have a higher baseline annexin V expression, the RBCs in both study groups responded in a similar manner to H_2O_2 induced oxidative stress. In both groups a significant increase in annexin V positivity was observed, but the increase was equivalent in both groups. This appears to confirm that the RBCs in HIV infection were not more sensitive *in vitro* to oxidative stress. Alternatively, oxidative stress *in vitro* may induce higher levels of RBC apoptosis which causes cell degradation, with degraded cells being excluded from RBC analysis. The finding that longer oxidative stress incubation times reduced annexin V binding (Fig 4.16) may be evidence for this, In which case a shift into late apoptosis was being detected as decreased early apoptosis. The damage to RBCs caused *in vivo* in HIV-1 infection does however translate into elevated overall RBC death following *in vitro* application of oxidative stress.

4.3.4. The effects of the anti-oxidant NAC on RBCs measured

The counter measure that the anti-oxidant (NAC) has on the oxidative stress induced in RBCs by H_2O_2 was measured by changes in annexin V expression. The anti-oxidant had an impact on the RBCs, buffering them almost completely from the harmful effects of the oxidative stressor. During this part of the study 20 control samples and 30 HIV-1 infected samples were processed. The impact of increasing concentrations of NAC on annexin V expression is illustrated in Figure 4.18.

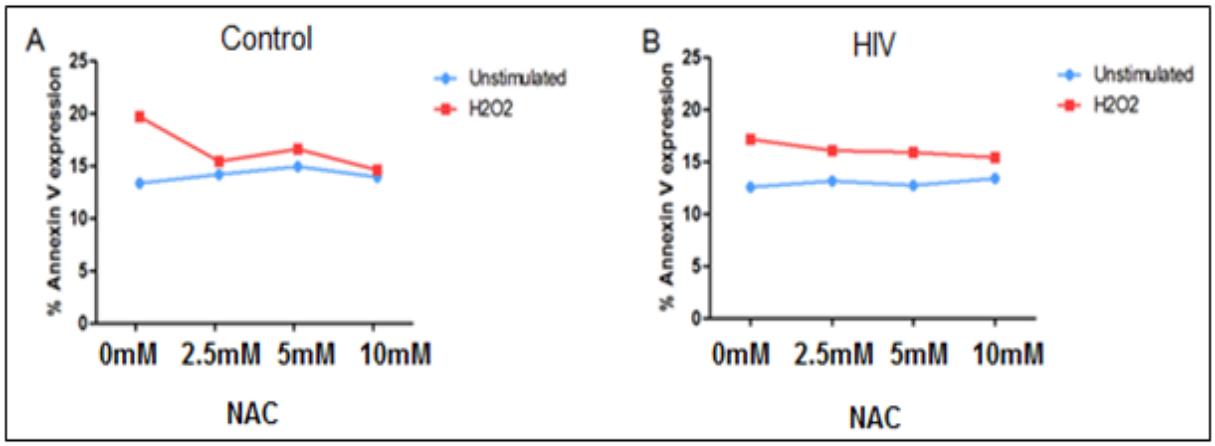

Figure 4.18. Dose response of NAC before and after inducing oxidative stress with H_2O_2. The graph illustrates the median % annexin V data between the control (n=20) group and HIV+ (n=30) group un-stimulated/ stimulated with a 5mM H_2O_2 for an hour in association with or without the anti-oxidant n-acetyl cysteine (NAC) at various concentrations (2.5mM, 5mM and 10mM). There was no significant difference between the control group and the HIV-1 positive group. The optimal inhibition by NAC occurred at the 10mM concentration for both study groups.

Table 4.11. Representation of median % annexin V expression at each stage of NAC dose

Stimulation	Control		HIV+	
	Un-stimulated	H_2O_2	Un-stimulated	H_2O_2
No NAC	13.6±4.1	20±5.1)	12.8 ±5.2	18.3 ±5.0
2.5mM NAC	14.2±3.4	14.9 ±4.1	13.1 ±4.6	16.8 ±5.1
5mM NAC	15.4 ±3.3	17.2 ±4.4	13.1 ±4.9	16 ±5.5
10mM NAC	14.3 ±3.4	15 ±4.4	13 ±5.2	16 ±5.2

Although NAC inhibited induced oxidative stress in both groups, the uninfected group displayed stronger inhibition. At 10mM NAC, the oxidative stress induced apoptotic percentage of RBCs was reduced from 20±5.1% to 15±4.4% (p=0.0063). In other words, the 6.4% increase due to oxidative stress was reduced to 1.4%. In the HIV-1 group, the oxidative stress induced apoptotic percentage of RBCs was reduced from 18.3±5.0% to 16±5.2%. (p=0.0649). In this case, the 5.5% increase due to oxidative stress was reduced to 3.2%. NAC thus appears less efficient in minimizing induced oxidative stress *in vitro* in the HIV-infected group.

4.4. Monocyte:RBC interaction

Having established that RBCs are depleted in chronic HIV and that this depletion is accompanied by increased annexin V expression, we next wanted to investigate the relationship of RBC depletion to monocyte cell numbers and function (particularly phagocytosis). Monocytes were purified as discussed in section 3.9. The purity of monocytes was assessed with the use of flow cytometry (see Figure 4.19).

Purity of separated monocytes

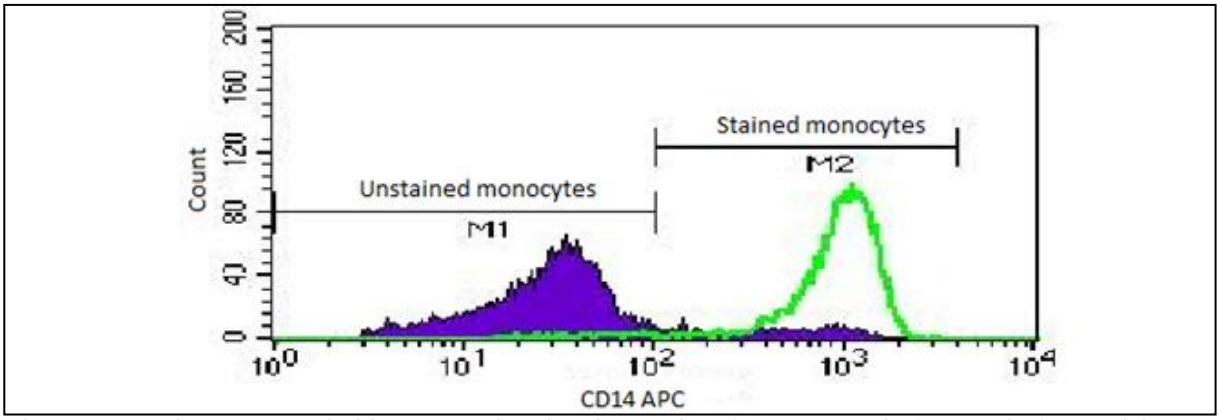

Figure 4.19. Flow cytometric histogram plot showing purity of monocytes before and after enrichment from whole blood. The graph represents a histogram measuring the CD14 expression in whole blood before purification (in purple) and after purification (green line) in order to obtain the percentage purified monocyte population. M1 measures the CD14-CD45+ population and M2 the CD14+CD45+. The percentage CD14+CD45+ monocytes (M2) obtained from whole blood was ±5.7% from total gated events before purification. The percentage monocytes (M2) obtained after purification was >70% of total gated events.

4.4.1. Comparison of the relative proportion of classical (CD14+CD16-) and inflammatory (CD14+CD16+) monocyte subsets between the study groups

The control group had a slightly (but statistically insignificant) higher percentage of classical monocytes when compared to the HIV-1 infected group. The control group had a median CD14+/16- monocyte % of 65.6±7.1 when compared to the HIV positive group of 63.4±8.8.

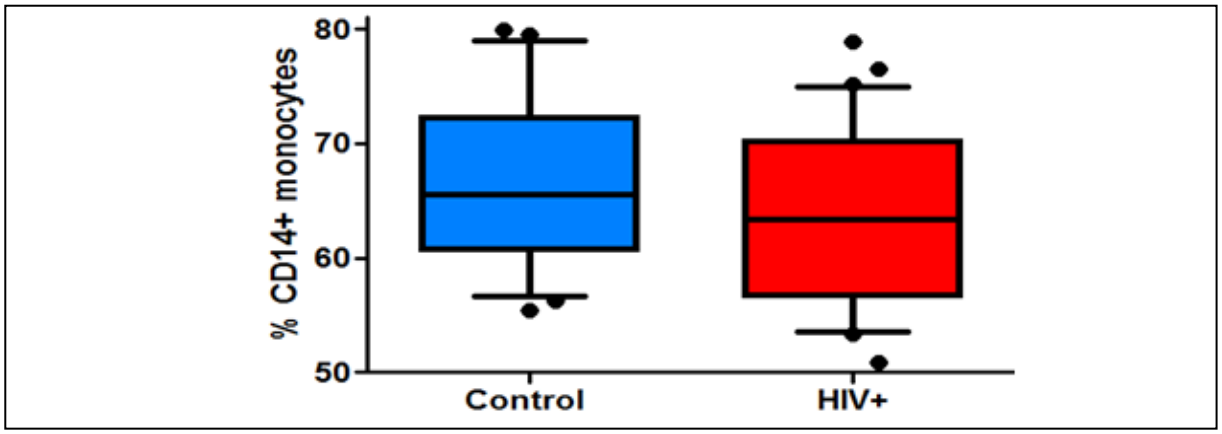

Figure 4.20. Comparison of the classical (CD14+/16-) monocyte subset between the two groups. The box-and-whisker plot illustrates the % classical (CD14+/16-) monocytes as % of total gated monocyte events between the two groups. Although median decreased in HIV-1 there was no statistically significant difference between the two groups with a p=0.1597.

The changes in classical monocyte percentages mirror the total monocyte count changes (Figure 4.10). Although both total monocyte count and inflammatory subset % differences (see below) were significant, this was not the case for the classical subset, as the data was fairly widely spread.

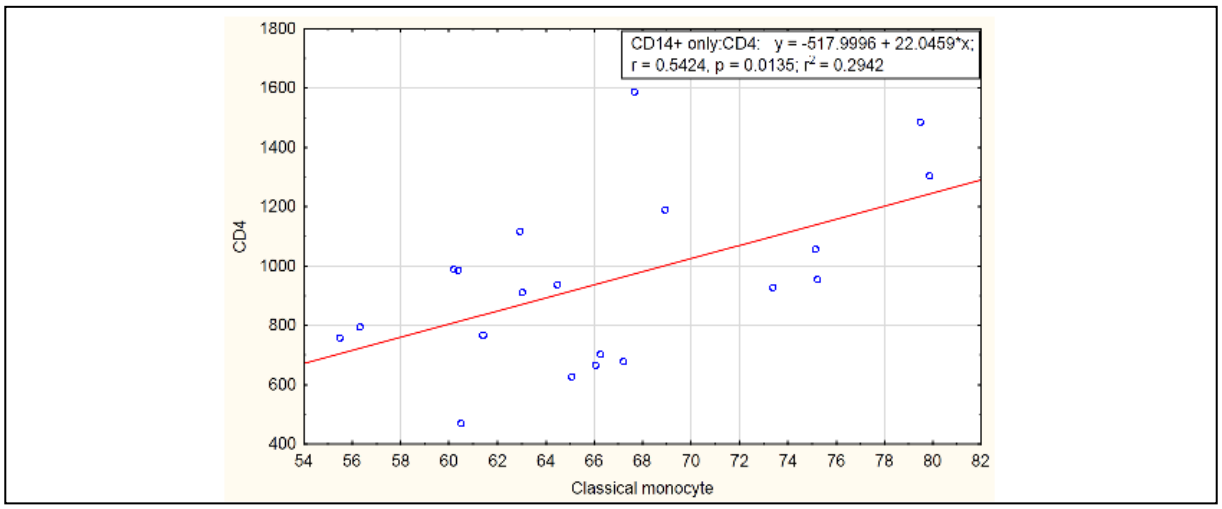

Figure 4.21. CD4 count versus classical monocyte correlation. The scatterplot illustrates the correlation between the CD4 count and the classical monocyte (CD14+CD16-) population in the control group. This was statistically significant with a p=0.0135 and r=0.5424

There was a significant correlation between the classical monocyte (CD14+CD16-) population and CD4 count in the control group, p=0.0135 and r=0.5424 illustrated in figure 4.21 above. There were no significant differences between the classical monocyte and any HIV-1 parameters or RBC parameters (see Table 4.12.) other than that described above.

Table 4.12. Correlations between the classical (CD14+CD16-) monocyte population and HIV-1 paramaters or RBC parameters

Classical monocyte (CD14+CD16-)	Control		HIV-1 infected	
	p-value	r-value	p-value	r-value
CD4 count	Significant	Significant	0.9900	-0.0024
RCC	0.1545	-0.3306	0.7439	0.0622
Hb	0.1129	-0.3657	0.7640	0.0572
Hct	0.0780	-0.4031	0.6587	0.0841
Annexin V baseline	0.3253	0.2318	0.8543	-0.0350
Annexin V	0.4528	-0.1780	0.7458	0.0618
CD38/8	0.4181	0.1917	0.4840	-0.1329
VL	N/A	N/A	0.3561	-0.1812

There was a significant increase in the % inflammatory monocytes in the HIV-1 infected group. The control group had a median inflammatory monocyte % of 5.3±3.8 when compared to the HIV-1 positive group of 8.3±3.5, p=0.0054.

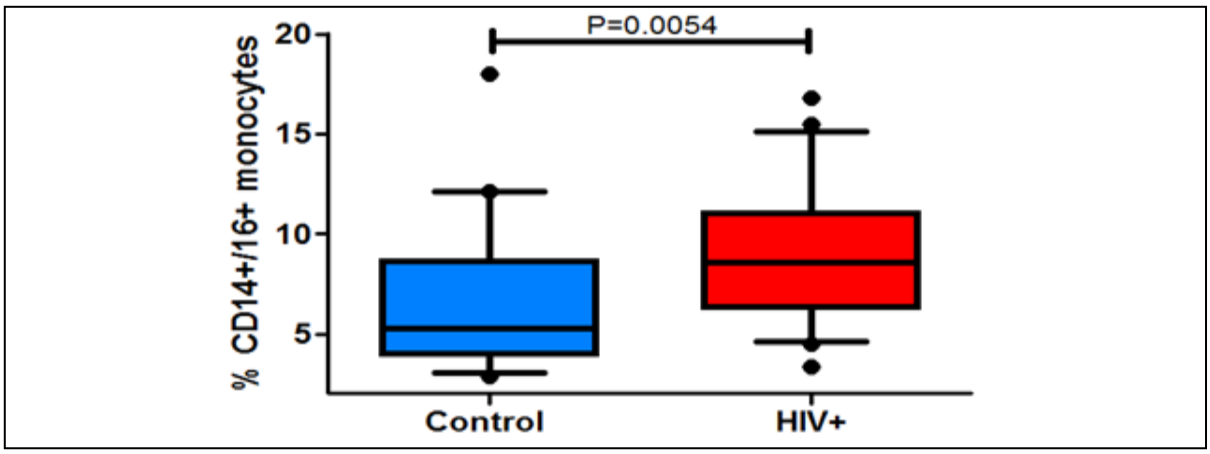

Figure 4.22. Comparison of the inflammatory (CD14+/16+) monocyte subset between the two groups. The box-and-whisker plot illustrates the inflammatory (CD14+/16+) monocyte between the two groups. There is a statistically significant difference between the inflammatory monocyte populations of the two groups with the HIV + group showing a statistical increase when compared to the control group with a p=0.0054.

The significant increase in the inflammatory subset of monocytes in HIV-1 infection may be due to the overall increase in immune activation (as evidenced by CD38 data). Although absolute monocyte counts were reduced in HIV-1, the % inflammatory cells were significantly increased. This would imply an overall increase in inflammatory monocytes. If 5.3% of monocytes were inflammatory in the uninfected group this would equate to $0.53x0.32x10^3$ cells/µl ($0.1696x10^3$ cell/µl) vs. 8.3% or $0.83x0.27x10^3$ ($0.2241x10^3$ cells/µl), representing almost double the number in the HIV-1 infected group.

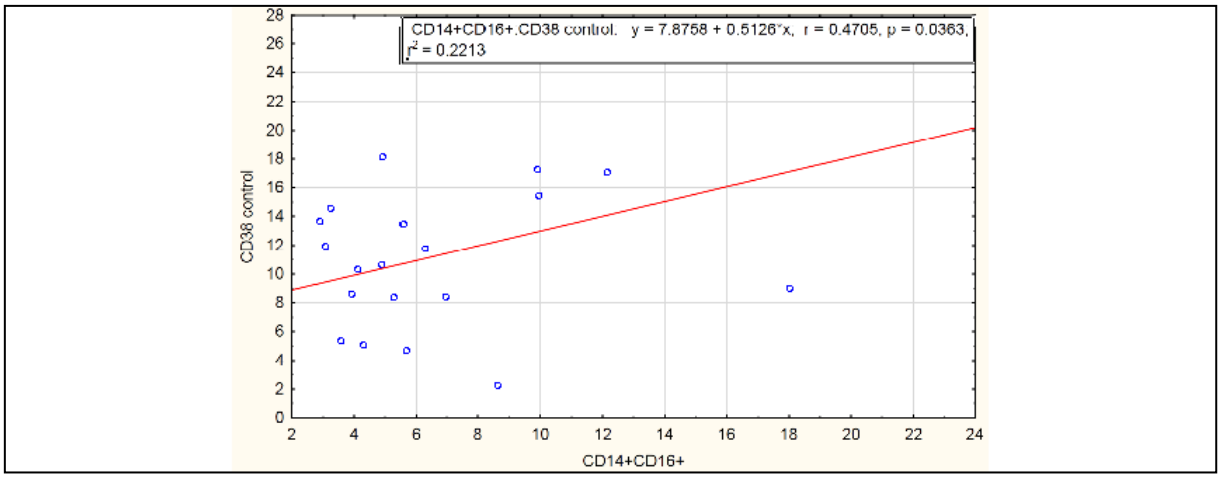

Figure 4.23. CD38+ CTL versus inflammatory monocyte correlation. The scatterplot illustrates the correlation between the CD38+ CTL and the inflammatory monocyte (CD14+CD16+) population in the control group. This was statistically significant with a p=0.0363 and r=0.4705

There was a significant correlation between the inflammatory monocyte (CD14+CD16+) population and CD38/8 expression in the control group, p=0.0363 and r=0.4705 illustrated in figure 4.23 above. There were no significant correlations between the classical monocyte and any HIV-1 parameters or RBC parameters (see Table 4.13.) other than that described above.

Table 4.13. Correlations between the classical (CD14+CD16-) monocyte population and HIV-1 parameters or RBC parameters

Inflammatory monocyte (CD14+CD16+)	Control		HIV-1 infected	
	p-value	r-value	p-value	r-value
CD4 count	0.1478	-0.3358	0.9712	0.0069
RCC	0.2409	-0.2748	0.9511	-0.0117
Hb	0.4671	-0.1725	0.9800	-0.0048
Hct	0.7344	-0.0810	0.9900	-0.0024
Annexin V baseline	0.9147	0.0256	0.8121	-0.0453
Annexin V	0.4423	-.01821	0.5244	-0.1209
CD38/8	Significant	Significant	0.2759	0.2055
VL	N/A	N/A	0.4553	0.1470

4.4.2. RBC phagocytotic potential of monocyte subsets at various monocyte to RBC ratios

The link between the monocyte and red cell compartments would most likely be at the level of apoptosis. Monocytes are the major cell involved in clearance of RBCs from the circulation – primarily in the spleen. Having established increased levels of apoptotic RBCs in HIV-1 infection, we investigated the interaction between monocytes and RBCs and how monocyte subsets differed in their ability to phagocytose these cells.

In order to test the ability of autologous monocytes to phagocytose RBCs, purified monocytes were exposed to RBCs at different monocyte:RBC ratios (as described in section 3.11.4.). Phagocytosis was measured by flow cytometry. RBCs were stained with CFSE prior to phagocytosis and the % of monocytes staining positive for CFSE was assessed at the end of the experiments. Figure 4.24 illustrates typical flow data generated.

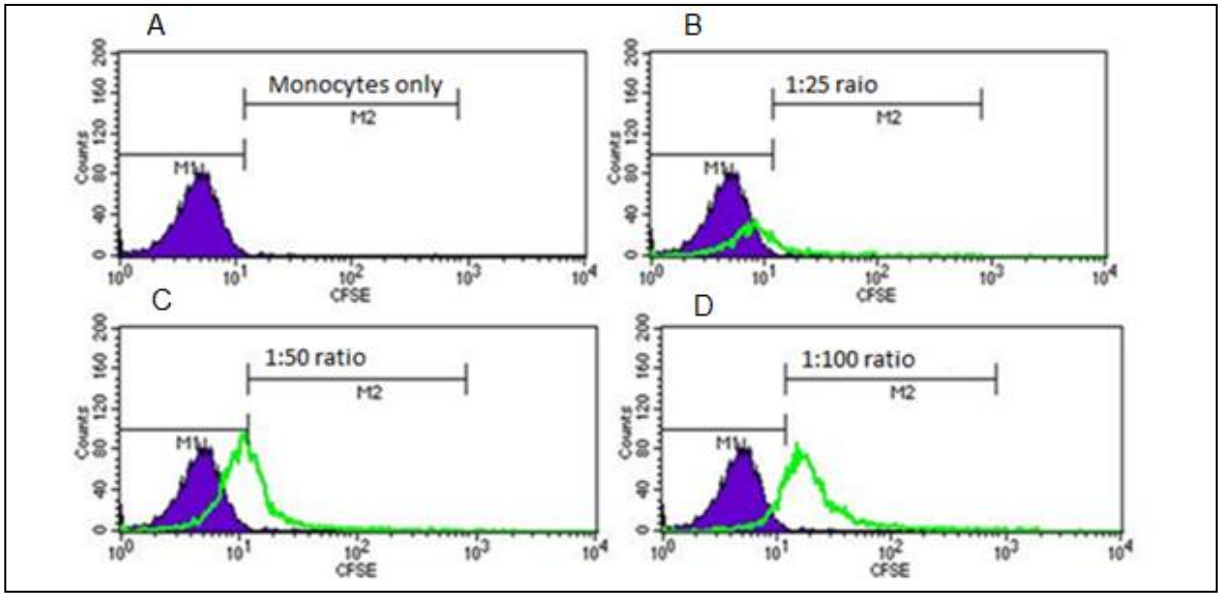

Figure 4.24. Phagocytosis of RBCs by monocytes at various monocyte:RBC ratios. (A) Representative histogram illustrating pure monocytes in purple containing no RBCs and showing placement of M2 CFSE erythrocyte marker. Graphs B-D represents the % f monocytes staining positive for CFSE, illustrated as a green line. Histogram B presents the number of monocytes taking up dead/dying RBCs when at a ratio of 1 monocyte to 25 stimulated RBCs (a total of 6.8% monocytes were CFSE positive). Histogram C represents a 1:50 ratio (total of 48.5% monocytes were CFSE positive) and histogram D a 1:100 ratio (total of 95.7% monocytes were CFSE positive).

4.4.3. 1 Monocyte to various RBC ratio's (25; 50 and 100)

In the phagocytosis experiments, the data was summarized as the median % of monocytes phagocytozing RBCs. The total monocyte fraction and the classical and inflammatory subsets were evaluated separately. Figure 4.25 shows the difference in phagocytotic potential of total monocytes. There was no significant difference in total monocyte phagocytic potential at all 3 ratios examined. Figure 4.26 illustrates that the same trend was observed when examining the classical (CD14+CD16-) monocyte subset. Figure 4.27 shows the phagocytic potential of the inflammatory (CD14+CD16+) monocyte subset, again showing no significant difference between the two study groups (i.e. HIV-1 negative versus HIV-1 positive).

These data illustrate that monocyte function is not impaired in HIV-1 infection, with comparable phagocytosis occurring at the designated monocyte:RBC ratios.

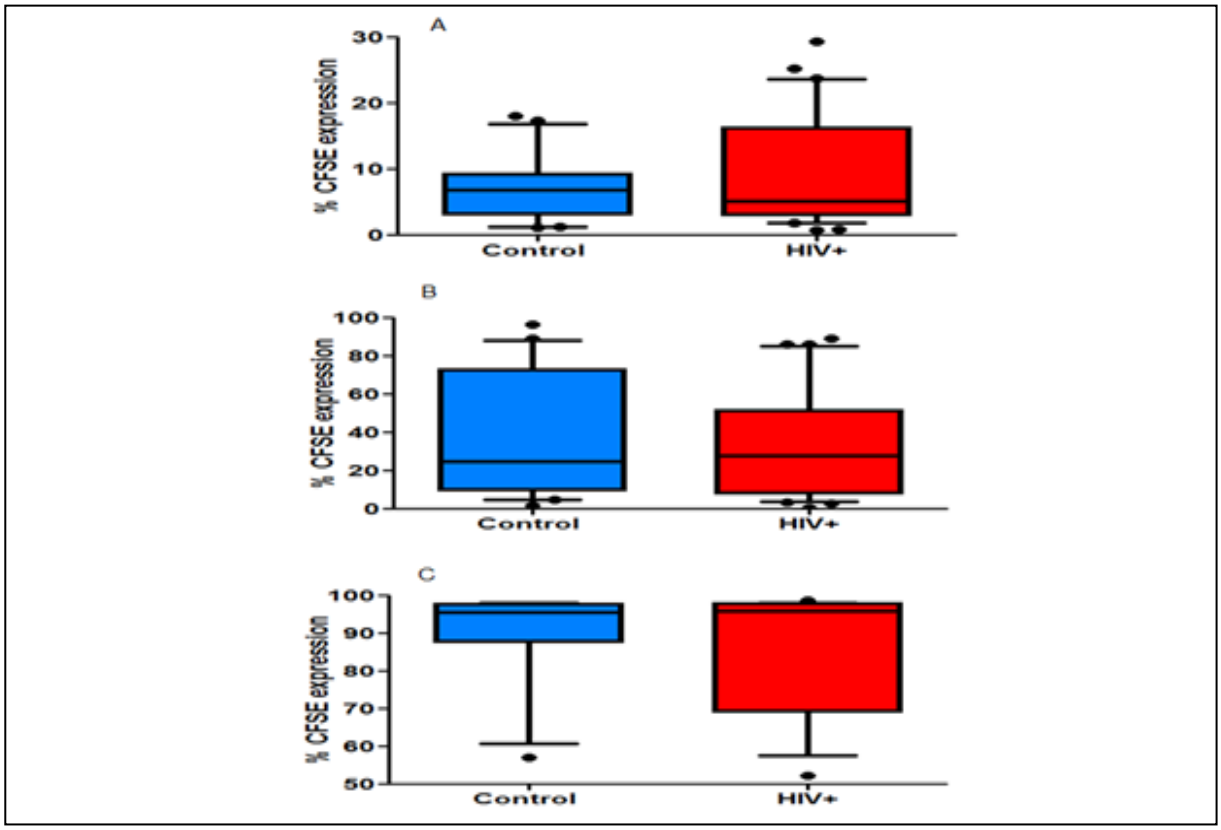

Figure 4.25. Phagocytosis of H_2O_2 stressed RBCs at different ratio's by monocytes. Graph A (box-and-whisker plot) illustrates a 1 monocyte to 25 stimulated RBC ratio between the two groups. Graph B illustrates a 1 monocyte to 50 stimulated RBC ratio between the two groups. Graph C illustrates a 1 monocyte to 100 stimulated RBC ratio between the two groups. There were no significant difference in the total number of monocytes between the control group (n=20) and the HIV-1 infected group (n=30) at any of the monocyte:RBC ratios.

The control group had a higher phagocytosis rate when compared to the total monocyte population of the HIV positive group at 1:25 ratio. There was no statistically significant difference between the two groups with a p=0.8897. At 1 monocyte to 50 stimulated RBC ratio between the two groups, the control group had a lower phagocytosis rate when compared to the HIV positive group. There was no statistically significant difference between the two groups with a p=0.5459. At 1 monocyte to 100 stimulated RBC ratio between the two groups, the control group had a lower phagocytosis rate when compared to the HIV positive group. There was no statistically significant difference between the two groups with a p=0.7478 (see Figure 4.25. and Table 4.14).

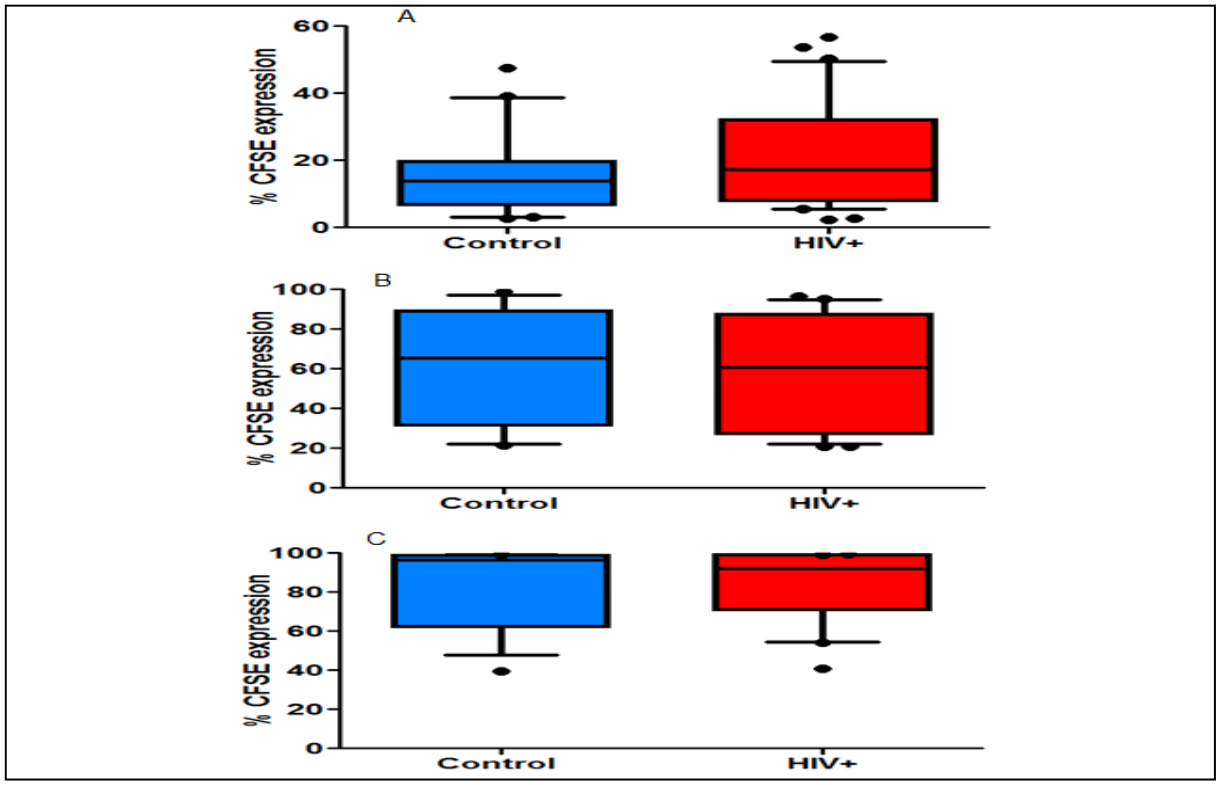

Figure 4.26. Phagocytosis of oxidative induced RBCs by the classical monocyte (CD14+/16-) subset. Graph A (box-and-whisker plot) illustrates a 1 classical monocyte (CD14+/16-) to 25 stimulated RBC ratio between the two groups. Graph B illustrates a 1 monocyte to 50 stimulated RBC ratio between the two groups. Graph C illustrates a 1 monocyte to 100 stimulated RBC ratio between the two groups. There were no significant difference between the control group (n=20) and the HIV-1 infected group (n=30) at any of the monocyte:RBC ratios.

The control group had a lower phagocytosis rate when compared to the classical monocyte population (CD14+/16-) of the HIV positive group at 1:25 ratio. There was no statistically significant difference between the two groups with a p=0.4458. At 1 classical monocyte to 50 stimulated RBC ratio between the two groups, the HIV-1 infected group had a lower phagocytosis rate when compared to the control group. There was no statistically significant difference between the two groups with a p=0.9290. At 1 classical monocyte to 100 stimulated RBC ratio between the two groups, the control group had a higher phagocytosis rate when compared to the HIV positive group. There was no statistical significant difference between the two groups with a p=0.5458 (see Figure 4.26. and Table 4.14).

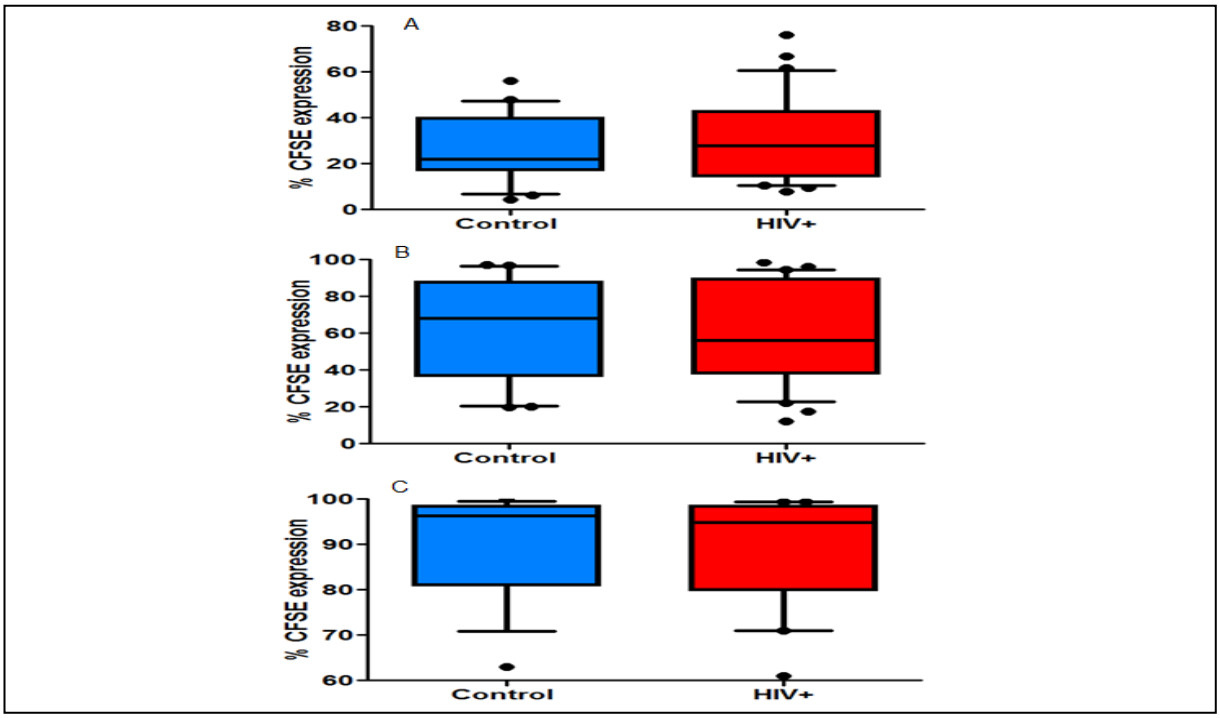

Figure 4.27. Phagocytosis of oxidative induced RBCs by the inflammatory monocyte (CD14+/16+) subset. Graph A (box-and-whisker plot) illustrates a 1 activated monocyte (CD14+/16+) to 25 stimulated RBC ratio between the two groups. Graph B illustrates a 1 monocyte to 50 stimulated RBC ratio between the two groups. Graph C illustrates a 1 monocyte to 100 stimulated RBC ratio between the two groups. There were no significant difference between the control group (n=20) and the HIV-1 infected group (n=30) at any of the monocyte:RBC ratios.

The control group had a lower phagocytosis rate when compared to the inflammatory (CD14+/16+) monocyte population of the HIV positive group at 1:25 ratio. There was no statistically significant difference between the two groups with a p=0.6136. At 1 activated monocyte to 50 stimulated RBC ratio between the two groups, the HIV-1 infected group had a lower phagocytosis rate when compared to the control group. There was no statistically significant difference between the two groups with a p=0.9921. At 1 activated monocyte to 100 stimulated RBC ratio between the two groups, the control group had a higher phagocytosis rate when compared to the HIV positive group. There was no statistically significant difference between the two groups with a p=0.8276 (see Figure 4.27 and Table 4.14).

Although there was no apparent difference in the phagocytotic potential of total monocytes or the subsets between the two groups, there was an enhanced capacity for phagocytosis by inflammatory monocytes in both study groups.

At the 25:1 ratio the inflammatory subset showed significantly enhanced phagocytosis as compared to the classical subset, in both the control and infected study groups. This would

appear to implicate the expanded, more phagocytic inflammatory subset in the clearance of the expanded apoptotic RBC population.

Table 4.14. Representation of median % CFSE expression and SD at each RBC:monocyte ratio

RBC:monocyte ratio	Classical		Inflammatory	
	Control	HIV-1 infected	Control	HIV-1 infected
25:1	13.8±12.9	17.2±15.6	22±14.3	27.9±18.1
50:1	24.8±29	27.9±32	68.1±27.5	56.3±26.9
100:1	96.4±21.1	92.3±18.3	96.4±11.2	94.8±11.6

4.4.4. Impact of RBCs oxidative stress on RBC up-take by the inflammatory (CD14+CD16+) monocyte subset at various monocyte to un-stimulated versus stimulated RBC ratios in the HIV+ group

Having established that the inflammatory subset is expanded in chronic HIV-1 infection and that the inflammatory subset is significantly more phagocytic of RBCs, we wished to investigate the impact of RBC apoptosis as induced by oxidative stress on the relative phagocytic potential of inflammatory monocytes. In section 4.3 we showed that H_2O_2 stressing led to approximately 18.5% of RBC becoming apoptotic. The increased red cell apoptosis induced by oxidative stress translated into increased phagocytosis at 25:1 ratio (5.2% vs. 2.9%), however this was not statistically significant. These data indicate that the *in vitro* oxidative stressing of the cells did not significantly impact on the phagocytic uptake. Increases in apoptotic RBCs of 3-4% were mirrored by a similar increase in phagocytosis (at 25:1 ratio) of 2.3%. There would appear to be a link between level of RBC apoptosis and phagocytosis, but due to moderate difference in apoptotic RBCs between the study groups, this did not lead to significant phagocytosis increase.

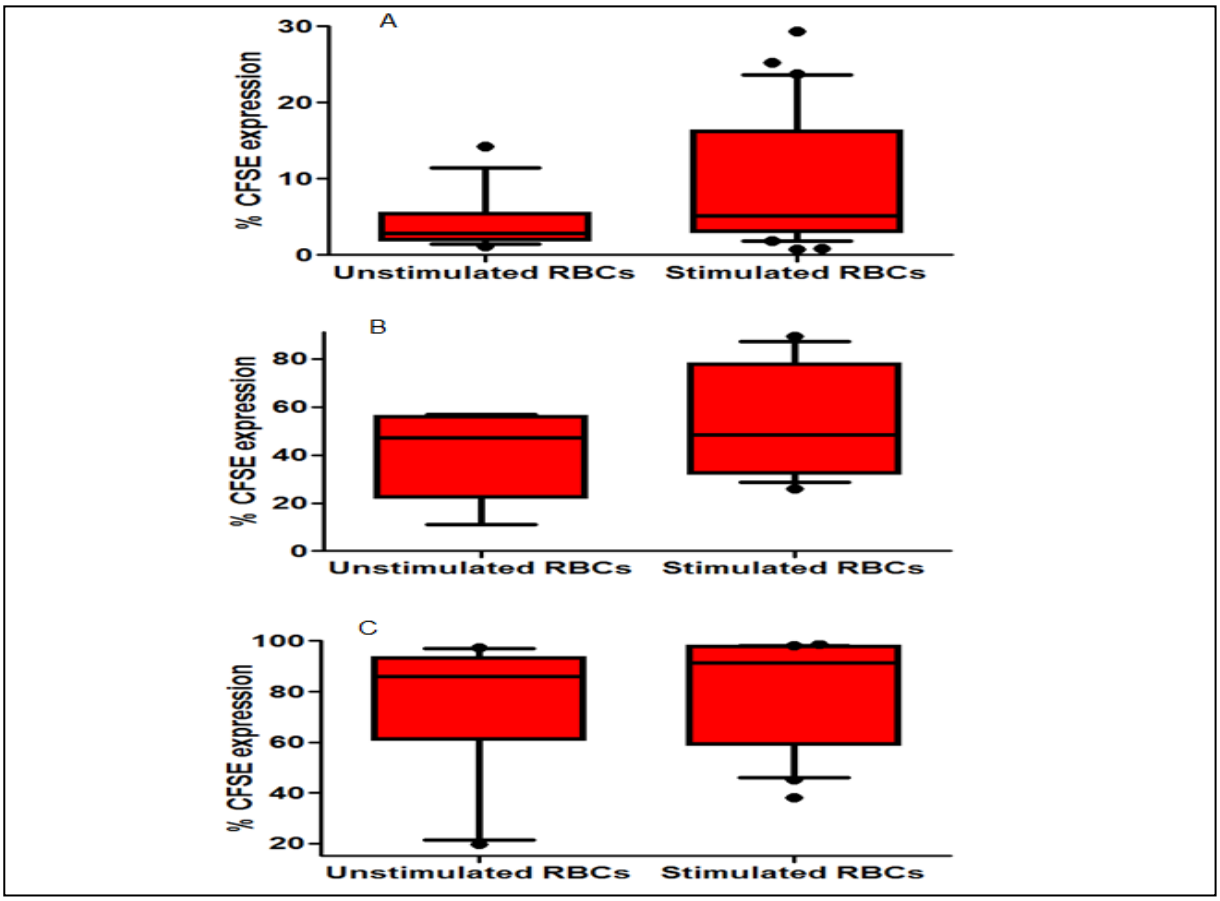

Figure 4.28. Determining the up-take capabilities of un-stimulated/stimulated RBCs by the inflammatory (CD14+CD16+) monocyte subset in the HIV-1 group. Graph A (box-and-whisker plot) illustrates a 1 activated monocyte (CD14+/16+) to 25 stimulated RBC ratio within the HIV-1 infected group. Graph B illustrates a 1 monocyte to 50 stimulated RBC ratio within the HIV-1 infected group. Graph C illustrates a 1 monocyte to 100 stimulated RBC ratio within the HIV-1 infected group. There were no significant differences between the uptake of un-stimulated RBCs (n=13) and the stimulated RBCs (n=13) by autologous monocytes at any of the RBC:monocyte ratios.

At a ratio of 1 activated monocyte (CD14+/16+) to 25 un-stimulated/stimulated RBC within the HIV positive group, the stimulated RBCs were phagocytosed twice as much by the inflammatory monocyte population as when RBCs were not stimulated with H_2O_2. There was no statistically significant difference between the two groups but there was a trend towards statistical significant with a p=0.0803. At 1 activated monocyte to 50 un-stimulated/stimulated RBC ratio within the HIV positive group, the un-stimulated RBCs were phagocytosed less by the inflammatory monocyte population as when RBCs were stimulated with H_2O_2. There was no statistically significant difference between the two groups with a p=0.2500. At 1 activated monocyte to 100 unstimulated/stimulated RBC ratio within the HIV positive group, the stimulated RBCs were phagocytosed more by the inflammatory monocyte population as when RBCs were not stimulated with H_2O_2. There was no statistically significant difference between the two groups but there was a trend towards statistical significance with a p=0.5000.

4.4.5. Phagocytosis of oxidatively stressed induced RBCs by the different monocyte subsets (classical (CD14+CD16-) and inflammatory (CD14+CD16+)) at various monocyte to RBC ratios

Having established that oxidative stress *in vitro* did not significantly alter phagocytosis by inflammatory monocytes between the 2 study groups, we next investigated how the two monocyte subsets differed in phagocytic ability within the study groups.

4.4.5.1. Classical/ Inflammatory monocytes at 25:1 RBC:monocyte ratios

The inflammatory monocyte subset phagocytosed almost twice as many erythroptotic RBCs when compared to the classical monocyte subset of the control group. The inflammatory subset had a median of 22±14.3% compared to 13.8±12.9 in the classical subset. p=0.0002. See figure 4.29

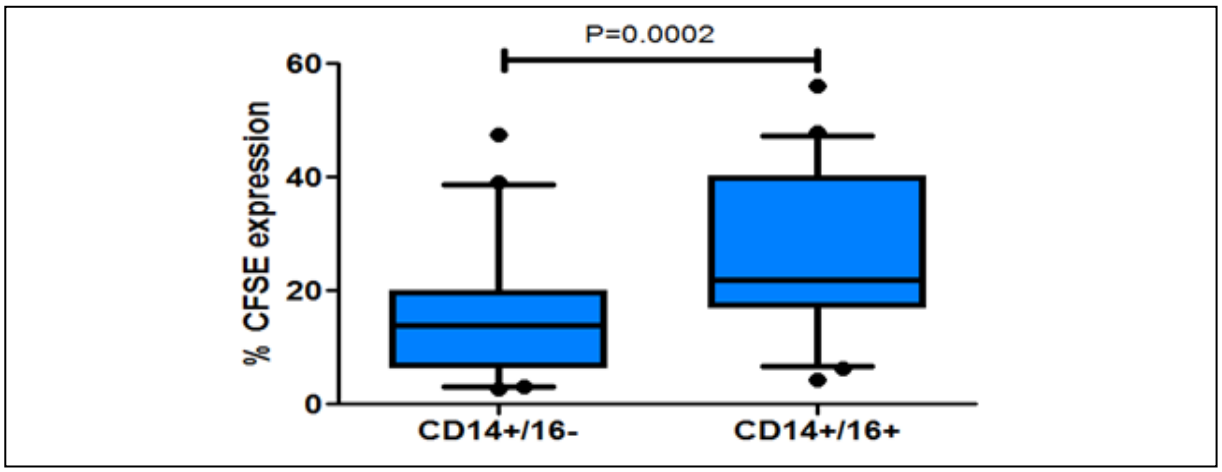

Figure 4.29. Comparison of the up-take capabilities between the different monocyte subsets in the control group at a 1 monocyte to 25 RBC ratio. The box-and- whisker plot illustrates classical (CD14+/16-) monocytes versus the activated monocytes (CD14+/16+) at a 1 to 25 stimulated RBC ratio within the control groups. There was a statistically significant difference between the two monocyte subsets with more activated monocytes engulfing damaged RBCs with a p=0.0002.

The classical subset phagocytosed 30% less erythroptotic RBCs when compared to the inflammatory monocyte subset in the HIV-1 infected group at a RBC:monocyte ratio of 25:1. The classical monocyte subset had a median of 17.2±15.6% phagocytic cells and the inflammatory monocyte subset a median of 27.9±18.1%, p<0.0001. See figure 4.30.

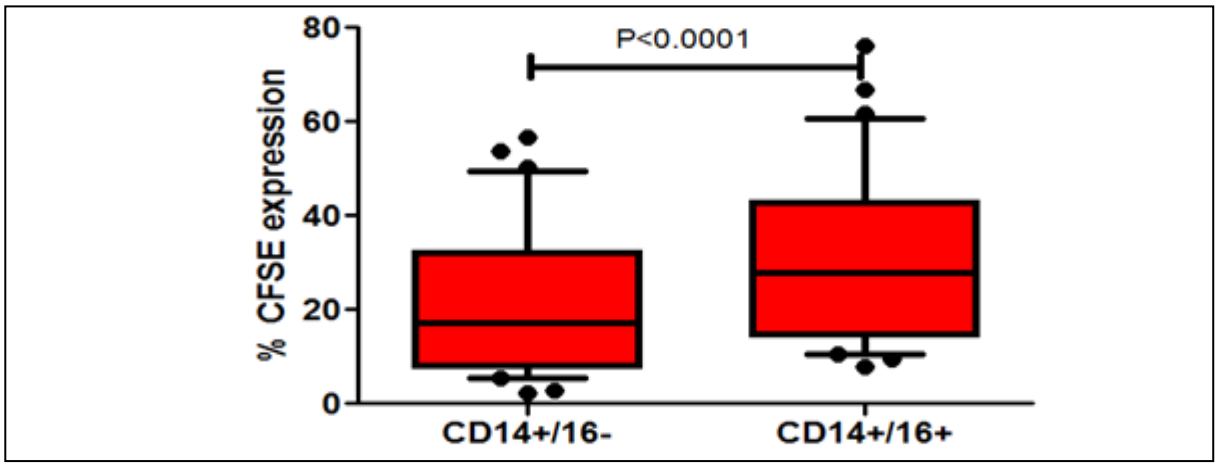

Figure 4.30. Comparison of the up-take capabilities between the different monocyte subsets in the HIV group at a 1 monocyte to 25 RBC ratio. The box-and-whisker plot illustrates classical (CD14+/16-) monocytes versus the activated monocytes (CD14+/16+) at a 1 to 25 stimulated RBC ratio within the HIV positive groups. There was a statistical significant difference between the two monocyte subsets with more activated monocytes engulfing damaged RBCs with a p<0.0001.

4.4.5.2. Classical/Inflammatory 50:1 RBC:monocyte ratio

The inflammatory monocyte subset phagocytosed more than 10% more erythroptotic RBCs when compared to the classical monocyte subset in the control group. The inflammatory subset had a median of 72.9±26.5% compared to 65.5±28.4%, p=0.0015 in the classical subset see figure 4.31.

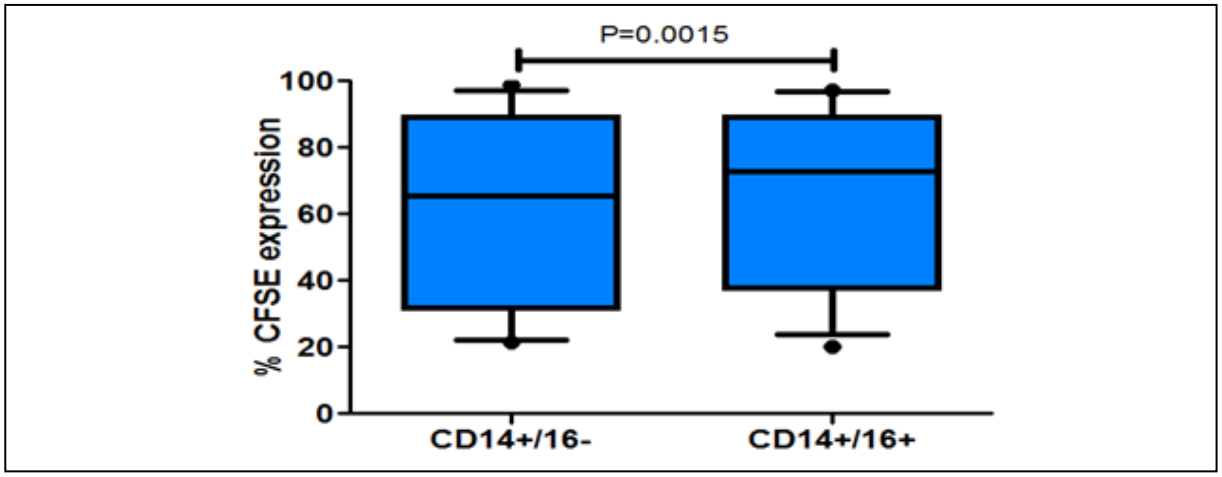

Figure 4.31. Comparison of the up-take capabilities between the different monocyte subsets in the control group at a 1 monocyte to 50 RBC ratio. The box-and-whisker plot illustrates classical (CD14+/16-) monocytes versus the activated monocytes (CD14+/16+) at a 1 to 50 stimulated RBC ratio within the control groups. There was a statistical significant difference between the two monocyte subsets with more activated monocytes engulfing damaged RBCs with a p=0.0015.

The inflammatory monocyte subset phagocytosed significantly less erythroptotic RBCs when compared to the classical monocyte subset in the HIV-1 infected group at this ratio. The

inflammatory monocyte subset had a median of 58.9±25.7% and the classical monocyte subset a median of 60.9±28.1%, p<0.0001. See figure 4.32.

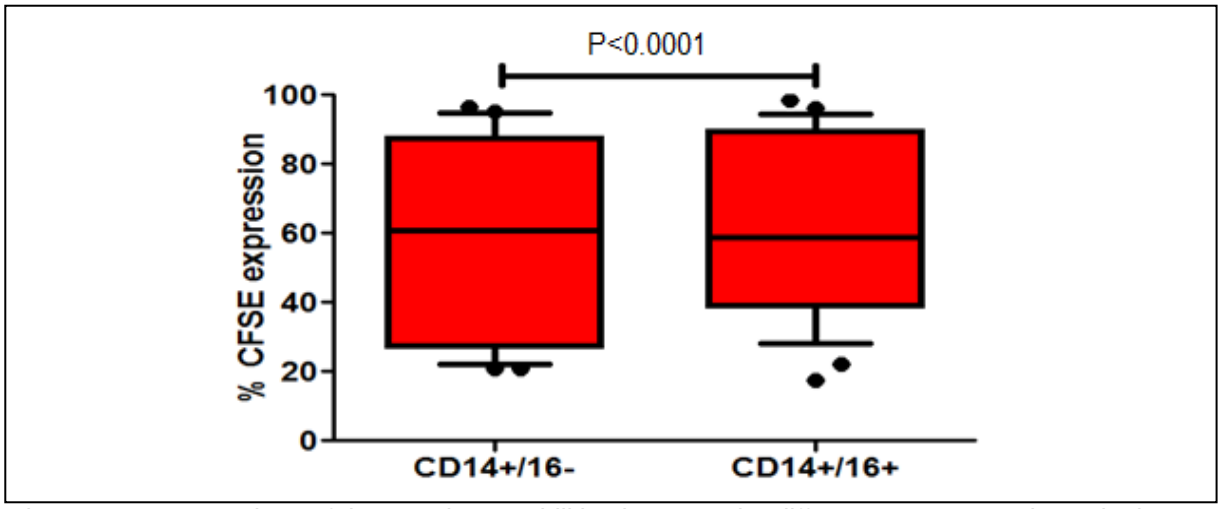

Figure 4.32. Comparison of the up-take capabilities between the different monocyte subsets in the HIV group at a 1 monocyte to 50 RBC ratio. The box-and-whisker plot illustrates classical (CD14+/16-) monocytes versus the activated monocytes (CD14+/16+) at a 1 to 50 stimulated RBC ratio within the HIV-1 positive groups. There was a statistical significant difference between the two monocyte subsets with more classical monocytes engulfing damaged RBCs with a p=0.0015.

4.4.5.3. 1 Classical/Inflammatory monocyte to 100 RBC ratio

The inflammatory monocyte subset phagocytosed a greater number of erythroptotic RBCs when compared to the classical monocyte subset in the control group. The inflammatory subset had a median of 95.6±26.5% compared to 96.4±28.4% in the classical subset, p=0.0465. See figure 4.33.

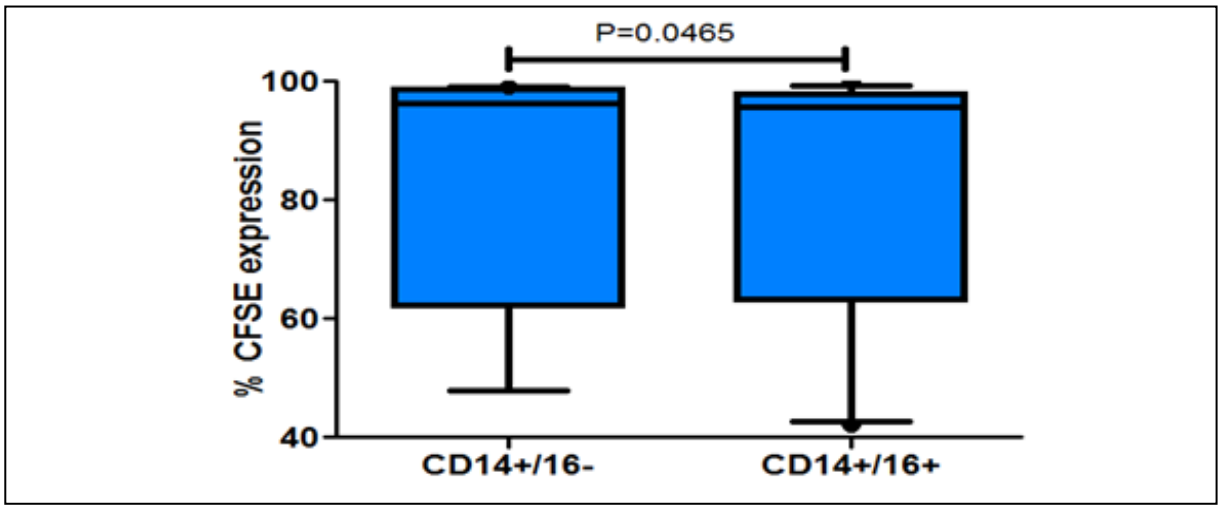

Figure 4.33. Comparison of the up-take capabilities between the different monocyte subsets in the control group at a 1 monocyte to 100 RBC ratio.The box-and-whisker plot illustrates classical (CD14+/16-) monocytes versus the activated monocytes (CD14+/16+) at a 1 to 100 stimulated RBC ratio within the control groups. There was a statistically significant difference between the two monocyte subsets with more activated monocytes engulfing damaged RBCs with a P=0.0465.

The inflammatory monocyte subset phagocytosed more erythroptotic RBCs when compared to the classical monocyte subset in the HIV-1 infected group. The inflammatory monocyte subset had a median of 94.8±11.6% and the classical monocyte subset a median of 94.6±16.4%, p=0.0066. See figure 4.34.

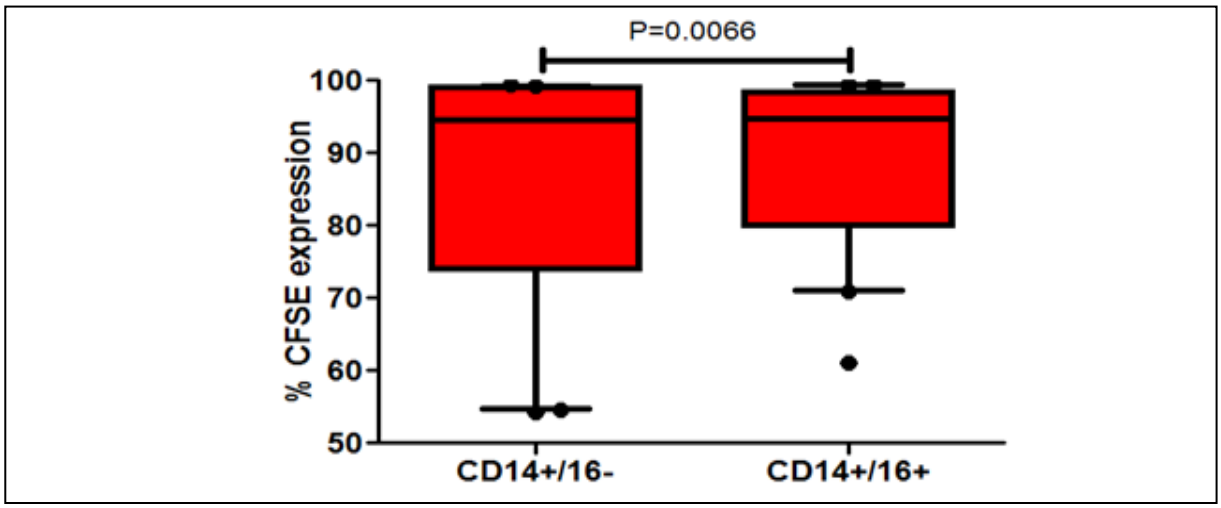

Figure 4.34. Comparison of the up-take capabilities between the different monocyte subsets in the HIV group at a 1 monocyte to 100 RBC ratio. The box-and-whisker plot illustrates classical (CD14+/16-) monocytes versus the activated monocytes (CD14+/16+) at a 1 to 100 stimulated RBC ratio within the HIV positive groups. There was a statistical significant difference between the two monocyte subsets with more activated monocytes engulfing damaged RBCs with a p=0.0066.

These data show that the inflammatory subset of monocytes was significantly more phagocytic than the classical subset. The expanded inflammatory monocyte subset in HIV-1 may be linked to the increased apoptotic red cell uptake of the expanded erythroptotic population.

Chapter 5. Discussion

Summary of data:

In the current study, we examined anaemia in chronic asymptomatic HIV-1 infection, with a particular focus on erythrocyte apoptosis, oxidative stress and immune activation, and the impact of changes in the erythrocyte compartment on monocyte-mediated phagocytosis. A summary of the major findings is outlined below, followed by a detailed discussion of the findings in relation to the published literature.

We have shown evidence for anaemia in chronic HIV-1 infection when compared to healthy HIV-1 uninfected individuals with significantly decreased RCC, Hb and Hct levels. The HIV-1 infected group had a median Hb of (12.9±1.8 g/dl) which was below the cut off level for anaemia (see section 2.7) and significantly lower than the control group (14.1±1.9 g/dl), p=0.0172. No significant correlates of red cell parameters with CD4 count, VL, or CD38/8 were detected – however trends were observed suggesting red cell changes may be related to HIV disease (e.g. RCC relationship to CD4 (+ve), VL (-ve) and CD38/8 (-ve). The HIV-1 infected group had a significantly higher baseline RBC annexin V expression when compared to the control group (13.4±4.7% vs. 10.4±5%, p=0.0189). This indicates that RBC damage occurs *in vivo*. Oxidative stress-induced upregulation of annexin V *in vitro* led to a 5% (control group) and 5.1% (HIV-1 infected group) increase in RBC-associated annexin V, indicating that the RBCs from HIV-1 positive individuals are not more sensitive to administered oxidative stress when compared to the RBCs from the control group.

Although NAC inhibited induced oxidative stress in both groups, the uninfected group displayed better inhibition. At 10mM NAC, the oxidative stress-induced annexin V expression was significantly reduced (from 20±5.1% to 15±4.4% (p=0.0063)). In other words, the 6.4% expression increase induced by oxidative stress was reduced to only 1.4% above baseline. In the HIV-1 group, the oxidative stress-induced annexin V expression was reduced from 18.3±5.0% to 16±5.2%. (p=0.0649). In this case, the 5.5% increase due to oxidative stress was reduced to 3.2%. NAC thus appears less efficient in minimizing induced oxidative stress *in vitro* in the HIV-infected group.

Absolute monocyte count was reduced in chronic HIV-1, with the control group having a median absolute monocyte count of $0.32x10^3$±0.1 cells/µl when compared to the HIV-1 positive group $0.27x10^3$±0.08 cells/µl (p=0.035). Although the control group had a higher CD14+/16- classical monocyte % of 65.6±7.1 when compared to the HIV positive group of

63.4±8.8 there was no statistical significance, p=0.1597. There was, however, a significant increase in the inflammatory (CD14+/16+) monocyte subset in the HIV-1 infected population when compared to the control population. The inflammatory subset in the control group constituted 5.3±3.8% when compared to the HIV-1 positive group of 8.3±3.5%, p=0.0054. The monocytes were equally phagocytic in the 2 study groups; however the inflammatory subset was significantly more phagocytic than the classical subset in both groups.

We have thus shown that anaemia is a feature of chronic HIV-1, even when patients are asymptomatic and CD4 count is relatively well maintained. This anaemia is multi-factorial and not due solely to the virus, CD4 T cell lymphopenia or generalised immune activation. Importantly, this study demonstrated significantly increased annexin V expression on erythrocytes, an indicator of erythroptosis. Increased oxidative stress is a feature of inflammation, and we were able to show that oxidative stress could increase baseline levels of annexin V expression. The antioxidant NAC was able to abrogate the induced oxidative stress damage *in vitro*, but elevated baseline erythroptosis in HIV-1 infection would appear to indicate that erythrocytes were “primed” to die *in vivo*.

Erythrocytes function primarily in homeostasis via haemoglobin-associated transport. Importantly, erythrocyte removal is mediated by monocytes and macrophages primarily located in the spleen but also in circulation. In this study we confirmed that monocytes were decreased in peripheral blood in chronic HIV-1 infection, however the inflammatory subset was significantly expanded. We also showed that the inflammatory subset of monocytes was the major phagocytic population and that phagocytosis of erythrocytes was affected by their annexin V expression.

5.1. Hypothesis

The original hypothesis of this study was that anaemia in chronic HIV-1 is linked to increased RBC death (erythroptosis), most likely due to oxidative stress, and that increased erythroptosis would be evident in the enhanced uptake (phagocytosis) of RBCs by monocytes.

We were able to partially verify the hypothesis: namely that RBC death was elevated in anaemic HIV-1 positive individuals. We also showed increased phagocytosis of erythroptotic RBCs by the expanded inflammatory monocyte subset. We could only partially verify a link between oxidative stress and erythroptosis, but did show partial inhibition of oxidative stress-induced apoptosis by NAC.

This is the first study to our knowledge to examine both erythrocyte death and associated monocyte uptake of erythrocytes in the context of chronic HIV-1 infection. Treating anaemic

HIV-1 patients with antioxidants (or reducing inflammation) would reduce erythrocyte death and remove the pressure on the monocyte population. There may also be downstream effects on monocytes, such as activation following phagocytosis, which could amplify the inflammation via secretion of cytokines. A very important finding is that changes in the monocyte population may be linked to enhanced erythrocyte death.

5.2. Basic indicators of HIV-1

It is well established that CD4 T cell numbers are decreased in chronic HIV-1 infection (Ford *et al.*, 2009; Aubert *et al.*, 2011; Ofotokun *et al.*, 2012). We found a statistically significant lower CD4 T lymphocyte count in the HIV-1 positive group compared to the control group. Not only are CD4 T lymphocytes directly infected by the virus, but indirect mechanisms such as 'bystander' apoptosis, also promote the loss of these cells (Badley *et al.*, 2000). CD4 T lymphocytes are therefore a valuable basic indicator of disease status in HIV infection.

Several studies have shown changes in the erythrocyte compartment in chronic HIV-1 infection. The changes may be related to anaemia of chronic disease or to unique HIV-1 infection associated features – such as virally induced changes, immune activation/inflammation changes and changes in other blood cell compartments. In the current study there was a statistically significant decrease in the RCC in the HIV-1 positive group when compared to the control group, $p=0.0009$. In a study by Abdollahi *et al.* (2010) conducted in Iran, RCC levels in 100 HIV-1 negative and 90 HIV-1 positive patients were assessed. The investigators showed a significantly lower RCC in the HIV-1 positive individuals as compared to the control group, $p<0.001$. The lower RCC could be due to a number of contributing factors; however, chronic immune activation with ROS production appears to have been the major exacerbating cause. Although the RCC levels in their study were slightly lower than the levels found in our study, we obtained a statistically lower RCC within the HIV-1 infected group compared to the control group, $p=0.0009$.

In a study by Obirikorang *et al.* (2009) a statistically lower Hb level in HIV-1 positive mothers was found when compared to the control group of HIV-1 negative mothers, $p\leq0.0001$. Their study was conducted in the Cape Coast in Ghana. In our study we also found statistically lower haemoglobin levels in the HIV-1 positive group when compared to the control group, $p=0.0172$. Since Hb forms part of RBCs, the decrease of Hb should be linked to the decrease in RBCs.

In our study, a significantly lower Hct level was found in the HIV-1 positive group compared to the control group. Omoregie *et al*. (2008) obtained similar results with $p=0.001$. Both the

haemoglobin and haematocrit levels are linked to the decreasing RCC levels in HIV-1 positive patients.

Anaemia is thus a well-described problem in HIV-1 infected individuals with decreased red cell parameters (RCC, Hb and Hct). The study group which we examined were not yet on ART; they were asymptomatic and had relatively well maintained CD4 counts.

Total monocyte count in chronic HIV-1 is not as well described as % monocyte subset distribution (see section 5.5. below). In a small study by Cobb *et al*. (2011) the total monocyte population in 8 healthy HIV-1 negative and 8 HIV-1 infected patients was measured. They found a small decrease in the HIV-1 infected group compared to the Control group, which was not significant p=0.079 (Cobb *et al*., 2011). The results we obtained in our study indicated a lower monocyte count in the HIV-1 infected group when compared to the control group, p=0.035. Although there was a statistical lower monocyte count in the HIV-1 group compared to the control group there was no clinical significance as the monocyte count still fell within the normal range. The difference in the results obtained between the two studies could be due to the smaller sample size used in their study. The overall monocyte count was lower in the HIV-1 infected group when compared to the control group in the current study. When the total monocyte count was divided into subsets, there was a lower classical monocyte population in the HIV-1 infected group compared to the control group (p=0.1597), but a statistical increase in the inflammatory population in the HIV-1 infected group when compared to the control group, p=0.0054. It is likely that monocytes are recruited to sites of infection/inflammation; therefore absolute counts appear decreased in the peripheral blood.

Numerous studies have researched the activation marker CD38 on CD8+ T cells in chronic HIV-1 infection. Steel *et al.* (2008) found a statistically significant increase in the percentage CD38 expression in HIV-1 positive patients compared to healthy controls, p<0.0001. In another study, Card *et al.* (2009) reported similar findings with an increase in CD38 expression in the HIV-1 positive group when compared to the healthy controls, p<0.001. These results agree with our findings and support the concept of activation of CTLs in HIV-1 positive individuals, p<0.0001.

Furthermore, increased CD38 expression has been shown to predict for a worse prognosis in HIV infection, irrespective of viral load or CD4 counts (Hazenberg *et al*., 2003).

5.3. Baseline annexin V expression on RBCs

There are many studies that have examined annexin V baseline expression on RBCs in other animals or on other cell types such as lymphocytes in HIV-1 infected individuals,

(Muratori *et al.*, 2009)(Gama *et al.*, 2012). However, our study is the first to our knowledge to examine these levels on RBCs in the context of HIV-1 infection. Our study is novel not only in the determination of these levels in RBCs, but also from the concept of measuring levels of expression of annexin V as an indication of *in vivo* inflammatory damage. In our study we measured the baseline expression *ex vivo* and found a statistically significant increase in the HIV-1 positive group when compared to the healthy non-infected controls. There are very few reports of impact of disease states on RBC baseline annexin V expression in humans. However Felder *et al.* (2011) determined the annexin V baseline expression on RBCs in healthy pigs and pigs infected with hemotrophic mycoplasma (HM). In the healthy controls they found almost undetectable levels of annexin V expression, but found much higher levels in the infected pigs (Felder *et al.*, 2011). The levels of annexin V baseline expression in the healthy pigs were much lower than those found in our study conducted on healthy non-infected humans. It is important to note that baseline annexin V levels in our study did not correlate with viral load; suggesting that factors other than the virus itself (such as the translocation of gut microbial products)(Ipp *et al.*, 2013), are likely to contribute to the inflammatory-induced oxidative stress sustained by the red blood cells.

5.4. Induction of Oxidative stress on RBCs with or without anti-oxidant NAC

A number of studies have looked at annexin V expression on various cells in various chronic conditions. In a study performed by Vota *et al.* (2012), the exposure of phosphatidylserine before and after incubation with aluminium to induce oxidative damage on RBCs was examined. Before stimulation, a low annexin V percentage was obtained and after stimulation the annexin V expression increased significantly, $p<0.05$ (Vota *et al.*, 2012). In our study, RBCs were stimulated with H_2O_2 and not aluminium as in their study. They reported much higher levels of annexin V expression than obtained in our study; nevertheless we also obtained significantly increased annexin V expression from baseline in both the control group ($p<0.0001$) and HIV-1 infected group ($p<0.0001$) as well as the maximum annexin V expression between the 2 groups after stimulation with H_2O_2, $p=0.0232$. In our study we found that oxidative stress *in vitro* increased RBC death, but the increase was equivalent in both the control and HIV-1 infected groups. On this basis we concluded that RBCs were not more sensitive to oxidative stress in the HIV positive group when compared to the control group, but had higher levels of damage already occurring *in vivo* most likely due to a more pro-apoptotic milieu. Healthy controls are likely to have a low inflammatory status allowing for compensated oxidative stress levels. Individuals that have high inflammatory environments such as HIV-1 positive individuals, produce significant amounts of oxidative stressors that are likely to contribute to the damage sustained by RBCs and result in increased exposure of phosphatidylserine.

Several studies have looked at the use of antioxidants to rescue cells (but not RBCs) from oxidative stress in HIV-1 infected individuals (Battin *et al.*, 2009)(Kamboj *et al.*, 2010). In a study conducted by Matarrese *et al.* (2005), oxidative stress was induced in RBCs by stimulation with 50 μM peroxynitrite ($ONOO^-$). Peroxynitrite is formed when hydrogen peroxide (H_2O_2) is mixed with nitrite. N-acetyl cysteine naïve samples stimulated with $ONOO^-$ expressed high annexin V levels due to the oxidative damage sustained. The samples incubated with the anti-oxidant NAC prior to stimulation with $ONOO^-$ expressed half the annexin V levels than was found when RBCs were incubated with only $ONOO^-$, suggesting that NAC dampened the damage caused by oxidative stress (Matarrese *et al.*, 2005). In our study we found annexin V expression levels similar to their study. In addition, we were able to demonstrate significant reduction in annexin V expression in the control group samples incubated with NAC, with levels returning almost to baseline within the control group, but with less well dampened levels in the HIV-1 infected group. This may indicate that NAC could prevent oxidative stress and thereby limit RBC death. This may also suggest that dampening oxidative stress *in vivo* may be beneficial in limiting the severity of anaemia in HIV infection.

5.5. Monocyte subsets and phagocytosis of erythroptotic RBCs

Unlike FBC monocyte count data, monocyte subsets have been more thoroughly investigated in HIV-1 infection. Han *et al.* (2009) conducted a study in 2009 on 97 HIV-1 non-infected and 68 HIV-1 infected individuals all recruited in Beijing, China. They divided the total numbers of isolated monocytes into their different subsets and found that there was a statistical decrease in the number of CD14+/CD16- (classical) monocyte population in the HIV-1 positive group when compared to the healthy control group, $p<0.0001$. They also found a significantly increased CD14+CD16+ (inflammatory) monocyte population of the HIV-1 positive group compared to the control group (Han *et al.*, 2009). Their finding of a statistical decrease in classical monocyte population in the HIV-1 positive group was similar to our study where we found a slightly lower classical monocyte population in the HIV-1 positive group when compared to the control group. Another study by Ansari *et al.* (2012) also found a similar trend when comparing the classical and inflammatory monocyte populations of HIV-1 infected individuals thus adding support to our findings. They also found a slight decrease in the classical monocyte population ($p=0.138$) and a significant increase in the inflammatory monocyte population in the HIV-1+ group when compared to the healthy control group, $p=0.004$ (Ansari *et al.*, 2012). These findings suggest that the CD14+CD16+ monocyte subset is expanded in HIV-1 infected individuals and this may be related to immune activation. The concurrent increase in inflammatory monocytes and apoptotic RBCs may also suggest that changes in the RBC compartment could affect the monocyte compartment.

Several studies have investigated phagocytosis of RBCs by macrophages but not specifically phagocytosis by monocytes in the peripheral blood; thus we have only macrophage data for comparison. We looked at monocytes due to their importance in inflammation and also due to their interaction with red cells in the bloodstream as well as being precursors of macrophages in the spleen. A study by Cambos *et al*. (2011) analysed the uptake of oxidized RBCs by macrophages. They measured RBC uptake by measuring CFSE expression in the macrophages the same way as we measured the oxidized RBC uptake in monocytes. In our study, we incubated three different ratios of oxidized RBCs to autologous monocytes (1:25, 1:50 and 1:100) in healthy and HIV-1 infected individuals; whereas in the Cambos study they incubated 200 oxidized RBCs to 1 macrophage. In our study, there was low to moderate uptake of oxidized RBCs by monocytes at the first two ratios in both the healthy and infected groups. The results obtained during our highest ratio (1:100) of RBCs to monocytes presented similar results when compared to their data (Cambos *et al.*, 2011).

This is the first study, to our knowledge, that has measured the phagocytosis of erythroptotic RBCs in HIV-1 infected individuals. Other studies have investigated the uptake capacity of the different monocyte subsets using various nanoparticles. Mosig *et al.* (2009) investigated the phagocytosis of oxidized low-density lipoproteins (LDL) by the classical (CD14+CD16-) monocyte population in a healthy control group compared with familial hypercholesterolemia (FH) group. They also investigated the phagocytic capacity of the inflammatory (CD14+CD16+) monocyte populations in the FH group and healthy controls. It was found that there was no difference between the uptakes of the oxidative LDL when comparing the classical monocyte population between the two groups. The inflammatory monocyte population showed a slight increase in the FH group compared to the healthy individuals but this did not reach statistical significance (Mosig *et al.*, 2009). These results, although not in the same chronic disease as our study; concurred with our findings indicating that the classical and inflammatory monocyte populations may be equally functional in the study group with disease as compared to the control group.

Ours is also the first study to our knowledge that investigated phagocytosis of RBCs by the different subsets of monocytes in HIV-1 infection. A study by Aguilar-Ruiz *et al.* (2011) researched the uptake efficacy of the classical monocyte population compared to the inflammatory monocyte population from healthy (HIV-1 negative) donors. Various cells were stimulated with zymosan (ligand found on fungi that stimulates a sterile inflammatory environment) or LPS and then incubated with either the classical or the inflammatory monocyte population. They found a statistically significant increase in the uptake of cells in the inflammatory monocyte population when compared to the classical monocyte population (Aguilar-Ruiz *et al.*, 2011). These results support our findings of the increased uptake of RBCs stimulated with H_2O_2 by the inflammatory subset. We also observed a significant

increase in the uptake in the autologous inflammatory monocyte population when compared to the autologous classical monocyte population. These results indicate that cells damaged by inflammatory environments such as in HIV-1 infection; are likely to be more readily taken up and disposed of by the expanded inflammatory monocyte population than the classical monocyte population.

This is also the first study to our knowledge that has investigated the up-take capabilities of un-stimulated versus stimulated apoptotic RBCs by the inflammatory monocyte subset in HIV-1 infected individuals. T. Mikołajczyk *et al.* (2009) researched the uptake capabilities of freshly isolated (un-stimulated) or apoptotic (stimulated) polymorphonuclear leukocytes (PMN) by the inflammatory (CD14+CD16+) monocyte population of healthy (HIV-1 negative) donors. The data obtained in their study indicated that only a low percentage of un-stimulated PMN cells were ingested by the inflammatory monocyte population. When the inflammatory monocytes were incubated with stimulated PMN cells there was a profound increase of percentage cells ingested (Mikołajczyk *et al.*, 2009). Their findings concur with the results we obtained when inflammatory monocytes of HIV-1 infected individuals were incubated with either healthy autologous RBCs or oxidative stressed autologous RBCs: there was also a statistically significant increase in the uptake of oxidatively stressed RBCs by the inflammatory monocyte population. Our findings suggest that the *in vivo* damage during inflammatory conditions, as seen in HIV infection, may drive a need for the increased disposal of dead/dying cells by the expanded activated inflammatory monocytes.

These results strengthen the idea that the inflammatory environment associated with HIV infection is an important factor leading to the development of anaemia. The free radicals (for instance H_2O_2) produced by monocytes (Bae *et al.*, 2009) during HIV-1 infection may not be the only oxidative stressor playing a part in the development of anaemia, but may be a major role player leading to its development (Johnson *et al.*, 2010). The activation of monocytes that remove dead/dying RBCs as a result of oxidative stress; is likely to contribute to the development of anaemia not only in HIV-1 infected individuals but also in other chronic inflammatory conditions.

5.6. Limitations of study

Our study had several limitations. The study had a cross-sectional design; so individuals could not be followed up to determine the prognostic value of these findings. The section (see section 4.4.4. above) focussing on up-take of un-stimulated/stimulated RBCs with H_2O_2 by the inflammatory monocyte population only incorporated analysis of the inflammatory monocyte population of the HIV-1 positive individuals and not of the controls. The work on oxidative stress and antioxidant rescue was performed *in vitro*. Detailed assessment of these

phenomena *in vivo* would require patient-based studies. Certain trends may also have been statistically significant with a larger sample size.

5.7. Summary of findings and future questions

In summary, RBCs were found to be damaged *in vivo* in HIV-1 infected individuals presenting a higher level of early apoptosis when compared to healthy non-infected individuals. Importantly, the HIV-1 infected group were clinically well, not on treatment and had relatively well maintained CD4 counts (mean: 400 cells/µl) and yet they were already showing signs of *in vivo* inflammatory-induced stress to their RBCs. The anti-oxidant NAC was found to dampen the damage caused to RBCs by oxidative stress (but less effectively in HIV-1 positive individuals). There was no difference in the total number of monocytes, but there was a shift in the monocyte subsets in the HIV-1 positive group. An increase in the inflammatory monocyte subset was detected and this is most likely a result of on-going immune activation in HIV infection. The inflammatory monocyte subset was more effective in phagocytosing damaged/dead RBCs than the classical monocyte subset. The inflammatory monocytes were also found to be more efficient at phagocytosing oxidative stressed RBCs compared to healthy RBCs.

5.8. Future questions

Future studies are needed to address the impact of RBC phagocytosis on monocytes and whether they become activated or whether they die. How the monocyte findings relate to macrophages also needs to be investigated. In addition, measuring oxidative stress and antioxidant levels in patients and relating those values to erythroptosis etc. needs to be studied. Finally, monitoring patient Hb and Annexin V levels in follow up cohort studies with an intervention arm incorporating the use of N-Acetyl cysteine needs to be investigated. These issues are being addressed in planned and ongoing studies.

Chapter 6. Conclusion

This was the first study to our knowledge describing increased erythroptosis at baseline level and after induced oxidative stress in chronic HIV-1. This is also the first study to link the expansion of the phagocytic inflammatory monocyte subset with erythrocyte damage. The red cell compartment may represent an underappreciated component in HIV-1 pathogenesis.

Studies have shown that anaemia is a common occurrence in HIV-1 infected individuals (Weiss, 2009)(Libregts *et al.*, 2011). An important contributing factor is persistent immune activation and inflammation. In support of this, we were able to demonstrate CTLs expressing higher levels of the activation marker (CD38/8) in HIV-1 positive individuals than in healthy individuals. The CTL activation marker was three times higher in the HIV-1 positive patients compared to the HIV-1 negative individuals which is in agreement with previous studies and this has significant implications for prognosis (Steel *et al.*, 2008; Funderburg *et al.*, 2012).

Monocytes are recruited to sites of infection and inflammation (Mikołajczyk *et al.*, 2009). Recruited monocytes produce ROS that could cause oxidative stress to surrounding cells (Zawada *et al.*, 2011). Damage to erythrocytes was higher in HIV-1 infected individuals compared to healthy non-infected individuals at baseline level suggesting that damage of cells already occurred *in vivo*. Erythrocytes stimulated with H_2O_2 *in vitro* showed equivalent increases in early apoptosis in both groups suggesting that RBCs from HIV-1 infected individuals are not more sensitive to oxidative stress than RBCs from healthy non-infected individuals.

The idea that anti-oxidants could be beneficial in chronic diseases was reinforced by our results. Anti-oxidants have previously been shown to reduce the level of erythroptosis (Matarrese *et al.*, 2005), but this is the first study to our knowledge to demonstrate this in the context of HIV infection. Our patients had not yet developed clinical anaemia, but already had significantly lower Hb, RCC and Hct levels than the uninfected controls. This suggests that enhanced removal of RBCs from the system was already occurring in this asymptomatic stage of HIV infection. We therefore propose that anti-oxidant therapy (or treatment with anti-inflammatory agents) would be beneficial in limiting the development of anaemia in the early stages of chronic HIV-1 infection. A longitudinal study will be important to determine the impact of anti-oxidant treatment on erythroptosis.

During chronic HIV-1 infection, as a result of ongoing immune activation, there is a change in the monocyte subset distribution resulting in an increase in the number of the inflammatory monocytes (Said *et al.*, 2010). This is the first study to our knowledge to demonstrate that the

expanded inflammatory monocytes in HIV-1 infection were more effective in phagocytosing autologous oxidatively stressed RBCs compared to the classical monocyte population. These results suggest that both inflammation and immune activation facilitate the development of anaemia not only by inducing more damage to RBC membranes, but also by stimulating the clearance of these RBCs through enhanced phagocytosis by activated monocytes. The use of anti-oxidants may inhibit the early apoptotic changes on RBCs and thereby limit their clearance from the system. In addition, treatment with anti-inflammatory agents may inhibit monocyte activation which occurs simultaneously with RBC damage.

References

Agrawal, L., Louboutin, J., & Strayer, D. S. (2007). Preventing HIV-1 Tat-induced neuronal apoptosis using antioxidant enzymes: mechanistic and therapeutic implications. *Virology*, *363*(2), 462–72.

Aguilar-Ruiz, S. R., Torres-Aguilar, H., González-Domínguez, É., Narváez, J., González-Pérez, G., Vargas-Ayala, G., Meraz-Ríos, M. a, et al. (2011). Human CD16+ and CD16- monocyte subsets display unique effector properties in inflammatory conditions in vivo. *Journal of leukocyte biology*, *90*(6), 1119–31.

Ajila, C. M., & Prasada Rao, U. J. S. (2008). Protection against hydrogen peroxide induced oxidative damage in rat erythrocytes by Mangifera indica L. peel extract. *Food and chemical toxicology : an international journal published for the British Industrial Biological Research Association*, *46*(1), 303–9.

Alter, G., & Moody, M. A. (2010). The humoral response to HIV-1: new insights, renewed focus. *The Journal of infectious diseases*, *202 Suppl* (Suppl 2), S315–22.

Andrew D. Badley, André A. Pilon, A. L. and D. H. L. (2000). Mechanisms of HIV-associated lymphocyte apoptosis. *Blood*, 2951–2964.

Ansari, a W., Meyer-Olson, D., & Schmidt, R. E. (2012). Selective Expansion of Pro-inflammatory Chemokine CCL2-Loaded CD14(+)CD16 (+) Monocytes Subset in HIV-Infected Therapy Naïve Individuals. *Journal of clinical immunology*, 14–16.

Aubert, R. D., Kamphorst, A. O., Sarkar, S., Vezys, V., Ha, S.-J., Barber, D. L., Ye, L., et al. (2011). Antigen-specific CD4 T-cell help rescues exhausted CD8 T cells during chronic viral infection. *Proceedings of the National Academy of Sciences of the United States of America*, *108*(52), 21182–7.

Auffray, C., Sieweke, M. H., & Geissmann, F. (2009). Blood monocytes: development, heterogeneity, and relationship with dendritic cells. *Annual review of immunology*, *27*, 669–92.

Bae, Y. S., Lee, J. H., Choi, S. H., Kim, S., Almazan, F., Witztum, J. L., & Miller, Y. I. (2009). Macrophages generate reactive oxygen species in response to minimally oxidized low-density lipoprotein: toll-like receptor 4- and spleen tyrosine kinase-dependent activation of NADPH oxidase 2. *Circulation research*, *104*(2), 210–8, 21p following 218.

Badley A.D., Pilon A.A., Landay A.,Lynch D.H. (2000). Mechanisms of HIV-associated lymphocyte apoptosis. Blood. 96, 2951-2964

Bain, B.J. (1997). The haematological features of hiv infection. *British Journal of Haematology*, *99*, 1–8.

Barbour, J. D., Ndhlovu, L. C., Xuan Tan, Q., Ho, T., Epling, L., Bredt, B. M., Levy, J. a, et al. (2009). High CD8+ T cell activation marks a less differentiated HIV-1 specific CD8+ T cell response that is not altered by suppression of viral replication. *PloS one*, *4*(2), e4408.

Battin, E. E., & Brumaghim, J. L. (2009). Antioxidant activity of sulfur and selenium: a review of reactive oxygen species scavenging, glutathione peroxidase, and metal-binding antioxidant mechanisms. *Cell biochemistry and biophysics*, *55*(1), 1–23.

Berahovich, R. D., Zabel, B. a, Penfold, M. E. T., Lewén, S., Wang, Y., Miao, Z., Gan, L., et al. (2010). CXCR7 protein is not expressed on human or mouse leukocytes. *Journal of immunology (Baltimore, Md. : 1950)*, *185*(9), 5130–9.

Berg, C. P., Engels, I. H., Rothbart, a, Lauber, K., Renz, a, Schlosser, S. F., Schulze-Osthoff, K., et al. (2001). Human mature red blood cells express caspase-3 and caspase-8, but are devoid of mitochondrial regulators of apoptosis. *Cell death and differentiation*, *8*(12), 1197–206.

Beyrer, C., Baral, S. D., Van Griensven, F., Goodreau, S. M., Chariyalertsak, S., Wirtz, A. L., & Brookmeyer, R. (2012). Global epidemiology of HIV infection in men who have sex with men. *Lancet*, *380*(9839), 367–377.

Boasso, A., & Shearer, G. M. (2008). Chronic innate immune activation as a cause of HIV-1 immunopathogenesis. *Clinical immunology (Orlando, Fla.)*, *126*(3), 235–42.

Bratosin, D., Tcacenco, L., Sidoroff, M., Cotoraci, C., Slomianny, C., Estaquier, J., & Montreuil, J. (2009). Active caspases-8 and -3 in circulating human erythrocytes purified on immobilized annexin-V: a cytometric demonstration. *Cytometry. Part A : the journal of the International Society for Analytical Cytology*, *75*(3), 236–44.

Brenchley, J. M., Schacker, T. W., Ruff, L. E., Price, D. a, Taylor, J. H., Beilman, G. J., Nguyen, P. L., et al. (2004). CD4+ T cell depletion during all stages of HIV disease occurs predominantly in the gastrointestinal tract. *The Journal of experimental medicine*, *200*(6), 749–59.

Briz, V., Poveda, E., & Soriano, V. (2006). HIV entry inhibitors: mechanisms of action and resistance pathways. *The Journal of antimicrobial chemotherapy*, *57*(4), 619–27.

Cambos, M., & Scorza, T. (2011). Robust erythrophagocytosis leads to macrophage apoptosis via a hemin-mediated redox imbalance: role in hemolytic disorders. *Journal of leukocyte biology*, *89*(1), 159–71.

Cassol, E., Malfeld, S., Mahasha, P., Van der Merwe, S., Cassol, S., Seebregts, C., Alfano, M., et al. (2010). Persistent microbial translocation and immune activation in HIV-1-infected South Africans receiving combination antiretroviral therapy. *The Journal of infectious diseases*, *202*(5), 723–33.

Chakrabarti, B. K., Pancera, M., Phogat, S., O'Dell, S., McKee, K., Guenaga, J., Robinson, J., et al. (2011). HIV type 1 Env precursor cleavage state affects recognition by both neutralizing and nonneutralizing gp41 antibodies. *AIDS research and human retroviruses*, *27*(8), 877–87.

Chun, T.-W., & Fauci, A. S. (2012). HIV reservoirs: pathogenesis and obstacles to viral eradication and cure. *AIDS (London, England)*, *26*(10), 1261–8.

Cobb, A., Roberts, L. K., Palucka, a K., Mead, H., Montes, M., Ranganathan, R., Burkeholder, S., et al. (2011). Development of a HIV-1 lipopeptide antigen pulsed therapeutic dendritic cell vaccine. *Journal of immunological methods*, *365*(1-2), 27–37.

Cohen, M., & Shaw, G. (2011). Acute HIV-1 infection. *New England Journal of Medicine*, *364*, 1943–1954.

Demchenko, A. P. (2012). Beyond annexin V: fluorescence response of cellular membranes to apoptosis. *Cytotechnology*, 65 (2), 157-172

Dey, B., Svehla, K., Xu, L., Wycuff, D., Zhou, T., Voss, G., Phogat, A., et al. (2009). Structure-based stabilization of HIV-1 gp120 enhances humoral immune responses to the induced co-receptor binding site. *PLoS pathogens*, *5*(5), e1000445.

Fauci, A. S. (2008). 25 years of HIV. *NATURE*, *453*(May), 289–290.

Federico, A., Morgillo, F., Tuccillo, C., Ciardiello, F., & Loguercio, C. (2007). Chronic inflammation and oxidative stress in human carcinogenesis. *International journal of cancer. Journal international du cancer*, *121*(11), 2381–6.

Felder, K. M., Hoelzle, K., Ritzmann, M., Schiele, D., Heinritzi, K., Groebel, K., & Hoelzle, L. E. (2011). Hemotrophic Mycoplasmas Induce Programmed Cell Death in Red Blood Cells. *Cellular Physiology Biochemistry and Biochemistry*, (27), 557–564.

Fendel, R., Mordmüller, B., Kreidenweiss, A., Rudat, A., Steur, C., Ambrosch, C., Kirstein, M., et al. (2007). New method to quantify erythrophagocytosis by autologous monocytes. *Cytometry. Part A : the journal of the International Society for Analytical Cytology*, *71*(4), 258–64.

Ford, E. S., Puronen, C. E., & Sereti, I. (2009). Immunopathogenesis of asymptomatic chronic HIV Infection: the calm before the storm. *Current opinion in HIV and AIDS*, *4*(3), 206–14.

Fu, Y., Fang, F., Lu, Z., Kuang, F., & Xu, F. (2010). N-acetylcysteine protects alveolar epithelial cells from hydrogen peroxide-induced apoptosis through scavenging reactive oxygen species and suppressing c-Jun N-terminal kinase. *Experimental lung research*, *36*(6), 352–61.

Funderburg, N. T., Zidar, D. a, Shive, C., Lioi, A., Mudd, J., Musselwhite, L. W., Simon, D. I., et al. (2012). Shared monocyte subset phenotypes in HIV-1 infection and in uninfected subjects with acute coronary syndrome. *Blood*, *120*(23), 4599–608.

Gama, L., Shirk, E. N., Russell, J. N., Carvalho, K. I., Li, M., Queen, S. E., Kalil, J., et al. (2012). Expansion of a subset of CD14highCD16negCCR2low/neg monocytes functionally similar to myeloid-derived suppressor cells during SIV and HIV infection. *Journal of leukocyte biology*, *91*(5), 803–16.

Ganz, T. (2006). Molecular pathogenesis of anemia of chronic disease. *Pediatric blood & cancer*, *46*(5), 554–7.

Geissmann, F., Manz, M. G., Jung, S., Sieweke, M. H., Merad, M., & Ley, K. (2010). Development of monocytes, macrophages, and dendritic cells. *Science (New York, N.Y.)*, *327*(5966), 656–61.

Gonzalez, V. D., Landay, A. L., & Sandberg, J. K. (2010). Innate immunity and chronic immune activation in HCV/HIV-1 co-infection. *Clinical immunology (Orlando, Fla.)*, *135*(1), 12–25.

Haas, A., Zimmermann, K., Graw, F., Slack, E., Rusert, P., Ledergerber, B., Bossart, W., et al. (2011). Systemic antibody responses to gut commensal bacteria during chronic HIV-1 infection. *Gut*, *60*(11), 1506–19.

Han, J., Wang, B., Han, N., Zhao, Y., Song, C., Feng, X., Mao, Y., et al. (2009). CD14(high)CD16(+) rather than CD14(low)CD16(+) monocytes correlate with disease progression in chronic HIV-infected patients. *Journal of acquired immune deficiency syndromes (1999)*, *52*(5), 553–9.

Harrison, K. M., Song, R., & Zhang, X. (2010). Life expectancy after HIV diagnosis based on national HIV surveillance data from 25 states, United States. *Journal of acquired immune deficiency syndromes (1999)*, *53*(1), 124–30.

Hazenberg, M. D., Otto, S. a, Van Benthem, B. H. B., Roos, M. T. L., Coutinho, R. a, Lange, J. M. a, Hamann, D., et al. (2003). Persistent immune activation in HIV-1 infection is associated with progression to AIDS. *AIDS (London, England)*, *17*(13), 1881–8.

Helweg-Larsen, J., Benfield, T., Atzori, C., & Miller, R. F. (2009). Clinical efficacy of first- and second-line treatments for HIV-associated Pneumocystis jirovecii pneumonia: a tri-centre cohort study. *The Journal of antimicrobial chemotherapy*, *64*(6), 1282–90.

Herrera, B., Fernández, M., Alvarez, a M., Roncero, C., Benito, M., Gil, J., & Fabregat, I. (2001). Activation of caspases occurs downstream from radical oxygen species production, Bcl-xL down-regulation, and early cytochrome C release in apoptosis induced by transforming growth factor beta in rat fetal hepatocytes. *Hepatology (Baltimore, Md.)*, *34*(3), 548–56.

Ipp, H., Zemlin, A. E., Glashoff, R. H., Van Wyk, J., Vanker, N., Reid, T., & Bekker, L.-G. (2013). Serum Adenosine Deaminase and Total Immunoglobulin G Correlate with Markers of Immune Activation and Inversely with CD4 Counts in Asymptomatic, Treatment-Naive HIV Infection. *Journal of clinical immunology*, *33*(3), 605–12.

Iwasaki, A., & Medzhitov, R. (2010). Regulation of adaptive immunity by the innate immune system. *Science (New York, N.Y.)*, *327*(5963), 291–5.

Jeang, K.-T. (2012). Multi-Faceted Post-Transcriptional Functions of HIV-1 Rev. *Biology*, *1*(2), 165–174.

Johnson, E. E., & Wessling-Resnick, M. (2012). Iron metabolism and the innate immune response to infection. *Microbes and infection / Institut Pasteur*, *14*(3), 207–16.

Johnson, R. M., Ho, Y., Yu, D., Kuypers, F. A., Ravindranath, Y., & Goyette, G. W. (2010). The effects of disruption of genes for peroxiredoxin-2, glutathione peroxidase-1, and catalase on erythrocyte oxidative metabolism. *Free radical biology & medicine*, *48*(4), 519–25.

Joshi, A., Nyakeriga, A. M., Ravi, R., & Garg, H. (2011). HIV ENV glycoprotein-mediated bystander apoptosis depends on expression of the CCR5 co-receptor at the cell surface and ENV fusogenic activity. *The Journal of biological chemistry*, *286*(42), 36404–13.

Kamboj, S. S., Vasishta, R. K., & Sandhir, R. (2010). N-acetylcysteine inhibits hyperglycemia-induced oxidative stress and apoptosis markers in diabetic neuropathy. *Journal of neurochemistry*, *112*(1), 77–91.

Kaoui, B., Biros, G., & Misbah, C. (2009). Why Do Red Blood Cells Have Asymmetric Shapes Even in a Symmetric Flow? *Physical Review Letters*, *103*(18), 1–4.

Karanam, B., Gambhira, R., Peng, S., Jagu, S., Kim, D.-J., Ketner, G. W., Stern, P. L., et al. (2009). Vaccination with HPV16 L2E6E7 fusion protein in GPI-0100 adjuvant elicits protective humoral and cell-mediated immunity. *Vaccine*, *27*(7), 1040–9.

Karsten, U., Butschak, G., Stahn, R., & Goletz, S. (2010). A novel series of anti-human glycophorin A (CD235a) antibodies defining five extra- and intracellular epitopes. *International immunopharmacology*, *10*(11), 1354–60.

Khan, H., Afridi, B., & Ishaq, T. (2007). HIV/AIDS transmission from mother to child with special attention toward transmission through breast feeding. *Rawal Medical Journal*, 1–6.

Kirchhoff, F. (2009). Is the high virulence of HIV-1 an unfortunate coincidence of primate lentiviral evolution? *Nature reviews. Microbiology*, *7*(6), 467–76.

Lang, K. S., Myssina, S., Lang, P. A., Tanneur, V., Kempe, D. S., Mack, A. F., Huber, S. M., et al. (2004). Inhibition of erythrocyte phosphatidylserine exposure by urea and Cl-. *American journal of physiology. Renal physiology*, *286*(6), F1046–53.

Lever, A. M. L. (2009). HIV: the virus. *Medicine*, *37*(7), 313–316.

Libregts, S. F., Gutiérrez, L., De Bruin, A. M., Wensveen, F. M., Papadopoulos, P., Van Ijcken, W., Ozgür, Z., et al. (2011). Chronic IFN-γ production in mice induces anemia by reducing erythrocyte life span and inhibiting erythropoiesis through an IRF-1/PU.1 axis. *Blood*, *118*(9), 2578–88.

Liu, L., Botos, I., Wang, Y., Leonard, J. N., Shiloach, J., Segal, D. M., & Davies, D. R. (2008). Structural basis of toll-like receptor 3 signaling with double-stranded RNA. *Science (New York, N.Y.)*, *320*(5874), 379–81.

Lu, S.-J., Feng, Q., Park, J. S., Vida, L., Lee, B.-S., Strausbauch, M., Wettstein, P. J., et al. (2008). Biologic properties and enucleation of red blood cells from human embryonic stem cells. *Blood*, *112*(12), 4475–84.

Lum, H., & Roebuck, K. A. (2001). Oxidant stress and endothelial cell dysfunction. *American Journal of Physiology*, *280*, C719–C741.

Lurie, M. N., & Rosenthal, S. (2010). Concurrent partnerships as a driver of the HIV Epidemic in sub-Saharan Africa? The evidence is limited. *AIDS and behavior*, *14*(1), 17–24; discussion 25–8.

Maitra, D., Byun, J., Andreana, P. R., Abdulhamid, I., Diamond, M. P., Saed, G. M., Pennathur, S., et al. (2011). Reaction of hemoglobin with HOCl: mechanism of heme destruction and free iron release. *Free radical biology & medicine*, *51*(2), 374–86.

Matarrese, P., Straface, E., Pietraforte, D., Gambardella, L., Vona, R., Maccaglia, A., Minetti, M., et al. (2005). Peroxynitrite induces senescence and apoptosis of red blood cells through the activation of aspartyl and cysteinyl proteases. *FASEB journal : official publication of the Federation of American Societies for Experimental Biology*, *19*(3), 416–8.

McMichael, A. J., Borrow, P., Tomaras, G. D., Goonetilleke, N., & Haynes, B. F. (2010). The immune response during acute HIV-1 infection: clues for vaccine development. *Nature reviews. Immunology*, *10*(1), 11–23.

Meidani, M., Rezaei, F., Maracy, M. R., Avijgan, M., & Tayeri, K. (2012). Prevalence, severity, and related factors of anemia in HIV/AIDS patients. *Journal of research in medical sciences : the official journal of Isfahan University of Medical Sciences*, *17*(2), 138–42.

Mikołajczyk, T. P., Skrzeczyńska-Moncznik, J. E., Zarebski, M. a, Marewicz, E. a, Wiśniewska, A. M., Dzieba, M., Dobrucki, J. W., et al. (2009). Interaction of human peripheral blood monocytes with apoptotic polymorphonuclear cells. *Immunology*, *128*(1), 103–13.

Mildvan, D., Creagh, T., & Leitz, G. (2007). Prevalence of anemia and correlation with biomarkers and specific antiretroviral regimens in 9690 human-immunodeficiency-virus-infected patients: findings of the Anemia Prevalence Study. *Current medical research and opinion*, *23*(2), 343–55.

Mogensen, T. H., Melchjorsen, J., Larsen, C. S., & Paludan, S. R. (2010). Innate immune recognition and activation during HIV infection. *Retrovirology*, *7*, 54.

Mohandas, N., & Gallagher, P. G. (2008). Red cell membrane: past, present, and future. *Blood*, *112*(10), 3939–48.

Mosig, S., Rennert, K., Krause, S., Kzhyshkowska, J., Neunübel, K., Heller, R., & Funke, H. (2009). Different functions of monocyte subsets in familial hypercholesterolemia: potential function of CD14+ CD16+ monocytes in detoxification of oxidized LDL. *FASEB journal : official publication of the Federation of American Societies for Experimental Biology*, *23*(3), 866–74.

Muratori, C., Cavallin, L. E., Krätzel, K., Tinari, A., De Milito, A., Fais, S., D'Aloja, P., et al. (2009). Massive secretion by T cells is caused by HIV Nef in infected cells and by Nef transfer to bystander cells. *Cell host & microbe*, *6*(3), 218–30.

Nicely, N. I., Dennison, S. M., Spicer, L., Scearce, R. M., Kelsoe, G., Ueda, Y., Chen, H., et al. (2010). Crystal structure of a non-neutralizing antibody to the HIV-1 gp41 membrane-proximal external region. *Nature structural & molecular biology*, *17*(12), 1492–4.

Odunukwe, N., Idigbe, O., Kanki, P., Adewole, T., Onwujekwe, D., Audu, R., Onyewuche, J., et al. (2005). Haematological and biochemical response to treatment of HIV-1 infection with a combination of nevirapine + stavudine + lamivudine in Lagos Nigeria. *Turkish Journal of Haematology*, *22*(3), 125–131.

Ofotokun, I., McIntosh, E., & Weitzmann, M. N. (2012). HIV: inflammation and bone. *Current HIV/AIDS reports*, *9*(1), 16–25.

Omoregie R., A. Egbeobauwaye, H. Ogefere, E.U. Omokaro, C. C. E. (2008). Prevalence of Antibodies to HAART Agents among HIV Patients in Benin city , Nigeria. *African Journal of Biomedical Research*, *11*(September 2007), 33–38.

Picker, L. J., & Watkins, D. I. (2005). HIV pathogenesis : the first cut is the deepest. *Nature immunology*, *6*(5), 430–432.

Pittman, R. N. (2010). Erythrocytes: surveyors as well as purveyors of oxygen? *American journal of physiology. Heart and circulatory physiology*, *298*(6), H1637–8.

Qu, C., Nguyen, V. A., Merad, M., & Randolph, G. J. (2009). MHC class I/peptide transfer between dendritic cells overcomes poor cross-presentation by monocyte-derived APCs that engulf dying cells. *Journal of immunology (Baltimore, Md. : 1950)*, *182*(6), 3650–9.

Quintó, L., Aponte, J. J., Menéndez, C., Sacarlal, J., Aide, P., Espasa, M., Mandomando, I., et al. (2006). Relationship between haemoglobin and haematocrit in the definition of anaemia. *Tropical medicine & international health : TM & IH*, *11*(8), 1295–302.

Raj, D. S. C. (2009). Role of interleukin-6 in the anemia of chronic disease. *Seminars in arthritis and rheumatism*, *38*(5), 382–8.

Ramoji, A., Neugebauer, U., Bocklitz, T., Foerster, M., Kiehntopf, M., Bauer, M., & Popp, J. (2012). Toward a spectroscopic hemogram: Raman spectroscopic differentiation of the two most abundant leukocytes from peripheral blood. *Analytical chemistry*, *84*(12), 5335–42.

Robbins, C. S., & Swirski, F. K. (2010). The multiple roles of monocyte subsets in steady state and inflammation. *Cellular and molecular life sciences : CMLS*, *67*(16), 2685–93.

Rockstroh, J. K., Gatell, J., Landman, R., & Antinori, A. (2010). Management of late-presenting patients with HIV infection. *Antiviral therapy*, *15 Suppl 1*, 25–30.

Said, E. a, Dupuy, F. P., Trautmann, L., Zhang, Y., Shi, Y., El-Far, M., Hill, B. J., et al. (2010). Programmed death-1-induced interleukin-10 production by monocytes impairs CD4+ T cell activation during HIV infection. *Nature medicine*, *16*(4), 452–9.

Seidler, S., Zimmermann, H. W., Bartneck, M., Trautwein, C., & Tacke, F. (2010). Age-dependent alterations of monocyte subsets and monocyte-related chemokine pathways in healthy adults. *BMC immunology*, *11*, 30.

Seki, E., & Schnabl, B. (2012). Role of innate immunity and the microbiota in liver fibrosis: crosstalk between the liver and gut. *The Journal of physiology*, *590*(Pt 3), 447–58.

Steel, A., John, L., Shamji, M. H., Henderson, D. C., Gotch, F. M., Gazzard, B. G., & Kelleher, P. (2008). CD38 expression on CD8 T cells has a weak association with CD4 T-cell recovery and is a poor marker of viral replication in HIV-1-infected patients on antiretroviral therapy. *HIV medicine*, *9*(2), 118–25.

Steele, M., & Narendran, A. (2012). Mechanisms of defective erythropoiesis and anemia in pediatric acute lymphoblastic leukemia (ALL). *Annals of hematology*, *91*(10), 1513–8.

Sundquist, W. I., & Kräusslich, H.-G. (2012). HIV-1 Assembly, Budding, and Maturation. *Cold Spring Harbor perspectives in medicine*, *2*(7), a006924.

Swirski, F. K., Nahrendorf, M., Etzrodt, M., Wildgruber, M., Cortez-Retamozo, V., Panizzi, P., Figueiredo, J., et al. (2009). Identification of splenic reservoir monocytes and their deployment to inflammatory sites. *Science (New York, N.Y.)*, *325*(5940), 612–6.

Tebit, D. M., & Arts, E. J. (2011). Tracking a century of global expansion and evolution of HIV to drive understanding and to combat disease. *The Lancet infectious diseases*, *11*(1), 45–56.

Trono, D., Van Lint, C., Rouzioux, C., Verdin, E., Barré-Sinoussi, F., Chun, T.-W., & Chomont, N. (2010). HIV persistence and the prospect of long-term drug-free remissions for HIV-infected individuals. *Science (New York, N.Y.)*, *329*(5988), 174–80.

Valko, M., Leibfritz, D., Moncol, J., Cronin, M. T. D., Mazur, M., & Telser, J. (2007). Free radicals and antioxidants in normal physiological functions and human disease. *The international journal of biochemistry & cell biology*, *39*(1), 44–84.

Vivier, E., Raulet, D. H., Moretta, A., Caligiuri, M. A., Zitvogel, L., Lanier, L. L., Yokoyama, W. M., et al. (2011). Innate or adaptive immunity? The example of natural killer cells. *Science (New York, N.Y.)*, *331*(6013), 44–9.

Volberding, P. a, & Deeks, S. G. (2010). Antiretroviral therapy and management of HIV infection. *Lancet*, *376*(9734), 49–62.

Vollbrecht, T., Brackmann, H., Henrich, N., Roeling, J., Seybold, U., Bogner, J. R., Goebel, F. D., et al. (2010). Impact of changes in antigen level on CD38/PD-1 co-expression on HIV-specific CD8 T cells in chronic, untreated HIV-1 infection. *Journal of medical virology*, *82*(3), 358–70.

Vota, D. M., Crisp, R. L., Nesse, A. B., & Vittori, D. C. (2012). Oxidative stress due to aluminum exposure induces eryptosis which is prevented by erythropoietin. *Journal of cellular biochemistry*, *113*(5), 1581–9.

Watts, J. M., Dang, K. K., Gorelick, R. J., Leonard, C. W., Bess, J. W., Swanstrom, R., Burch, C. L., et al. (2009). Architecture and secondary structure of an entire HIV-1 RNA genome. *Nature*, *460*(7256), 711–6.

Weiss, G. (2009). Iron metabolism in the anemia of chronic disease. *Biochimica et biophysica acta*, *1790*(7), 682–93.

Wertheim, J. O., & Worobey, M. (2009). Dating the age of the SIV lineages that gave rise to HIV-1 and HIV-2. *PLoS computational biology*, *5*(5), e1000377.

Wilen, C. B., Tilton, J. C., Doms, R. W., Craigie, R., & Bushman, F. D. (2012). HIV : Cell Binding and Entry. *Cold Spring Harbor perspectives in medicine*, a006866.

Worobey, M., Gemmel, M., Teuwen, D. E., Haselkorn, T., Kunstman, K., Bunce, M., Muyembe, J.-J., et al. (2008). Direct evidence of extensive diversity of HIV-1 in Kinshasa by 1960. *Nature*, *455*(7213), 661–4.

Yan, H.-L., Xue, G., Mei, Q., Ding, F.-X., Wang, Y.-Z., & Sun, S.-H. (2008). Calcium-dependent proapoptotic effect of Taenia solium metacestodes annexin B1 on human eosinophils: a novel strategy to prevent host immune response. *The international journal of biochemistry & cell biology*, *40*(10), 2151–63.

Yan, N., & Lieberman, J. (2011). Gaining a foothold: how HIV avoids innate immune recognition. *Current opinion in immunology*, *23*(1), 21–8.

Zawada, A. M., Rogacev, K. S., Rotter, B., Winter, P., Marell, R.-R., Fliser, D., & Heine, G. H. (2011). SuperSAGE evidence for CD14++CD16+ monocytes as a third monocyte subset. *Blood*, *118*(12), e50–61.

Zeng, M., Smith, A. J., Wietgrefe, S. W., Southern, P. J., Schacker, T. W., Reilly, C. S., Estes, J. D., et al. (2011). Cumulative mechanisms of lymphoid tissue fibrosis and T cell

depletion in HIV-1 and SIV infections. *The Journal of clinical investigation*, *121*(3), 998–1008.

Zhang, J.-Y., Zou, Z.-S., Huang, A., Zhang, Z., Fu, J.-L., Xu, X.-S., Chen, L.-M., et al. (2011). Hyper-activated pro-inflammatory CD16 monocytes correlate with the severity of liver injury and fibrosis in patients with chronic hepatitis B. *PloS one*, *6*(3), e17484.

Zheng, Y.-H., Lovsin, N., & Peterlin, B. M. (2005). Newly identified host factors modulate HIV replication. *Immunology letters*, *97*(2), 225–34.

Ziegler-Heitbrock, L., Ancuta, P., Crowe, S., Dalod, M., Grau, V., Hart, D. N., Leenen, P. J. M., et al. (2010). Nomenclature of monocytes and dendritic cells in blood. *Blood*, *116*(16), e74–80.

Zimmermann, H. W., Seidler, S., Nattermann, J., Gassler, N., Hellerbrand, C., Zernecke, A., Tischendorf, J. J. W., et al. (2010). Functional contribution of elevated circulating and hepatic non-classical CD14CD16 monocytes to inflammation and human liver fibrosis. *PloS one*, *5*(6), e11049.

Zwaal, R. F., & Schroit, a J. (1997). Pathophysiologic implications of membrane phospholipid asymmetry in blood cells. *Blood*, *89*(4), 1121–32.